Assessment Of Repolarization Sequence From The QT Interval In The Body Surface Electrocardiogram

By

Shirley Wong

Submitted in partial fulfillment of the requirements
for the degree of Doctor of Philosophy

at
Dalhousie University
Halifax, Nova Scotia, Canada
February 1, 1996

Canada

Name _____

Dissertation Abstracts International and Masters Abstracts International are arranged by broad, general subject categories.
Please select the one subject which most nearly describes the content of your dissertation or thesis. Enter the corresponding
four-digit code in the spaces provided.

Physiology
SUBJECT TERM

|0|4|3|3| **UMI**
SUBJECT CODE

Subject Categories

THE HUMANITIES AND SOCIAL SCIENCES

COMMUNICATIONS AND THE ARTS
Architecture 0729
Art History....................................0377
Cinema 0900
Dance 0378
Fine Arts 0357
Information Science........................0723
Journalism 0391
Library Science 0399
Mass Communications 0708
Music..0413
Speech Communication..................0459
Theater 0465

EDUCATION
General 0515
Administration 0514
Adult and Continuing 0516
Agricultural 0517
Art...0273
Bilingual and Multicultural 0282
Business 0688
Community College........................0275
Curriculum and Instruction 0727
Early Childhood.............................0518
Elementary 0524
Finance 0277
Guidance and Counseling 0519
Health 0680
Higher 0745
History of 0520
Home Economics 0278
Industrial 0521
Language and Literature 0279
Mathematics 0280
Music 0522
Philosophy of 0998
Physical...0523

Psychology 0525
Reading 0535
Religious 0527
Sciences 0714
Secondary 0533
Social Sciences 0534
Sociology of 0340
Special 0529
Teacher Training 0530
Technology 0710
Tests and Measurements 0288
Vocational 0747

LANGUAGE, LITERATURE AND LINGUISTICS
Language
  General 0679
  Ancient 0289
  Linguistics 0290
  Modern 0291
Literature
  General 0401
  Classical 0294
  Comparative 0295
  Medieval 0297
  Modern 0298
  African 0316
  American 0591
  Asian 0305
  Canadian (English) 0352
  Canadian (French) 0355
  English 0593
  Germanic 0311
  Latin American 0312
  Middle Eastern 0315
  Romance 0313
  Slavic and East European 0314

PHILOSOPHY, RELIGION AND THEOLOGY
Philosophy.....................................0422
Religion
  General 0318
  Biblical Studies 0321
  Clergy 0319
  History of 0320
  Philosophy of 0322
Theology 0469

SOCIAL SCIENCES
American Studies 0323
Anthropology
  Archaeology 0324
  Cultural 0326
  Physical 0327
Business Administration
  General 0310
  Accounting 0272
  Banking 0770
  Management 0454
  Marketing 0338
Canadian Studies 0385
Economics
  General 0501
  Agricultural 0503
  Commerce-Business 0505
  Finance 0508
  History 0509
  Labor 0510
  Theory 0511
Folklore 0358
Geography 0366
Gerontology 0351
History
  General 0578

Ancient 0579
Medieval 0581
Modern 0582
Black 0328
African 0331
Asia, Australia and Oceania 0332
Canadian 0334
European 0335
Latin American 0336
Middle Eastern 0333
United States 0337
History of Science 0585
Law...0398
Political Science
  General 0615
  International Law and
    Relations 0616
  Public Administration 0617
Recreation 0814
Social Work 0452
Sociology
  General 0626
  Criminology and Penology ...0627
  Demography 0938
  Ethnic and Racial Studies 0631
  Individual and Family
    Studies 0628
  Industrial and Labor
    Relations 0629
  Public and Social Welfare 0630
  Social Structure and
    Development 0700
  Theory and Methods 0344
Transportation 0709
Urban and Regional Planning 0999
Women's Studies 0453

THE SCIENCES AND ENGINEERING

BIOLOGICAL SCIENCES
Agriculture
  General 0473
  Agronomy 0285
  Animal Culture and
    Nutrition 0475
  Animal Pathology.........................0476
  Food Science and
    Technology 0359
  Forestry and Wildlife 0478
  Plant Culture 0479
  Plant Pathology 0480
  Plant Physiology 0817
  Range Management 0777
  Wood Technology 0746
Biology
  General 0306
  Anatomy 0287
  Biostatistics 0308
  Botany 0309
  Cell 0379
  Ecology 0329
  Entomology 0353
  Genetics 0369
  Limnology 0793
  Microbiology 0410
  Molecular 0307
  Neuroscience 0317
  Oceanography...............................0416
  Physiology 0433
  Radiation 0821
  Veterinary Science.........................0778
  Zoology 0472
Biophysics
  General 0786
  Medical 0760

EARTH SCIENCES
Biogeochemistry.............................0425
Geochemistry 0996

Geodesy 0370
Geology..0372
Geophysics 0373
Hydrology 0388
Mineralogy......................................0411
Paleobotany 0345
Paleoecology 0426
Paleontology 0418
Paleozoology 0985
Palynology 0427
Physical Geography 0368
Physical Oceanography 0415

HEALTH AND ENVIRONMENTAL SCIENCES
Environmental Sciences 0768
Health Sciences
  General 0566
  Audiology 0300
  Chemotherapy 0992
  Dentistry 0567
  Education 0350
  Hospital Management 0769
  Human Development 0758
  Immunology 0982
  Medicine and Surgery 0564
  Mental Health 0347
  Nursing 0569
  Nutrition 0570
  Obstetrics and Gynecology ..0380
  Occupational Health and
    Therapy 0354
  Ophthalmology 0381
  Pathology 0571
  Pharmacology 0419
  Pharmacy 0572
  Physical Therapy 0382
  Public Health 0573
  Radiology 0574
  Recreation 0575

Speech Pathology 0460
Toxicology 0383
Home Economics 0386

PHYSICAL SCIENCES

Pure Sciences
Chemistry
  General 0485
  Agricultural 0749
  Analytical 0486
  Biochemistry 0487
  Inorganic 0488
  Nuclear 0738
  Organic 0490
  Pharmaceutical..............................0491
  Physical 0494
  Polymer 0495
  Radiation 0754
Mathematics 0405
Physics
  General 0605
  Acoustics 0986
  Astronomy and
    Astrophysics 0606
  Atmospheric Science 0608
  Atomic 0748
  Electronics and Electricity 0607
  Elementary Particles and
    High Energy 0798
  Fluid and Plasma 0759
  Molecular 0609
  Nuclear 0610
  Optics 0752
  Radiation 0756
  Solid State 0611
Statistics 0463

Applied Sciences
Applied Mechanics 0346
Computer Science 0984

Engineering
  General 0537
  Aerospace 0538
  Agricultural 0539
  Automotive 0540
  Biomedical 0541
  Chemical 0542
  Civil 0543
  Electronics and Electrical 0544
  Heat and Thermodynamics ...0348
  Hydraulic 0545
  Industrial 0546
  Marine 0547
  Materials Science 0794
  Mechanical 0548
  Metallurgy 0743
  Mining 0551
  Nuclear 0552
  Packaging 0549
  Petroleum......................................0765
  Sanitary and Municipal 0554
  System Science 0790
Geotechnology 0428
Operations Research 0796
Plastics Technology 0795
Textile Technology 0994

PSYCHOLOGY
General..0621
Behavioral.......................................0384
Clinical..0622
Developmental 0620
Experimental 0623
Industrial 0624
Personality 0625
Physiological 0989
Psychobiology 0349
Psychometrics 0632
Social...0451

Table of Contents

Lists of Figures and Tables

Figures

Tables

Abstract

The concept of "reverse sequence of repolarization" is traditionally presented to account for the mainly concordant polarity of the T wave, with respect to the QRS complex in the body surface ECG during normal ventricular conduction. However, it is generally observed that in complete bundle branch blocks the T waves are discordant, i.e. of opposite polarity to the QRS complex, suggesting a concordant rather than reverse sequence of repolarization. The present investigation was initiated as a systematic effort to investigate the influence of spatial sequence of left ventricular excitation on the spatial/temporal sequence of repolarization in terms of concordance and discordance and its effects on the QT interval of the electrocardiogram. ECG data files of various North American population groups collected between the years 1976 - 1984 were used to construct vectorcardiograms and QRS-T correlation maps for the orthogonal X, Y and Z leads in normal ventricular conduction and in various categories of ventricular conduction defects. Several linear regression models were introduced to assess the contribution of the QRS duration to QT and JT intervals. The results indicate that the QRS duration has a small but significant influence on the QT interval in normal ventricular conduction, this influence becoming pronounced in complete bundle branch blocks. This finding suggests that even in normal conduction, repolarization is not universally reverse. It becomes prominently concordant in complete bundle branch blocks, particularly in left bundle branch block and complete bundle branch blocks of undetermined type. The local spatial direction of the excitation fronts may play an important role in determining excitation-repolarization relationships. It is suggested that in normal conduction, repolarization is mainly reverse. However, repolarization is likely to change from reverse to at least partially concordance sequence during repolarization of the posterior basal left ventricular wall, and possibly in portions of the ventricular septum where there is a higher likelihood of excitation propogating in an apex to base direction. In the left bundle branch block the repolarization process becomes mainly concordant, as regional/temporal sequence of excitation is mainly in a apex to base direction. A large fraction of the observed total QT interval variability remains unexplained. It is suggested that local and global differences in action potential duration gradients with regional and global contractility and other factors in addition to heart rate to be carefully considered in future development of more advanced repolarization models.

List of Symbols and Abbreviations

α - (alpha) regression coefficient, QT_{max} for univariate regression of QT on RF

γ - counterpart of the intercept in linear univariate regression

Δ - (delta) changes in a variable

$\pm$ - range of standard deviation

$<$ - less than

$>$ - more than

$^\circ$ - degree, unit of angular displacement

Ω - root-mean-square variation value; solid angle

β - (beta) a measure of the slope for a regression line

$\emptyset$ - estimated values for the QRS/T angle

μ - micro

$\longrightarrow$ - vector

$\bar{A}, \bar{P}, \bar{R}, \bar{L}, \bar{S}, \bar{I}$ - directions of main activation and repolarization in the orthogonal Cartesian coordinate system - directing toward anterior, posterior, right, left, superior and inferior

AP/APs - action potential/action potentials

APD/APDs - action potential duration/action potential durations

APDendo - action potential duration of endocardium

APDepi - action potential duration of epicardium

APD_L - action potential duration of the ventricular myocardial region which repolarizes latest

APD_O - action potential duration in the myocardial fibers excited earliest

APD_{max} - limited value of action potential duration after a long pause

$\hat{A}QRS$ - QRS integral vector: $\overrightarrow{|AQRS|}$ (μvs)

$\hat{A}R$ - area under R wave vector

$\hat{A}T$ - area under T wave vector

AT - activation time

aT - peak of T wave

AV - atrioventricular node

aVF, aVL, aVR - augmented unipolar limb leads devised by Goldberg

CV - coefficient of variation

DP_O - duration of plateau at endocardium

DP3 - the duration of the fast phase of repolarization

dQT/dHR - an expression for the predicted change in QT per unit increase in heart rate from a given steady state level

ECG - electrocardiogram

ET_O - excitation time in the myocardial fibers excited earliest

ET_L - excitation time of the ventricular myocardial region which repolarizes latest

ETendo - excitation time of the endocardium

ETepi - excitation time of the epicardium

eT - end of T wave

ER - end of repolarization

f(HR) - function of heart rate

f(ET) - function of excitation time

FRPs - functional refractory periods

$\vec{G}$ - ventricular gradient vector

HHANES - Hispanic Health and Nutrition Examination Survey

HR - heart rate

IVCD - complete block of unspecified type

IRBBB - incomplete right bundle branch block

ILBBB - incomplete left bundle branch block

I, II, III - standard limb leads devised by Einthoven

J point - the end of excitation

JT - represents ventricular repolarization; QT minus QRS duration

k - constant

LBBB - left bundle branch block

LV - left ventricle

MAP/MAPs - monophasic action potential/monophasic action potenials

MC - Minnesota Code

MI - Myocardial infarction

mm - millimeter

ms/msec - millisecond, an unit of time

N - total number

NHANES 1 - the first National Health and Nutrition Examination Survey

NHANES 2 - the second National Health and Nutrition Examination Survey

P wave - a deflection in the ECG that represents repolarization of the atria

Q - a deflection in the ECGs that expresses depolarization of the septum

QT- electrical systole of the ventricles

QT_{100} - QT at HR = 100/min

QTI - QT prolongation index; QTI = (QT/QTp) x 100

QT_c - QT interval corrected for heart rate

QT_{LC} - the linearly corrected QT interval in second

QT_o - QT after a long pause

QT_p - predicted QT; QTp = 656/(1 + 0.01HR)

QT_{max} - maximum prediction QT after a long pause; 1/a = 656 ms

QR_2 - total electromechanical systole obtained from the systolic time interval

QRS complex - deflection in the ECG that represents depolarization of the   ventricle

R^2 - squared multiple correlation coefficient

ΔR^2 - the increment in R2 values with the inclusion of QRS duration on QT and JT
prediction formulas

RBBB - right bundle branch block

RF - the rate correction factor defined as 1/(1 + 0.01 HR)

RMS - root-mean-square value

RMSE (ms) - the root-mean-square error of prediction

RP - refractory period

RR - length of time between QRS waves in the electrocardiogram

RT - repolarization time

RT$_L$ - myocardial regions repolarize last

RV - right ventricle

SAS - a statistical computer software

SD - standard deviation

SR - start of repolarization

ST - segment of electrocardiogram between QRS and T wave

T wave - a deflection in the ECG that represents repolarization of the ventricles

TQ - the subinterval of RR interval

X,Y,Z - corrected orthogonal lead system devised by Frank; components of a dipole
in a orthogonal system: +X = to the left; +Y = to inferior (downward); +Z =
to posterior (to the back)

U wave - a small deflection in the ECG followed the T wave.; exact mechanism of
generation unknown

VCD - ventricular conduction defects

VG - ventricular gradient, VG = |G|

V1-V6 - precordial leads, unipolar leads devised by Wilson

Acknowledgments

To pursue a PhD in Physiology and Biophysics is one of the biggest challenges in my career development. The completion of my thesis would not have been possible were it not for the assistance given me by several persons. I would like to acknowledge them with my warmest thanks.

My deepest gratitude and thanks go to my supervisor, Dr. P. M. Rautaharju, Director of the EPICORE Centre of the University of Alberta, for guiding me with innovative and exciting ideas for my research, and for providing me with financial assistance during my stays in Edmonton, Alberta. His patience and priceless criticism made the writing of this thesis an enjoyable task rather than a burdensome chore.

I give many thanks to the members of my Supervisory Committee: Dr. H. Wolf, my Co-Supervisor, Dr. J.A. Armour and Dr. G. Klassen , who have made helpful suggestions to my thesis. Special heart felt gratitude goes to Dr. J.A Armour for his support during the most difficult period of my study in the program.

For their assistance in computer work, I would like to thank Dr. H. Calhourn, a member of the EPICORE Centre of the University of Alberta; Mr. B. Hoyt and Mr. J. Warren, the members of the Dalhousie University Medical computer staff and M s.Vivien Hanon, a member of Dalhousie Computer Centre. Thanks are due to all the staff of EPICORE, University of Alberta for their friendship and help during my stays in Edmonton.

Last but not the least I would like to give a special heartfelt thanks to my brother Dr. Alan Wong and my sister Julia Wong for their unconditional support and encouragement, which meant a lot to me.

During the course of the work I was supported by Dalhousie Graduate scholarship.

CHAPTER 1
INTRODUCTION AND HYPOTHESES

1.1. Introduction

The conventional QT interval in the body surface electrocardiogram (ECG) is measured from the earliest onset of the QRS complex to the terminal portion of the T wave, and it reflects the duration of total ventricular excitation and repolarization.

It is well established that ventricular repolarization is strongly influenced by heart rate and the spatial sequence of ventricular excitation. Numerous formulas have been proposed for the prediction of QT interval from steady state heart rate or the RR interval of ECG in order to correct QT for differences produced by heart rate variations. Bourdillon et al.[1] were the first to suggest that the inclusion of the QRS duration improves QT prediction accuracy and may enhance detection of the QT prolongation. None of the current QT prediction formulas took QRS duration into account until recently, when Rautaharju et al.[2] demonstrated that QRS duration is a significant independent determinant of the QT interval even in normal conduction.

More recently, clinical application of changes in the duration of QT has become a topic of growing interest. The reason for this is its wide utility over an increasingly investigated range of applications, including drug-induced QT prolongation [3] , the reported association between prolonged QT interval and serious ventricular arrhythmias [4] , and the identification of a QT interval as a prognostic factor for sudden death [5].

1

Prolongation of the QT interval may be caused by prolongation of ventricular activation, changes in heart rate, and action potential duration prolongation, manifested as prolongation of myocardial refractoriness [6]. To date, the mechanisms responsible for the QT prolongation still remain speculative. The fact that the inclusion of the QRS duration contributes significantly to the QT prediction, has important theoretical implication to modelling of QT and ventricular repolarization. This in turn is likely to improve prediction of a prolonged QT interval in ventricular conduction defects.

There is a paucity of information on the QT interval prediction in ventricular conduction defects. This poses a problem in attempts to identify the QT prolongation in the presence of bundle branch blocks. A recent report on 72 patients with various types of ventricular conduction defects suggested that QT prolongation was entirely secondary to prolonged depolarization [7]. Thus far there are no published reports on how the QRS duration variations will influence excitation time, and action potential duration in those myocardial regions, which repolarize latest and determine the QT interval length.

It is known that the normal T waves in the ECG leads with mainly positive QRS complexes (left-lateral leads) are, in general, concordant (morphology of T wave is upright and positive) with a QRS complex in normal conduction. The concept of "reverse sequence of repolarization" has been introduced to account for the mainly concordant polarity of the T wave in normal persons. In its simplest form, this concept implies that excitation in the free wall of the left ventricle spreads from the endocardial surface towards the epicardium, and repolarization proceeds in the opposite direction from the epicardium to the endocardium. Thus some areas of early activation have longer action potentials than do areas that are excited late. This means that the action potential durations must progressively shorten from endocardium to epicardium in such a fashion that the action potential duration differences (APDendo - APDepi) are larger than the differences in excitation time (ETepi - ETendo). However, it is generally

observed that in complete bundle branch blocks, the T waves are discordant, i.e. of opposite polarity to the QRS complex. This observation would tend to support the concept of a concordant rather than discordant sequence of repolarization. Thus, considerable differences can be anticipated in the excitation-repolarization relationship between normal conduction and ventricular conduction defects, and consequently in QT prediction. It is not known, however, to what extent the reverse sequence concept holds in normal subjects and to what extent the concordant sequence concept is valid in various kinds of ventricular conduction defects. The present study was initiated as a systematic effort to investigate the effect of ventricular excitation sequence on the QT interval of the electrocardiogram, with the expectation that it will provide a better understanding of excitation-repolarization relationships in various types of ventricular conduction.

1.2. Scope of investigation

This inquiry contains three essentially exploratory studies. The first project investigates the evolution of ventricular excitation and repolarization patterns with age in relation to the QT interval of the ECG in normal adult men and women. In the next project, association between ventricular excitation time and QT and JT intervals is investigated in ventricular conduction def..cts. The third project attempts to quantify the excitation-repolarization relationship by means of QRS-T correlation maps, determined for normal conduction and for various categories of ventricular conduction defects. The objective here is to gain an improved understanding of the reasons why variations in the excitation-repolarization relationship influence QT and JT intervals.

1.3. Working hypotheses

The following working hypothesis was postulated to build a conceptual structure for evaluating the results from various analyses performed:

The spatial sequence of left ventricular excitation has a strong influence on the spatial/temporal sequence of left ventricular repolarization, so that local spatial excitation-repolarization relationship largely contributes to concordant/discordant type of repolarization in normal conduction and ventricular conduction defects, and the inter-regional temporal excitation-repolarization relationship mainly determines the QT interval. Thus, the inclusion of QRS duration as a

covariate will significantly improve the accuracy of QT and JT prediction.

CHAPTER 2
LITERATURE REVIEW

This literature review contains two main sections. The first section presents the determinants of the QT interval as background information. In the second section, the mechanism of the generation of the QT interval is considered, with special attention paid to the genesis of QRS in normal ventricular conduction and in bundle branch blocks, and the genesis of the T wave and repolarization changes in bundle branch blocks.

2.1 Determinants of the QT Interval

2.1.1. The relation of the QT interval to ventricular rate

The rate-dependent changes in the QT duration are basically due to the fact that the ventricular action potential duration (APD) is rate dependent [8] . The duration of the refractory period of cardiac tissue shortens at a fast heart rate and lengthens at a slow rate [9]; [10]. However, the QRS duration, one of the QT components, is independent of the heart rate.

Although APD dependence on a steady state stimulus interval has been reported to follow a single exponential relationship in frog ventricular muscle [8], this functional relationship is more complex in rabbit ventricular muscle, in dog and sheep Purkinje fibers [11], as commented by Elharrar and Surawicz [12]. These investigators

6

reported that even a sum of two exponentials fitted poorly with their experimental data on dog Purkinje fibers and papillary muscle preparations.

The steady state APD-basic cycle length relation, reaches a plateau at a slow rate. As noted previously, in the canine ventricular fibers [13] [14] the anticipated prolongation of APD failed to occur at extremely slow heart rates. Elharrar and Surawicz [12] confirmed this observation in their study of dog Purkinje and ventricular fibers. They documented the limited value of APD (APD_{max}) at infinitely long cycle length, being 531 ms for Purkinje fibers and 330 ms for ventricular fibers.

Mines [15] was the first to relate the duration of the refractory phase to the length of the QT interval of the ECG. The steady state QT interval can be anticipated to approach a lower limit when the heart becomes slow. It is evident that QT values gradually reach a finite limit after a rest, or long pause, or plateau, at slow stimulus rates [16].

Empirical experimental data on isolated canine ventricular muscle preparation [12] indicate that steady state action potential duration (APD), relates to the stimulus interval Z according to the formula: $(APD)=Z/(aZ + b)$, where Z is cycle length in ms. The basic cycle lengths in Elharrar & Surawicz's data [12] could be maintained from 300 to 5000 ms corresponding to heart rate (HR) ranging from 12 to 200/min. 1/a is given as the limit value of APD (APD_{max}) after a long pause [12].

QT prediction equations

The effects of HR (or its reciprocal value, the RR interval) have been studied by many authors in an effort to adjust the QT interval for steady state differences in HR. This is essential for defining the normal QT interval and for detection of QT prolongation.

In 1920, Fridericia [17] presented a formula in which the QT interval in the human ECG is proportional to the cubic root of the length of the cardiac cycle, whereas Bazett [18], in the same year, stated that it was related to the square root of the RR interval. Since that time a number of formulas have been proposed to improve the accuracy of the QT prediction. Adams [19], Schlamowitz [20], and Simonson et al.[21] promoted a linear regression of QT on the RR interval. Hodges et al.[22] suggested that a linear correction with heart rate provided a better fit than Bazett's formula. Arhras and Richards [23], and Boudoulas et al [24] introduced a formula for the linear QT regression on the heart rate which had been advocated by Kovacs [25]. Using the RR interval instead of HR as an independent variable, Sarma et al.[26] proposed an exponential three parameter formula which is similar to a slightly simpler two parameter expression derived by Carmeliet [8]. Puddu et al.[27] advocated the cubic root equation of Fridericia over Bazett's formula. In 1991 Dickhuth et al. [28] re-examined the relationship between the HR and QT interval during atrial stimulation in ten healthy males. After comparing the modified Bazett's equation, with Sarma and Kovacs' functional expression for a QT correction for heart rates, they proposed an exponential three parameter formula that is mathematically expressed as $QT = ae^{-b(HR-60)}$. They concluded that this formula is a more precise assessment of the QT interval for rate changes under physiological conditions. However the validity of their conclusion should be taken with caution, as their results are limited to findings under atrial stimulation by an external pacemaker, and to the small sample of subjects. Most

recently, Sagie et al.[29]reported on a new linear correction formula, for adjusting the QT interval for heart rate based on ECGs of 5,018 subjects from the Framingham Heart Study. Their formula is expressed as $QT_{LC} = QT + k(1-RR)$, where QT_{LC} is the linearly corrected QT interval in second and RR is cycle length in second, k is a constant of 1.54 for both men and women.

Critical flaws with the currently used QT prediction formulas have been reported. Simonson et al.[21] noted that while many formulas are satisfactory over heart rates in the mid range, discrepancies become apparent at high and low heart rate. Their observation is further supported by Rautaharju et al.[2], who evaluated a number of one-, two- and three- parameter formulas for the correction of the QT interval for heart rate throughout a wide range of heart rates in sinus rhythm. They also found that practically all QT rate correction formulas function fairly well within a limited range of heart rates, producing nearly equivalent results in a 55 to 85 beat/min. heart rate range, but often fail at low or high heart rates. Kovacs [25] criticized all commonly cited formulas as an arbitrarily selected algebraic function to a set of data with wide variations. None of the current statistical empirical formulas are based on physiological models or experimental electrophysiological data. Rautaharju et al.[2] noted that with many of the prediction formulas, QT increased to infinity at the low end of the HR range and approached zero at very high heart rates. From a physiological point of view, these formulas for the QT rate correction do not meet realistic functional behaviors. Therefore, the inadequate performance of power functions of RR, and linear functions of RR and heart rate, makes accurate detection of QT prolongation difficult.

Functional expressions for QT prediction, should preferably take a form which is suitable for characterizing the dependence of action potential duration on stimulus cycle length. One critical parameter in such equations is the asymptotic value of action potential duration after a long rest, or the hypothetical value of the QT when heart rate approaches zero. Comparing a set of 13 QT prediction formulas on a random

subsample of a 1,920 community-based population, Rautaharju et al.[30] established

an optimal heart rate correction factor for QT. They derived the asymptotic value of QT

(QT_0- represents QT after a long pause), by transferring the constant b of Elharrar and

Surawicz's equation [12] into a regression parameter for heart rate, with the expression

of the form:

$$APD = 1/(a + b'HR), \qquad (1)$$

where, for dog Purkinje fibers $a = 1.96 \times 10^{-3}$ and $b' = 1.82 \times 10^{-5}$.

It is noted that these values for a and b' are numerically nearly equal except for a

difference by a factor of 100.

The predicted value of QT (QT_p) for their expression is of the form:

$$QT_p = 1/(a+bHR). \qquad (2)$$

The values of coefficients a and b in the above formula in normal

conduction, were closely equal, except differing by a factor of 100. With coefficient

b=a/100, it was possible to further simplify the formula for QT_p. Thus the predicted

heart-rate corrected QT is expressed as:

$$QT_p = QT_{max}/(1+0.01HR), \qquad (3)$$

where $QT_{max} = 1/a = 656$ ms

Rautaharju et al. [30] noted that with their functional expression, the predicted QT is one half of QT_{max} at heart rate 100. This simplest formula for predicted QT(QT_p) meets reasonable physiological constraints regarding QT_{max}(maximum predicted QT after a long pause), and also functional behaviors of QT rate sensitivity. QT rate sensitivity is the slope of various functions used to predict QT for various values of the heart rate. As used in this context, dQT/dHR is an expression for the predicted change in QT per unit increase in heart rate, from a given steady state level. Drastically diverging functional behavior has been documented for different QT prediction formulas regarding the QT rate sensitivity, which ranged from inverse power functions to exponential functions, and inverse square functions, of the heart rate. An unrealistic functional behavior is reflected in the QT rate sensitivity functions which approach minus infinity at low heart rates [30]. Rautaharju's formula suggests that the QT rate sensitivity is inversely proportional to the square of HR and that individual values of QT_{max} can be predicted from ambulatory or exercise ECGs, using the formula $QT_{max} = 2 \times QT_{100}$, where QT_{100} is QT at HR = 100/min..

This universal formula of Rautaharju et al. for the rate correction of QT also includes a modification for incorporation of QRS duration and age correction for males. In addition, these authors provide normal standards for the accurate detection of QT prolongation. However, this optimal heart rate correction factor for the QT was derived for normally conducted ventricular complexes. Similar universal formulas for QT prediction in the presence of various categories of ventricular conduction defects, do not exist.

Dynamic behavior of QT interval

It is known that the duration of the cardiac action potential, does not adjust immediately to a new steady state cycle length, and that a full adjustment may require

several hundred beats [31, 32]. In a dynamic situation, cardiac action potential duration is a fairly complex function of the timing sequence of preceding excitation cycles [12]. In a steady state situation, the time interval from the onset of the previous action potential appears to be a stronger determinant of the subsequent action potential duration than, for instance, the interval from the end of the preceding action potential [16]. This is perhaps the primary rationale for choosing the RR or heart rate, rather than the TQ interval in the models used to predict normal QT.

2.1.2. Influence of the autonomic nervous system on QT interval

The in-vitro experimental results of the relation between APD and heart rate, are not necessarily comparable to the effect of HR on the QT interval of the electrocardiogram, since the in situ heart rate changes may be caused by a variety of factors which influence APD in other ways.

The QT response to rate change induced by pacing alone, have been reported to be different from the QT change with heart rate induced by neural and humoral factors in situation like exercise. Rickards and Norman [33], Milne [34] and Sarma et al.[26] have shown that changes in HR produced by pacing cause less shortening of the QT than comparable changes induced by an increased level of circulating catecholamine in exercised subjects. It has been suggested, that this sympathetic action may be even more important than the heart rate alone in determining changes of the QT duration.

Ventricular repolarization is believed to be predominantly under beta adrenergic control as beta-adrenergic stimulation shortens APD and the absolute refractory period [35]. Normally, sympathetic stimulation shortens the QT interval; however, Boudoulas et al.[36] reported that adrenergic stimulation produces a relative

prolongation of the QT interval in relation to QR2 -- total electromechanical systole obtained from the systolic time interval -- whereas QT-QR2 remains normal when the heart rate is increased with atrial pacing. They concluded that adrenergic stimulation causes a shortening of the QR2, but does not always produce a shortening of the action potential and the duration of the QT interval. A study of the autonomic influence on rate dependent changes of the QT interval indicates that a vagal tone increases intrinsic dependence of the QT interval on cycle length variation, but a sympathetic tone does not seem to interfere significantly [37].

The QTc shortening is generally considered as a potential protective mechanism of the action of the beta blockade. A number of studies have reported shortening of the QTc with the beta blockade administration [38]; [34, 39] . On the other hand, several studies demonstrate that, at a constant heart rate, intravenous administration of propranolol or chronic beta adrenergic blockade causes either no significant change in QTc or a slight QTc prolongation [40, 41]. Lecocq et al.[42] showed that with proper rate correction, the QT remained unchanged with a beta blocking agent. These authors used a single exponential formula of the form QT = A+Bexp(-kRR) proposed by Sarma et al.[26] for the rate correction of QT.

The lengthening of the QT interval has been found with both bilateral sympathetic ablation and asymmetric sympathetic stimulation [43-45]. However, the role of autonomic system imbalance, unilateral stellate stimulation or blockade, or complete denervation in modulating a QT interval [46], remains an unresolved issue regarding the management of the long QT syndrome. Finley and Armour [47] in their brief communication, express their support of Till's conclusion that "the sympathetic imbalance theory of the long QT must be questioned".

Recently the effect of sympathetic stimulation on the QT interval has been re-examined. Savard et al.[48] provided new evidence that substantial regional (local) variations can take place in the repolarization pattern at the epicardial surface in dogs

with neural stimulation. Local QT durations were either shortened or did not change. These changes are not reflected in changes in global body surface QT measurement.

2.1.3. Sex differences in QT interval age-trends

Age has been recognized as the most important single physiological factor with a dominating influence on the variation of ECG patterns throughout the life span [49]. Sex differences in the QT duration have also been shown to exist ever since the original report of Bazett in 1920. Age differences in the QT interval were pointed out by Ashman in 1943 [50], and Simonson's QT prediction formula contains a term for age trend correction [21]. The QT intervals of normal women corrected for heart rate by Bazett's formula are known to be longer than those of normal men [49]. Consistent with this finding, Kujath [51] reported significant differences in the QT intervals of females, with women's QT intervals longer than those in men. Similarly, Rautaharju [52] observed that the rate-corrected QT values in females in their reproductive years are indeed significantly longer than those in men. However, these sex differences appeared to be due to a significant decrease by about 20 ms in the rate-corrected QT after puberty in males, followed a gradual, closely linear, increase until about age 55. In contrast, the mean values of the QTc remained quite stable in females throughout the growth, maturation and reproductive years. The mechanism of the QT shortening in males following puberty remains unknown.

One of the objectives of the present study was to examine to what extent the effect of QRS on JT and QT interval is changing with normal aging.

2.1.4. Long QT syndrome and other conditions with prolonged QT: congenital and acquired long QT syndromes

A prolonged QT may be the result of slowed depolarization or prolonged repolarization. In other words, the increased duration of one or more of its components namely QRS, the ST segment, or T wave, could prolong the QT interval. The normal upper limit for the QT interval when corrected for HR with the Bazett formula, is usually given as 0.44 sec. Moss et al.[53] used QTc > 0.44 sec. as a criterion for diagnosing the so called long QT syndrome. The long QT syndrome refers to an association of prolongation of the QT interval with recurrent attacks of syncope, and with sudden death [53].

Etiology of the long QT syndromes can be broadly categorized into congenital and acquired types. Both are associated with an increased likelihood of serious ventricular arrhythmia [54]. This association is particularly evident in patients with a congenital long QT syndrome. The autosomal recessive Jervell-Lange-Nelson syndrome is the clinical entity of a prolonged QT interval, congenital deafness, syncope, and sudden death. The pathogenesis of a congenital long QT syndrome is not well understood. Schwartz and associates [55] postulated that imbalance in the cardiac sympathetic innervation of the heart with a dominant left-sided sympathetic influence is the plausible mechanism.

The most common type of acquired long QT syndrome is secondary to the use of antiarrhythmia agents and drugs. For example, drugs such as quinidine, calcium antagonist bepridil, sotalol (in high doses), and some antibiotics (erythromycin), can induce QT prolongation, leading to torsades de pointes, particularly in hypokalemic patients. This tachycardia is characterized by progressive changes in the amplitude and polarity of the QRS complex, such that the QRS complex appears to be twisting around

the isoelectric baseline. On the other hand, profound QT prolongation with amiodarone serotonin/antagonist ketanserin [56] and sotalol (except in high doses) is rarely associated with torsades de pointes or other forms of tachyarrythmias. This holds true also for conditions such as QT prolongation with hypocalcemia and hypothyroidism.

The prognostic value of a QT interval prolongation in post MI patients has been recognized since 1976. Schwartz and Wolf [57] have observed that patients with a prolonged QT interval following a MI are at a considerably higher risk of sudden death. In 1984 Ahnve [5] confirmed the prognostic implication of QTc prolongation in post infarction patients. The studies in 1991 by Algra et al. [58] and Schouten [59] and associates, extended the knowledge about the prognostic importance of QTc for mortality. The occurrence of malignant ventricular arrhythmia in patients with acute MI is likely in those with a prolonged QT as opposed to normal QTc intervals. Schwartz [60] suggested that the mechanisms of the QTc prolongation in high risk patients with acute and subacute coronary diseases, may be linked to heterogeneity of repolarization, alteration in calcium flux, and imbalance in sympathetic activity. In contrast, results of other studies [61, 62] indicated that QTc has little predictive value in determining survival rate, and long term prognosis on subsequent cardiac events.

Other known causes of acquired QT prolongation include electrolyte abnormalities e.g. hypokalemia and hypocalcemia, cerebral diseases, modified liquid-protein diet and infection [53]. It is evident that QT prolongation is not a single uniform pathophysiological entity.

2.2. Mechanisms responsible for generation of the QT interval

2.2.1. Genesis of QRS in normal conduction

Anatomy of ventricles

The anatomy of the ventricles greatly influences the three-dimensional forces created by ventricular excitation, and the arrangement of myocytes into fibers also has an important effect on the electrical behavior of cardiac muscle. The experimental evidence shows that the conductivities along the fibers (axial) are larger than those in the transverse (radial) direction [63]. This greatly affects the current flows in the fibers. Corbin and Scher [64] demonstrated in the epicardium of canine hearts, that a current flows from the activation wavefront to the resting tissue, only when the wavefront propagates along the longitudinal direction of fibers; whereas the flow of current is from the resting tissue towards the wavefront when excitation is traveling transversely to the fibers.

Myocardial tissues consist of individual cells of roughly cylindrical shape around 100 μ long and 15 μ in diameter. They are interconnected by a low resistance junction called an intercalated disc, which causes the flow of current between and among the cells. Although the fibers branch and interdigitate, at each point within the myocardium, there is a discernible fiber orientation.

Anatomically the right ventricle is located more anteriorly than rightward, and conversely, the left ventricle is more posteriorly than leftward [65]. The ventricular septum is anatomically mainly a portion of the left ventricle. The anterior paraseptal wall of the left ventricle is oriented anteriorly, leftward and superiorly; the posterior paraseptal area directed posteriorly, rightward and inferiorly. The apex is a small

portion of the left ventricular muscular area. Both ventricles are much thinner at the apex than at the base. The right ventricular wall is roughly one-third as thick as the free wall of the left ventricle.

Ventricular depolarization in normal conduction

Depolarization consists of excitation waves moving through myocardial tissues by means of active propagation. During the spread of excitation, all myocardial fibers undergo rapid depolarization and a slow repolarization of the cell membrane, which begins immediately following the depolarization of each cardiac cell. It consists of a slow phase 2 (plateau) and a rapid phase 3 of the action potential. Hoffman and Suckling [66] were the first to show the temporal relationship between the depolarization phase of the action potential and the QRS deflection, and between the repolarization phase and the T wave. The time course and sequence of the excitatory process of the normal heart would be of value for the understanding of the QRS complex.

The activation process in the ventricle is closely related to a specialized conduction system. Starting at the AV node, the electrical pathway into the ventricles is the bundle of His, which divides promptly into left and right branches. The anatomy of the left bundle branch is less predictable than that of the right bundle branch. In the embryonic heart, the left bundle branch has been recognized as a fanlike structure while the right bundle branch is cordlike. In most cases, the left bundle branch has two main subdivisions- anterosuperior and posteroinferior. Rosenbaum [67] described the left bundle branch as a bifascicular system and explained many bundle branch block patterns on the basis of this system. Occasionally, a third septal subdivision of the left bundle may also be identified. This trifascicular concept was first introduced by Tawara [68] who depicted three fascicles in the left ventricle, and was later supported by

Demoulin and Kulbertus [69] However, in other cases, the branching pattern of the left bundle is not clearly defined. Although the anatomic basis of the trifascicular concept is still occasionally questioned, this concept does provide a meaningful correlation with electrocardiographic findings, as the destinations of the three divisions of the left bundle branch correspond to the earliest areas of endocardial activation reported by Durrer et al.[70]. The right bundle branch does not subdivide until the base of the right anterior papillary muscle is reached on the endocardial surface of the right ventricle near the interventricular septum; it divides and fans out into the right ventricular wall.

The specialized conduction system normally functions as one continuous medium [71] for the propagation of activation. Thus, the anatomical distribution of the conduction system determines the overall time sequence of ventricular activation.

The pathway of the excitation spread in the ventricular myocardium has been the subject of numerous investigations. Sites of very early activation of 0 to 5 ms are noted in three endocardial areas after the start of the left ventricular activity potential [70]. These areas become confluent in 15 to 20 ms. They are located: 1) high on the anterior paraseptal wall just below the attachment of the mitral valve; 2) central on the left surface of the interventricular septum and 3) about one third of the distance from apex to base in the posterior paraseptal area.

Excitation of the myocardium of the human and of the canine heart occurs mainly in an endocardial to epicardial direction [70]; [72].. Septal excitation sequence appears more complex. In the study by Scher and co-workers [73], the septum was found to be predominantly excited from the left. The net effect of septal activation seems to be determined by the mid septal region and is perpendicular to the septal wall anteriorly, superiorly and slightly to the right. Thus the orientation of the interventricular septum can be described by a vector from the left to the right endocardial surface oriented anteriorly, superiorly, and slightly to the right.

Soon after the beginning of the septal and paraseptal activation, the impulse rapidly proceeds towards the apex and the endocardial surface of the left ventricle through the Purkinje network. The activation of the left ventricle is the result of the transmission of the electrical impulse through two main branches of the left ventricle. Because of the absence of Purkinje fibers in much of the endocardium of the right ventricle, activation of the right ventricle is much slower than that of the left ventricle. Earliest activity took place just above the anterior papillary muscle on the right about 5 to 10 ms after the onset of left ventricular activation [70]. Most of the endocardium of the ventricular free walls is excited within the first 30 ms of activation [74]. Further depolarization occurs from endocardial to epicardial surfaces in both right and left ventricles. Durrer et al. [70] reported that it took 20 to 40 ms for excitation to travel from the endocardium to the epicardium in the apex of the human heart. The most recent experimental evidence shows that right ventricular epicardial breakthrough occurs approximately 25 ms after the onset of left ventricular depolarization, that is about 10 ms before activation reaches the left ventricular epicardial surface [75]. In humans epicardial breakthrough occurs 7 - 25 ms after the onset of the QRS complex [76]. The "mosaic-like" pattern of the breakthrough on the anterior and posterior ventricular surfaces has been demonstrated [77]. This pattern may result from the irregular geometry of the ventricular wall. It has been reported that the overall pattern of epicardial activation is in an apex to base direction [78].

The last regions of the ventricles to be excited are the posterobasal paraseptal region, or a more lateral location of the left ventricle [70]. Depolarization of the pulmonary conus of the right ventricle also occurs at this time. The impulses arrive late in these regions because of their poor supply of the specialized conduction system. In the basal septum the wave proceeds toward the base and is from the left to the right.

There is a paucity of information on the excitation time in various regions of the human heart. Selvester and his associates [79] simulated the duration of

depolarization of 20 segments of the human heart based on Scher's work in the sequence of ventricular myocardial depolarization in the dog heart. They provided an approximation of the direction assigned to the vector representing each segment. According to Selvester's model, the approximated excitation time for the left ventricle is 45 ms.

Spatial vectors

The sequence of normal ventricular activation has been approximated by a vectorial approach [80]. Vector 1, the initial phase, represents the activation of the middle segment of the interventricular septum. Vector 2 represents the second phase, which is the mean vector of the activation of the free ventricular walls. Vector 3 represents the terminal phase, produced by the thick posterolateral and basal wall of the left ventricle and the septum. Deflections recorded in any lead simply reflect the degree to which the cardiac vectors are projected on the axis (lead vector) of that lead.

The sequence of cardiac excitation has been applied to the explanation of the QRS. In general, the dispersion of excitation times in the ventricles (QRS duration) with normal conduction is about 80-90 ms. The QRS could be anticipated to influence QT duration if action potential durations were equal in the ventricles or if regional dispersion of action potential durations were less than that of the dispersion of excitation time, resulting in a totally or partially concordant sequence of repolarization. Present evidence indicates that the geographic gradients of APD do exist.

2.2.2. Genesis of QRS in bundle branch blocks

Ventricular depolarization in the left bundle branch block

Reported studies reveal conflicting results as to the mechanism of QRS prolongation in left and right bundle branch blocks. Rodriquez and Sodi-Pallares [81] maintained that an abnormal intraseptal barrier causes considerable delay in the advancement of the impulse across the septum. In contrast, other investigators demonstrated that the excitatory wave front advances throughout the septum at a uniform speed. However, the alteration of the septal activation in complete bundle branch blocks is responsible for most of prolongation of the QRS duration [82].

There are different opinions on the sequence of activation of the free wall of the left ventricle in LBBB. Some believe that the free wall of the left ventricle is activated in a normal fashion, in spite of the delayed excitation [83, 84]. Others have found that there is also alteration in the pattern of activation in the free wall, namely that the excitation spreads from epicardium to endocardium [82, 85]. Pruitt et al.[86] suggested that the mechanism of slow transeptal conduction in LBBB was due to the perpendicular direction of the septal wavefront, relative to the orientation of the myocardial fibers in the long axis of the septum. Our current understanding of ventricular sequence in human LBBB is derived from epicardial mapping [76] and endocardial catheter mapping [87]. Wyndham et al.[76] examined epicardial activation sequence in patients with LBBB. They found that septal crossing by the leftward-moving wave front was initiated in the right ventricle. The timing of completion of the anteroseptal region and the inferoseptal region was about 56 ms and 102 ms respectively. The left ventricle was activated by anterior and inferior wavefronts traversing the septal region slowly. The timing of the latest RV activation and the latest

LV epicardial activity ranged from 50-110 ms and from 113-140 ms after the onset of QRS respectively.

Vassallo et al.[87] have shown through endocardial catheter mapping, that the initial site of the right ventricular activation was on the right ventricular septum. Right ventricular activation then followed. Total right ventricular endocardial activation time was 36 ms which corresponded to $21\pm 7\%$ of the surface QRS complex. Left ventricular septal breakthrough occurs at 52 ± 17 ms after the onset of the surface QRS complex. The mean total duration of left ventricular activation was 91 ± 36 ms. The last left ventricular area to be activated was found to be at the basal part of the anterolateral wall, and was at 142 ± 36 ms from the onset of surface QRS complex. These investigators suggested that right ventricular endocardial activation began before the initiation of left ventricular activation in all 18 patients with LBBB, and that longer duration of left ventricular endocardial activation correlated with an increasing QRS duration.

Van Dam [75] reported that right ventricular epicardial breakthrough in LBBB occurred approximately 20 ms after the onset of ventricular activation. The excitation enters the left ventricular myocardium through the interventricular septum at approximately 40 ms after the onset of right ventricular septum.

By correlating the sequence of activation with the spatial vector, the ventricular activation in LBBB could be arbitrarily simplified into three vectors. Due to the block in the left bundle, activation starts first in the right septum and the free wall of the right ventricle. The initial vector of ventricular activation is directed anteriorly to the left and inferiorly, in agreement with the way the activations are spread. As the right to left septal activation continues and proceeds slowly over the left septal mass and its adjacent myocardium of the free wall of the left ventricle, the vector 2 is directed to the left, inferiorly and posteriorly. The late activation of the left ventricular mass generates electrical forces (vector 3) which direct toward the left, posteriorly and inferiorly [88].

Incomplete left bundle branch block

Sodi-Pallares and associates[89], on the basis of experimental animals, have described various degrees of incomplete left bundle branch block. Their data indicated that as the degree of block increases, reversal of the direction of septal activation occurs. Schamroth and Bradlow's report [90] provided for the first time convincing evidence of the existence of incomplete LBBB in man.

In an incomplete left bundle branch block, the impulse conduction through the left bundle branch occurs at a slower rate [91]. Consequently the right septal surface supplied by the right bundle branch system is activated first. The activation process spreads transeptally from right to left and activates the left septal mass. This explains the abnormal initial QRS forces in the incomplete left bundle branch block. Depolarization of the remaining left ventricular free wall proceeds in a normal fashion [88]. Sodi-Pallares and co-workers [91] suggested that the morphology, rather than the duration of the QRS complex, provides the most valuable means in assessing the functional capacity of incomplete LBBB.

Ventricular depolarization in the right bundle branch block

The site of block in RBBB may vary [92-94]. Overall, the block in the right bundle causes a delay of activation in the right ventricle. Right ventricular excitation is dependent on myocardial conduction, and on the continuation of left ventricular excitation in the anterior and posterior walls and through the interventricular septum [95]. Moore et al.[96] studied epicardial activation in chronic, complete RBBB in the canine heart, and noted that 45 ms were required for right ventricular epicardial

activation after the sectioning of the septal right bundle, whereas activation in the normal conduction system was complete within 25 ms. However, the left ventricle is activated normally and septal activation occurs in the normal left to right direction. Thus the initial part of the QRS complex remains unchanged. However, because of the absence of double septal envelopment due to the block, septal depolarization was prolonged over 40 ms [97]. The delayed, abnormal, activation of the right ventricular free wall causes changes in the late QRS complex. Although no real right ventricular epicardial breakthrough has been identified, the first epicardial areas excited are noted in anterior and posterior paraseptal parts. The last areas activated are the top of the pulmonary conus or the anterior basal ventricular wall [75].

Like a normal activation process, the left septum is activated initially in the complete right bundle branch block. The direction of the spread of excitation is from left to right, the vector 1 being directed to the right, anteriorly and superiorly. As the activation involves the rest of left septum and the free wall of the left ventricle, the vector 2 is directed leftward, inferiorly, and either anteriorly or posteriorly. The abnormal left-to-right activation of the right septum, and the free wall of the right ventricle, can be expressed as vector 3, which is directed to the right, anteriorly and either superiorly or inferiorly [88].

Incomplete right bundle branch block

In the canine heart with incomplete RBBB, Moore and co-workers [92] observed that the earliest site of epicardial activity was located in the mid right ventricle near the interventricular sulcus, and that there was a slight discrepancy of about 10 ms in the time of depolarization of the right ventricular outflow tract. A normal QRS complex was inscribed in lead II. These investigators concluded that incomplete right

bundle branch block can occur as a result of a block in the peripheral right Purkinje system.

In incomplete right bundle branch block, the left ventricular septum, and the free wall, activate first. Then the right septum and right ventricular free wall are activated by the right and left bundle branches. Similar to complete RBBB, only the late part of the depolarization is deviated to the anterior and rightward direction [88]. There is sufficient evidence indicating that in bundle branch blocks the activation of the ventricles is altered. However, the effect of this altered activation on repolarization and the electrocardiographic QT interval has not yet been established.

2.2.3. Genesis of the T wave in normal conduction

The T wave represents the uncancelled potential difference of ventricular repolarization. Surawicz [98] states that because of the cancellation of electromotive forces, the T wave area is estimated to exhibit only 1-8 % of the total time x voltage product of the cardiac excitation/repolarization cycle.

In spite of recent advances in cellular cardiac electrophysiology, the elucidation of the sequence of ventricular repolarization on the T wave still poses a challenging problem. The following literature review describes what is known of the recovery process as it affects the genesis of the T wave.

Repolarization in historical perspective

The invention of the string galvanometer by Einthoven [99] provided a means for recording ECG with enhanced accuracy. However, a fundamental understanding of the nature and genesis of ECG was not achieved, until the

introduction of the microelectrode for recording the potential difference which exists across the membranes of single cells.

The study of the T wave started about 120 years ago. Burden-Sanderson and Page in 1880 and 1883 [100, 101] recorded potential changes on the surface of the frog heart. They were the first to recognize the duration of electrical activity in the ventricular myocardium. They observed that the initial positive wave was followed by the negative wave, with the base of the ventricle becoming negative first. Based on this result, they concluded that the diphasic potential changes were consistent with the wave of excitation traveling from the base to the apex. Their modeling of the potential difference created the picture of the modern QRS, and the T wave. However in mammals, the second wave is usually not negative but positive. Waller in 1887 [102], was the first scientist who noticed the positive T wave that was recorded in the human ECG from the body surface. Bayliss and Starling in 1892 [103], offered an explanation for the concordance of the QRS and T deflections of a dog's electrogram. They postulated that the durations of the actic. potentials at the base of the ventricle are longer than those at the apex.

Around the same time period, other theories of the T wave emerged. Hoffman [104], Samojloff [105] and others speculated that the R wave is an expression of electrical excitation, whereas the T wave is a manifestation of a different process. Samojloff [105] tested the effect of an excitation sequence on T wave by producing an extrasystole on the apex of the frog's heart. He found that the T wave was still the same as that in response to a normal auricular beat. Samojloff suggested that the T wave was essentially independent of excitation.

In the early 1930's, Wilson et al. [106] introduced a more realistic model of the heart as a source of electrical potential. They explained the underlying mechanism of the genesis of the T wave as a result of the rate of the repolarization process in different parts of the ventricle, and felt that it occurred independently of the time of the

depolarization process. The work of these earlier scientists laid an important foundation for subsequent work on the nature of T wave.

Reverse Sequence of Repolarization

The theoretical explanation for the apparent paradox of the T wave concordant in the mammalian ECG is that the depolarization and repolarization waves in the major portion of the ventricles travel in opposite directions. For such inverse relation to occur, a gradient in APD among myocardial regions would be present, and the differences of APD must be greater than the differences of excitation time. Currently there are two major regional differences in APD which are advanced to explain the concordant T wave: a transmural gradient between endocardium and epicardium, and gradients between the base and the apex or both. In addition, regional differences in APD between left and right ventricles and between anterior and posterior walls have been explored. Excitation time also plays an important role in th's inverse sequence.

a) Regional inhomogeneity of action potential durations

The difference in duration of the action potentials in the epicardium and endocardium, is an important factor in determining the polarity of the T wave in the normal ECG. Early studies [107-109] have provided adequate evidence that the refractory periods in the endocardial layers were 10 to 25 ms longer than those in the middle and subepicardial layers. However, methods used by these earlier investigators only provide information about one moment during the relatively long time course of ventricular repolarization. Inoue et al.'s mathematical model [110] of the electrical activity of the heart suggested that the positive T wave was obtained when the

transmural gradient was more than 30 msec/cm. The difference of repolarization time between endocardium and epicardium was about 20-30 msec, with the longer repolarization time in the endocardium.

Higuchi et al.[111] studied in dogs the relation between the difference in duration of the action potentials in the epicardium and endocardium (transmural gradient), and the polarity of the T wave, from electrogram recordings. They found that the required activation time (AT) from endocardium to epicardium for the polarity of the T wave, was 6 to 13 msec. A negative epicardial T wave was obtained when APDendo was 14 ms longer than APDepi, and a positive T wave when APDendo was 48 ms longer than APDepi. These authors suggested that a larger difference in duration of APs between epicardium and endocardium was necessary for a normal upright T wave in the ECG. A similar transmural gradient is also found in man, as measured from monophasic action potentials [112]. The epicardial repolarization time (the sum of activation time and action potential duration) measured $80.7 \pm 3.9\%$ of the QT interval, whereas endocardial values were $87.1 \pm 4.4\%$ of the QT interval. Thus, earlier repolarization occurs at the epicardium and is in a direction opposite to that of depolarization. This is compatible with the T wave concordance in the surface of ECG.

This transmural difference is the basis of the "theoretic model" of the T wave proposed by Harumi et al.[113]. In their model, the reversed spatial orientation of recovery and activation wavefronts, explains the concordant nature of epicardial QRS and T wave polarities.

Different regions of the heart have different action potential durations [114, 115]. Unfortunately, gradients between the base and apex of the ventricle are not well established. The apex to base repolarization concept was strongly advocated by Noble and Cohen [116] in their review paper in 1978. Experimental evidence [107, 117] postulated that APD is about 10-30 ms longer in base than in apex. In contrast, the refractory period measurements by Burgess et al.[108] and the monophasic action

potential duration measurements by Abildskov et al. [109] and by Toyoshima [118], suggested a base to apex repolarization sequence with action potential about 5 to 20 msec longer at the apex than at the base. The fact that the T vector in the majority of normal cases is directed towards left-inferior, left anterior or left [119], provides additional support for the concept of apex to base as the general direction of the normal repolarization process. This implies that the base rather than apical region determines the length of QT.

Gradients between the anterior and posterior walls and those between left and right ventricles, have also been reported. By studying with a suction electrode, Autenrieth and co-workers [120] reported that the MAP at the anterior base ends 17 ms, whereas that of the posterior base ends 33 ms, before the end of the T wave respectively. Thus the dispersion of repolarization was 16 ms. This observation is confirmed with a positive T wave in inferior ECG leads.

The gradients between left and right ventricles are not as clearly presented as those observed between the posterior and anterior walls. Burgess et al. [108] noted that there was no systematic relationship between FRPs in the free wall of the right ventricle compared to those in the free wall of the left ventricle. However, they documented a left to right gradient of APD in the septum, with the left septum about 1-11 ms longer. On the other hand, Solberg et al. [121], found that the left and right papillary muscles of the dog had the same APDs, whereas Watanabe [122] observed that APDs in the endocardium and papillary muscle in the left ventricle of the rat heart was almost twice as long as those in the corresponding parts in the right ventricle. Different species studied by these investigators may account for the inconsistent findings.

Although the relative contributions of transmural and other gradients to the T wave remains speculative, the current evidence tends to suggest that a transmural gradient is the probable cause of positive T waves in the left lateral ECG leads during sinus rhythm. Van Dam and Durrer [107] considered that regional differences, such as

those between base and apex, are more important than transmural differences. Therefore, no valid prediction of the temporal and spatial sequence of repolarization of the whole hea^{rt}, could be made on the basis of the measurement of gradients between the endocardial and epicardial surface.

b) The effect of excitation time on the repolarization process

The ventricular gradient of an electrocardiographic lead is defined as a time integral of the ECG over a complete cardiac cycle [123]. It is a measure of recovery properties of the cardiac tissues. The old dogma of the ventricular gradient, showed that the ventricular gradient is independent of the activation sequence [124]. Adequate experimental evidence indicates that this concept is no longer tenable. Franz et al. [112] stated that the T wave is a reflection of regional difference in repolarization time, which is the sum of activation time and action potentials (APD). A ventricular repolarization gradient deducted only from regional differences in APD may be invalid, as they ignore the variations of activation time in different sites of the heart. In their experiment, an inverse correlation between activation time (AT) and action potential duration, at both the endocardial and epicardial surface was observed. These researchers noted that the averaged dispersion of APD is significantly more than the dispersion of AT $(41 \pm 14$ ms vs 24 ± 61 ms respectively).

Measurements of the functional refractory periods of the ventricular muscle, the indirect study of the repolarization process [109, 125] lend further support to the evidence that sequence of excitation affects local recovery properties. Kuo et al. [126] found the dispersion of the termination of simultaneously recorded monophasic action potentials in dogs to be substantially determined by differences in regional activation time as well as APDs.

By recording MAPs intraoperatively, Cowan et al. [127] have found in man a relationship between epicardial repolarization time gradients, and the configuration of the T wave. In ten patients with an upright T wave, they observed an inverse relationship between the APD and the activation time (AT). The areas of latest activation (the posterobasal regions) repolarized first, whereas the anterior and posterior septum, which were excited earliest, were the last to repolarize. However, no such relation was observed in four patients with an inverse T wave. In patients with an upright T wave, the dispersion of repolarization time was less than that of AT (14 & 23 msec respectively). In contrast, the dispersion of repolarization time was greater than that of AT (31 & 26 msec respectively) in patients with inverse T waves.

Measurement of the dispersion of repolarization times

It is generally accepted that the time differences of phase 3 of ventricular action potentials are responsible for the normal T wave [98]. However, the true meanings and the measure of dispersion of repolarization times are still uncertain.

Repolarization times can be accurately determined from monophasic action potentials [128, 129]. Surawicz [98] determined the dispersion of repolarization times by using the suction electrode to record monophasic action potentials (MAPs) in dogs. They obtained the mean maximum dispersion of the MAP duration as 22 ± 9 ms, which was in good agreement with the averaged MAP dispersion of 25 ms, observed on the surface of the isolated cat heart [130]. According to these researchers, the maximum of the local gradients of APs during repolarization coincides with the peak of the T wave, and takes place when the earlier terminating AP has the steepest slope of repolarization. It was then assumed that the duration between the peak of the T wave (aT) and the end of the T wave (eT) reflected the dispersion of repolarization in the entire heart. These

authors concluded that the dispersion of APD on the entire ventricular surface, exceeds the transmural differences of refractory periods.

Franz et al. [112] reported that the longest endocardial repolarization time, was nearly as long as the simultaneously recorded QT interval. Their observations dispute those made by Watanabe et al. [131], who pointed out that endocardial and epicardial action potentials in the guinea pig ventricle were too short to account for the entire T wave duration.

Mirvis [132] estimated the dispersion of repolarization times from timing differences of the end-point of the T wave, from the body surface potential map data in 30 patients with acute myocardial infarction, and in 50 normal subjects. He found that in each case, the variation of timing of the end of the T wave was significantly greater than that of the onset of QRS complex. Consequently he concluded that the variation in the T wave termination, rather than QRS onset, is the major determinant of the QT interval range. However, considerable uncertainty about the end of the T wave, due to the overlapping of T and U waves and errors in using individual leads instead of global estimation from several leads at a time, make Mirvis's estimated dispersion of repolarization time questionable. The above evidence indicates that the meaning of repolarization duration, repolarization time, and the dispersion of repolarization times, varies in different contexts.

2.2.4. Ventricular repolarization changes in bundle branch blocks

The QRS complex and the T wave correspond to the depolarization and repolarization of the ventricle. Several studies have attempted to analyze either quantitatively or qualitatively the excitation and repolarization relationship from body surface ECG and body surface potential distribution [133, 134].

The relationship of the QRS and T wave in clinical application is ventricular gradient. It has clearly been demonstrated in a homogeneous strip of cardiac muscle that repolarization generally begins at the same point where depolarization begins [124], and spreads at a uniform velocity. The areas under R and T waves must be opposite in polarity as well as equal in magnitude. The ventricular gradient would be zero. However, in the human heart, there are local variations in the durations of the excitation state, $\hat{A}_R$ does not equal $\hat{A}_T$. Thus, the sum of these areas on the frontal plane is not equal to zero [135].

The relationship of the T wave direction with that of QRS deflection can be expressed by an equation [136]:

$$|\overrightarrow{AQRS}| + \overrightarrow{AT} = \overrightarrow{G}$$
$$\text{thus} \quad \overrightarrow{AT} = \overrightarrow{G} - |\overrightarrow{AQRS}|$$

It becomes evident from this equation that the direction of the mean electrical axis of T can be altered either by a change in the VG vector, or by a change in the direction or magnitude of QRS area vectors.

In a primary T wave change, repolarization is altered independently of depolarization and results from a change in the direction or magnitude of the mean VG vector. This abnormal change of G is usually indicative of some myocardial abnormalities. In a secondary T wave change, an alteration in repolarization is due to some alteration in the time sequence of the onset of depolarization throughout the heart muscle and is evidenced by a change in the mean electrical axis of QRS but with a constant VG. A secondary T wave change is not in itself indicative of myocardial repolarization abnormalities.

The existence of a secondary T wave change has been demonstrated clinically by the effect of Isoproterenol on the T wave. After administration of Isoproterenol to 106 patients with abnormal negative T waves, Daoud et al. [137]

found that the T waves remained abnormal in patients with averaged QRS duration of 106 ms, and in patients with myocardial infarction or pericarditis. The T wave abnormality was reversed in 96% of patients with averaged QRS duration of 85 ms. Isoproterenol shortened the QT interval in all patients, but did not change the QRS complex. These researchers concluded that conduction delay by 21 ms is responsible for the secondary T wave inversion in the left precordial leads.

It has been demonstrated by the studies in epicardial electrocardiogram that the polarity of the T wave is correlated with the sequence of recovery across the ventricular wall [138]. The T wave was negative when the epicardium recovered later than endocardium, whereas the positive T wave occurred when recovery was delayed in the deeper layers.

In normal adults, the T wave is always upright in the precordial leads (V3 - V6), in lead I and in lead II. Positive, negative, or diphasic T wave may be found in lead III and aVF. It has been reported that the onset of LBBB gives rise instantaneously to T wave changes with ST and T vectors directed opposite to the main QRS vector [88]. In the surface leads, the left precordial leads (V5, V6, I and aVL) have a depressed ST segment and inverted T wave in the opposite direction to the widened R wave. Reciprocal changes (ST segment elevation and positive T wave) may be seen in the leads over the right precordium (leads III and aVF).

In RBBB, the abnormal changes in the course of repolarization as the result of an abnormal activation sequence give rise to a depressed ST segment and an inverted T wave in V1 and V2, and an upright T wave in lead V5 and V6. The T vector is in an opposite direction to that of the terminal QRS forces.

All categories of conduction defects and fascicular blocks will have a certain degree of secondary repolarization abnormalities due to the changed sequence of excitation and QRS morphology. Conduction defects would be theoretically stratified into two subgroups: a) those likely to have primary repolarization abnormalities, and b)

those not likely to have primary repolarization abnormalities. However, very often, the ST-T findings are generally ignored if conduction defects are present. Thus far, there are no previous reports on attempts to separate primary and secondary repolarization abnormalities, or to identify QT prolongation in the presence of ventricular conduction defects.

CHAPTER 3
METHODS

3.1. Introduction

The source data for the three projects were derived from the large community-based data files of the ECG archives of Dalhousie's Heart Disease Research Centre and the data pool of the Epicore Centre of the University of Alberta. This data bank has been collected during the past thirty years in connection with several epidemiologic studies, particularly cross-sectional health surveys such as the First National Health and Nutrition Examination Survey (NHANES 1), the Second National Health and Nutrition Examination Survey (NHANES 2), and the Hispanic Health and Nutrition Examination Survey (HHANES) conducted in the USA between the years of 1976 -80, and 1982-1984 respectively. Various aspects relevant to the geographically weighted probability sampling procedures of the last two surveys of the noninstitutionalized United State population were documented in a previous communication [139, 140]. ECGs of 24,142 subjects were extracted from the total data bank of 43,360 ECGs which were all collected using strictly standardized procedures. The ECG-normal data file was created by excluding primary ECG abnormalities known to influence the QT intervals. Excluded were AV and ventricular conduction defects identified on the basis of a computer measurement of the PR and QRS duration. Subsequent exclusion criteria (for ages 13 years and over) included Minnesota Code [141] categories 1, 4 and 5 (Q, QS and related items, ST and T wave abnormalities).

37

QT measurements (QRS onset and T offset), HR measurements, and QRS measurements, were derived after a selective averaging procedure from 10 second long sample records of the standard 12-lead electrocardiograms, and in selected subgroups from the orthogonal Frank-lead ECGs. A statistical computer software SAS had been used to analyze the ECG measurements.

3.2. QT measurement

QT measurements were made after the selective averaging of normally conducted QRS-ST complexes by a computer program, the Novacode, which was designed for the simultaneous measurement of all ECG leads [142]. A high resolution graphics terminal, with scaling enlarged by the factor of six, was used to visually verify the proper detection of the QRS onset and the end of the T wave for each of the 20 class intervals. Leads with artifacts or excessive residual noise were rejected automatically, or by the human operator. Care was taken to avoid including U or P waves on the measurements. All QT measurements were expressed in msec. A representation of the QT measurement is shown in Figure 3.1.
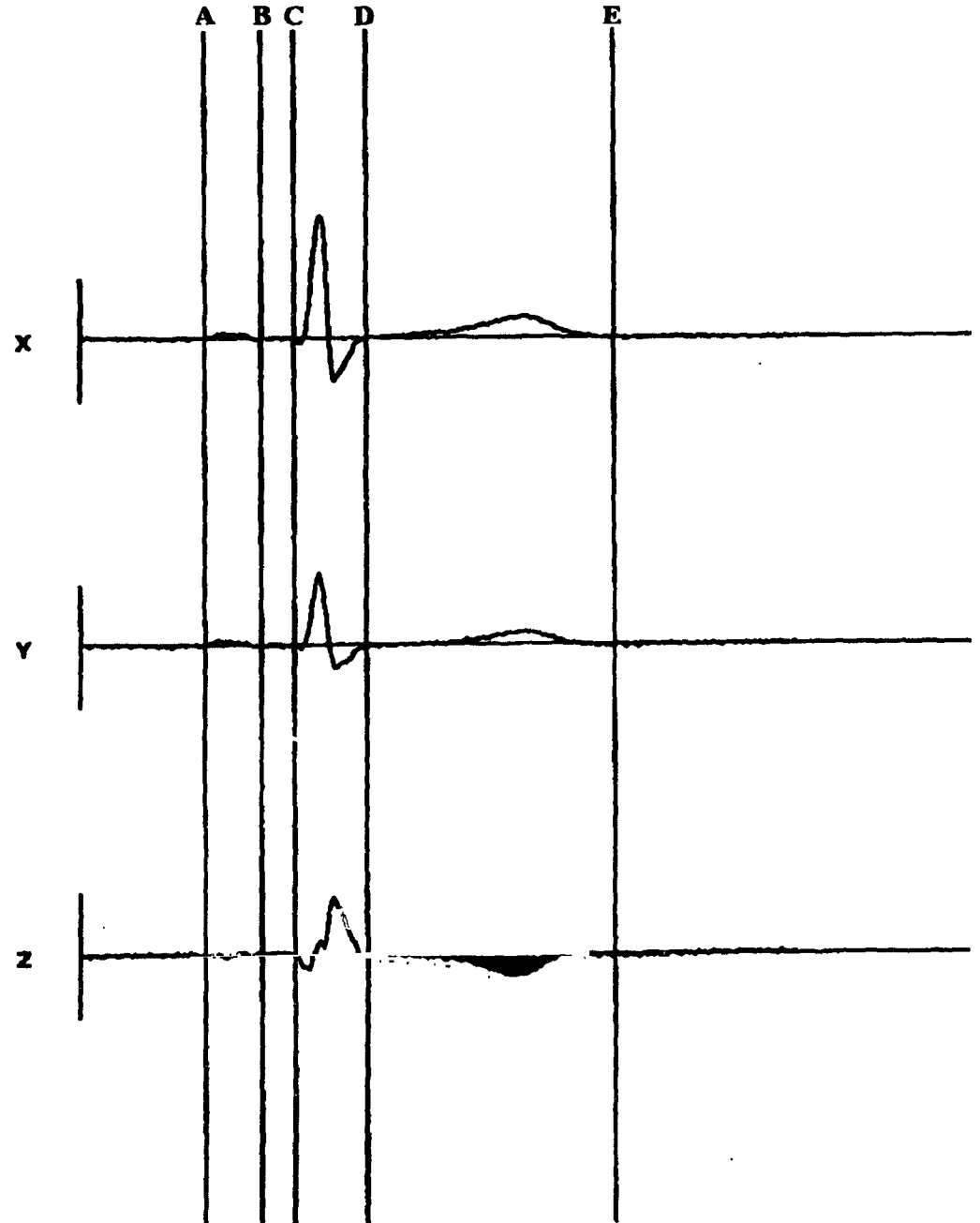
Figure 3.1: A representation of the QT measurement. Time demarcation lines A to E identify common reference time points for the beginning and end of atrial depolarization (A - B), ventricular depolarization (C - D), and the end of ventricular repolarization (E). The display provides an option for the ECG operator to make corrections to various time reference lines, such as end of the T wave (line E), which, in this case appears to be too late according to the visual inspection.

A critical point in the QT measurement act is the method of determining the point of onset of the Q wave and the end of the T wave. Substantial variations in QT duration estimates have been reported from lead to lead, from lead group to lead group, and from one QRS-T complex to another [127]. To reduce this source of variation, all QT measurements were performed on simultaneously sampled 8 independent components of the standard 12 lead ECG. The simultaneous leads and selective averaging of complexes used for coding provide a more precise and less variable measurement.

3.2.1. Error analysis and the assessment of QT measurement precision

All QT measurements were performed by the ECG measurement program, and verified by trained ECG editors using a high resolution ECG editing terminal as described earlier. A decision was made to accept QT measurements by the program unchanged, when the absolute QT difference between computer and visual measurement was less than 15 ms, and to accept visual measurement if the difference exceeded 15 ms. In this way the occasional larger QT measurement errors by the program were corrected. Otherwise the precisely defined measurement algorithms of the program for the QRS onset and the T offset were accepted without permitting measurement changes by the operators.

In the ECG measurement program, a single set of global onsets and offsets were determined for P, QRS and T wave (Figure 3.1). The ECG operator was required to make corrections if the various time reference lines appeared either too early or too late according to visual inspection. The following methods were used to guide the ECG operator's visual measurement. The landmarks for onset and offset

of QRS were the beginning of descending portion of the Q waves, and the end of descending portion of the S waves respectively. The onset of T wave was determined by J point plus 7/16 of JT interval and the point where a tangent joined the baseline was considered the end of the T wave.

Digitized ECG data files were used to assess the variability of the QT measurements by human operators, when performing the QT measurements without the global time lines inserted by the computer program. This was done by calculating the root-mean-square (rms) variation or (Ω) defined as:

$$\Omega = [\sum_{i=1}^{n} (X1i - X2i)^2/(2n - 1)]^{1/2}, \qquad (3.1)$$

Where X1i and X2i refer to the first and second measurement of the QT interval from record i. The rms variation can be expressed as a percent of the mean QT or a coefficient of variation (CV):

$$CV = (\Omega / \overline{QT})X100 \qquad (3.2)$$

To assess the reliability of the QT measurement by human operators, the disagreements between replicate determination in a series of the QT measurement was investigated. Two operators (the investigator and a medical student) participated in a test after an initial training session under the supervision of experienced editors. A file of 100 ECGs was used in the study. The intrareader and interreaders' variability was computed by calculating the standard deviation difference between pairs of measurement using the following formula:

$$\sqrt{\frac{S(x_1 - x_2)^2}{n-1}} \qquad (3.3)$$

where x_1 = individual first measurement/first reader's measurement

x_2 = individual second measurement/second reader's measurement

n = total number of measurements

The values of standard deviation difference for the interreader and in the intrareader were SD = 6.4 and SD = 5.6 respectively. t test for significance indicated that the difference were statistical signifcant at p value of 0.005. These values of SD fell below the level of the accepted values of variation (11 ms), which were established for a combination of two operators, who regularly participate in the ECG editing procedure [142].

A comparison was also made between the QT measurements derived by reader 1 and the QT measurement derived by the computer, and no significant difference (SD = 5.8, p< 0.0001) in the QT measurement was demonstrated.

3.2.2. QT measurement of VCD subgroups

An ECG data bank derived from community-based population samples was classified for the presence of various types of VCD according to the Minnesota Code (MC). This special subgroup of individuals with VCD was used for the measurement of the association of QT with interindividual variations in QRS duration. The QT measurements were made by the Novacode computer program and all measurements were visually verified as previously described.

3.3. Statistical method

A statistical software (SAS) was used for data analysis. Several linear multiple regression models were introduced to assess the contributions of QRS durations to QT and JT intervals in various study subgroups. In the first step, optimal correction was made for heart rate by introducing so called rate factor (RF) into the QT predicted from the formula QT = 656/(1+0.01HR) which in a previous study was observed to produce the best correction for heart rate (HR) variations using 13 functional formulas evaluated [2]. The two primary regression equations used were:

$$QT = a_1RF + b_1QRS \qquad \text{(Model 1)}$$

$$\text{and} \quad JT = a_2RF + b_2QRS \qquad \text{(Model 2)}$$

Two additional regression models were subsequently used to evaluate JT prediction accuracy without the inclusion of QRS duration as a covariate:

$$JT = a_3RF + \gamma_3 \qquad \text{(Model 3)}$$

$$\text{and} \quad JT = a_4RF \qquad \text{(Model 4)}$$

R-square values were used to evaulate what fraction of the total QT or JT variance can be accounted for by each prediction formula.

3.4. Vectorcardiogram and correlation maps

The orthogonal Frank lead ECG measurements from the second National

Health and Nutrition Survey (NHANES 2) were used for this substudy. A right -

handed orthogonal cartesian coordinate system was employed, with positive X,Y

and Z direction pointing to the left, inferiorly and posteriorly respectively. The T

wave duration was determined by J point plus 7/16 of JT(i.e. onset of T wave) and

the offset of the T wave.

QRS and T intervals were normalized and divided into 20 units in time. Each

QRS and T vector have X, Y and Z components from X, Y and Z leads separately.

Thus, there were 20 QRS and 20 T vectors corresponding to 20 time units, that

made 120 measurements for each subject. Mean QRS and T vectors were

constructed from differences of maximum positive and negative deflections in three

leads. An approximation of the spatial QRS/T angle (ø) was calculated for the

analysis of excitation/repolarization spatial relationships by using these mean

vectors of QRS and T. The spatial angle was calculated by the following formula:

$$(\emptyset) = \text{arc } \cos \frac{(X_{QRS}X_T + Y_{QRS}Y_T + Z_{QRS}Z_T)}{\sqrt{(X^2_{QRS} + Y^2_{QRS} + Z^2_{QRS})} \bullet \sqrt{(X^2_T + Y^2_T + Z^2_T)}} \qquad (3.5)$$

The range of the angles is from 0 to 180. Repolarization patterns were

categorized into five groups according to the estimated values of the QRS/T angle :

(ø) 0 to 36 indicating mainly reverse sequences of repolarization, (ø) 36 to 72 semi-

reverse, (ø) 72 to 108 intermediate, (ø) 108 to 144 semi-concordant. and (ø) 144 to

180 mainly a concordant sequence of repolarization.

A laser printer was used to plot the X and Y amplitudes and to obtain the

frontal plane QRS and T vector loops. Similarly, the horizontal and sagittal plane

vector loops were obtained by plotting X and Y, and Z and Y amplitudes respectively. The second step was to calculate the correlation coefficients for a "20 x 20" matrix, containing the QRS and T amplitudes for each orthogonal lead separately. The correlation coefficients were from 1 to -1, which were multiplied by a factor of 100. The spatial relationship was shown from 100 to -100, with 100 indicating QRS and T in the same direction, whereas -100 denoted QRS and T in opposite direction. 0 signifies that the angle between QRS and T at that moment is 90 degrees. A sample of a "20 x 20" correlation matrix is shown in Table 3.2. A correlation contour map was plotted for each correlation matrix by a Fortran program (Figure 3.2). The positive values and negative values show positive correlation and negative correlation respectively, and signify the maxima and minima for each lead respectively.

NHA:TES 2 NORMALS (NO REJECTED LEADS AND 1.0 AND 4.0 AND 5.0 AND 6.0 AND 7.0)

LEAD Z N=5828

T

	1	2	3	4	5	6	7	8	9	10	11	12	13	14	15	16	17	18	19	20
1	28	26	24	21	17	14	11	7	4	1	-1	-4	-6	-9	-12	-13	-12	-5	4	6
2	25	26	26	25	23	21	20	17	15	12	9	6	2	-1	-5	-7	-7	-1	5	8
3	18	19	20	21	20	20	19	18	17	15	13	10	7	4	1	-1	-1	1	4	6
4	17	20	21	22	23	23	23	23	22	20	18	16	13	9	6	4	4	6	8	8
5	12	14	16	18	19	20	21	21	21	20	19	17	15	13	11	9	9	10	10	10
6	3	5	8	10	11	13	14	15	16	16	16	16	15	15	15	15	16	15	14	13
7	-7	-5	-3	0	2	4	5	7	8	10	11	12	13	15	16	18	20	19	16	14
8	-13	-13	-11	-9	-7	-5	-3	-1	1	3	5	7	10	13	16	19	22	20	16	14
9	-17	-18	-17	-15	-14	-12	-11	-9	-7	-5	-2	1	4	8	13	17	20	19	15	13
10	-21	-23	-22	-21	-20	-19	-18	-17	-15	-13	-10	-6	-2	3	8	14	17	17	13	12
11	-22	-25	-26	-25	-25	-24	-23	-22	-21	-19	-16	-12	-8	-3	4	9	13	14	11	10
12	-22	-26	-28	-28	-28	-28	-27	-27	-26	-24	-22	-18	-14	-8	-2	4	8	9	8	8
13	-18	-23	-25	-26	-26	-26	-27	-27	-26	-25	-23	-20	-17	-12	-7	-2	2	4	3	3
14	-13	-18	-20	-21	-22	-23	-23	-24	-24	-23	-22	-20	-17	-14	-9	-5	-2	-1	0	0
15	-6	-11	-13	-14	-15	-16	-17	-17	-18	-18	-17	-16	-14	-11	-8	-5	-3	-2	-2	-2
16	2	-2	-4	-5	-6	-7	-8	-9	-10	-10	-10	-9	-8	-6	-4	-2	-1	-1	-2	-1
17	23	17	14	11	9	8	5	3	1	-1	-1	-1	1	3	5	6	7	7	7	8
18	51	44	41	39	36	33	30	27	23	20	19	18	18	18	18	17	17	17	17	18
19	73	67	64	61	58	55	51	47	42	38	35	34	32	30	28	26	24	24	26	27
20	84	80	77	74	70	67	63	58	53	49	45	42	40	37	34	30	27	28	30	31

(Q R S — row labels)

Table 3.1: A "20 x 20" correlation matrix for Z lead on subjects with normal ventricular conduction. Correlation coefficients for each element are multiplied by a factor 10^2.
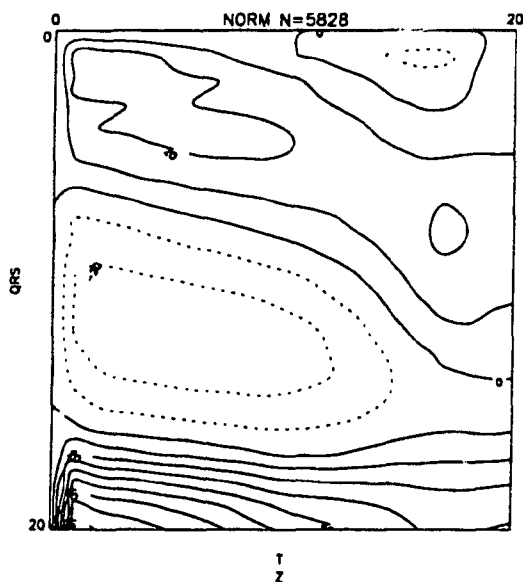
Figure 3.2. Z component of QRS-T correlation map for normal conduction

CHAPTER 4
RESULTS

4.1. Regression models for QT and JT prediction

Critical flaws with currently used QT prediction formulas have been recognized. With many of the prediction formulas, QT increased to infinity at the low end of the HR range and approached zero at very high heart rates. Rautaharju et al. [30] established an optimal heart rate correction factor for the QT. They noted that QTmax is the limiting value of QT when the heart rate approaches zero. Their expression for predicted QT of the form:

$$QT = 1/(a + bHR) \qquad (4.1)$$

has certain interesting functional properties. Expressed in a slightly different form:

$$\frac{QTmax\text{-}QT}{QT} = (b/a)HR \qquad (4.2)$$

$$= HR/100 \text{ for } a = 100b \qquad (4.3)$$

QT_{max} in this expression is the asymptotic value of QT at HR = zero which can be taken to represent QT after a long pause. This relationship indicates that for any given HR, the proportional QT shortening from QT_{max} to actual QT at that HR is a

constant (HR/100). At HR = 100, this ratio is 1, i.e. the QT has shortened to 1/2 of

QT_{max}. QT_{max} = 656 msec is the estimated asymptotic value of QT for the

functional formula used. This expresses the rate-corrected QT interval as a constant

divided by $(1 + \frac{HR}{100})$

$$\text{Thus the rate factor (RF)} = 1/(1 + 0.01 \times HR) \qquad (4.4)$$

In this investigation, several regression models shown in Tables 4.1 and

4.2 were evaluated, using the aforementioned RF in the models in order to obtain

the best regression equation for QT and JT.

The QT interval has a complex relation to the heart rate. A self-correlation

problem may arise when the dependent variable in a regression model is an integral

component of the independent variable, as is the case with the QT prediction from

the RR intervals. Spodick [143] objects to the use of RR to predict the QT based

on his observation that at high heart rates, most of the cardiac cycle is indeed QT. It

is of interest to include TQ, the subinterval of RR as an independent covariate in the

regression model, to account for the total variance of the QT and JT intervals.

4.1.1. Population description

The source data for the present investigation of regression models consisted

of the data file of the North American population of children and adults described in

chapter three. It was composed of 21,512 normal subjects, 234 subjects with left

bundle branch block (LBBB), 677 with right bundle branch block (RBBB), 622

with IVCD, 613 and 740 with incomplete left bundle branch block (ILBBB) and

incomplete right bundle branch block (IRBBB) respectively.

4.1.2. R-square values for five QT and five JT prediction models

Table 4.1: QT regression models for six categories of ventricular conduction

	Model 1 QT=aRF+b			Model 2 QT=aQRS+bTQ+c				Model 3 QT=aRF+bQRS+c			
	a	b	R2	a	b	c	R2	a	b	c	R2
Category											
Normal	0.95	23.34	0.87	0.71	0.15	256	0.87	0.90	0.53	-5.5	0.88
LBBB	0.91	96.17	0.81	1.00	0.13	243	0.82	0.86	0.85	-14.0	0.87
RBBB	0.80	117.9	0.78	0.89	0.11	250	0.79	0.76	0.78	20.2	0.85
IVCD	0.83	98.88	0.79	1.03	0.10	240	0.77	0.85	0.99	-36.9	0.85
IRBBB	0.95	27.64	0.88	0.69	0.16	250	0.84	0.90	0.56	-8.7	0.90
ILBBB	0.79	94.97	0.84	0.31	0.12	312	0.77	0.90	0.53	-5.54	0.88

RF = 1/(1+0.01HR)

Table 4.2: JT regression models for six categories of ventricular conduction

Category	Model 1 JT=aRF+b			Model 2 JT=aQRS+bTQ+c				Model 3 JT=aRF+bQRS+c			
	a	b	R2	a	b	c	R2	a	b	c	R2
Normal	0.86	-30.3	0.86	-0.28	0.15	256	0.79	0.90	-0.4 6	-5.5	0.88
LBBB	0.86	-32.5	0.80	0.00	0.13	243	0.75	0.86	-0.14	-14.0	0.83
RBBB	0.75	-7.0	0.80	-0.10	0.11	250	0.71	0.76	-0.21	20.2	0.81
IVCD	0.85	-38.2	0.83	0.03	0.10	240	0.71	0.85	-0.00	-36.9	0.83
IRBBB	0.87	-37.0	0.87	-0.30	0.16	250	0.82	0.90	-0.43	-8.7	0.88
ILBBB	0.79	94.97	0.84	-0.68	0.12	312	0.77	0.79	-0.70	64.9	0.84

$RF = 1/(1+0.01HR)$

When two or more independent variables are used, the index of correlation is the multiple correlation coefficient symbolized as R, which shows the strength between several independent and a dependent variable. The R-square values for QT and JT regression in subjects with normal conduction and the five categories of ventricular conduction defects are shown in Tables 4.1 and 4.2.

Model 3 for QT and JT predictions included the rate correction factor (RF) and QRS duration as independent covariates. They yielded the highest R-square values.Similar R-square values for model 2 (QT and JT = aQRS+bTQ+c) and model 3 (QT and JT = aRF+bQRS+c) indicated that TQ could predict QT and JT reasonably well provided that the QRS duration is included as a covariate.

4.2. Evolution of ventricular excitation and repolarization patterns with age in relation to the QT interval of the electrocardiogram

Significant sex differences were recently demonstrated in the age-evolution of the QT interval after careful adjustment of the measured QT values for differences in the heart rate, with shorter rate-corrected QT values in younger age groups of adult males than in females [52]. Furthermore, there is evidence indicating that ventricular excitation time i.e. QRS duration was significantly associated with the QT duration in subjects with normal ventricular conduction [52]. It is expected that the heart rate and QRS duration would contribute in a varying degree to the variation of the QT interval during the aging process.

Two linear multiple regression equations were introduced to assess the contribution of QRS duration to QT and JT intervals in various age groups. In the first step, optimal correction was made for the heart rate by introducing the rate factor (RF) into the QT predicted from the formula QT = 656/(1+0.01HR), which, in a previous study was observed to produce the best correction for heart rate (HR) among 13 functional formulas evaluated [2]. The two linear multiple regression equations used in this study were:

$$QT = \alpha_1 RF + \beta_1 QRS + \gamma_1 \qquad (4.5)$$

$$JT = \alpha_2 RF + \beta_2 QRS + \gamma_2 \qquad (4.6)$$

where

QT, JT and QRS intervals were expressed in milliseconds.

The significance of sex differences in the mean values of HR, QRS duration, measured QT and QTI were evaluated by using a t test. The sex- related differences between the QT and QRS duration were explored by means of an analysis of variance. The differences were considered statistically significant at p value < 0.05.

4.2.1. Population description

The study population of 20,565 for this investigation was a sub-sample of the total population of 43,246 North American children, adolescents, and adults aged from birth to 99 years used in the previous investigation [2]. Excluded were AV and ventricular conduction defects identifed on the basis of computer measurement of PR and QRS durations. Subsequent exclusion criteria included Minnesota Code Categories 1, 4 and 5 (MC1, MC4, MC5, Q, QS and related items; ST and T wave abnormalities). Also excluded from the original pooled sample were 2984 subjects with ECGs sampled at 250 samples per second after pilot studies indicated that a 2 ms (millisecond) sample interval (500 sample/second/lead) will be required for QT measured with adequate resolution. These exclusion left 14,379 normal ECGs for final analysis. The distribution of this total sample by age and gender is listed in Table 4.3.

Table 4.3 : The distribution of the study population of 18,622 normal adults by age and gender

Age	Men N	Women N
20-29	684	1250
30-39	717	1115
40-49	1559	2533
50-64	3425	4750
65-75	839	1340
75+	147	216
Total	7371	11,251

The total population included 7,371 men and 11,251 women. Six age subgroups from 20 to 75+ were studied : 20-29, 30-39, 40-49, 50-64, 65-74 and 75+. In each age group, there were more women than men.

4.2.2. Mean values

Distribution of mean values of heart rate, QRS duration, measured QT and QT Prolongation Index by gender and age are listed in Table 4.4.

Table 4.4: Mean values (standard deviations) for heart rate, QRS duration, measured QT interval and QT Prolongation Index in adult males and females by age

Males

Age (years)	N	Heart Rate	QRS duration	Measured QT	QTI
20-29	684	66±11.2	90±8.7	383±29	97±4.1
30-39	717	68±11.6	90±8.6	379±28	97±4.1
40-49	1559	66±10.3	95±9.6	394±27	100±4.3
50-59	3425	66±10.8	95±9.8	401±29	101±4.5
60-74	839	66±11.6	91±10.2	400±33	101±4.6
75+	147	64±10.0	94±9.0	408±28	102±4.8

Females

Age (years)	N	Heart Rate	QRS duration	Measured QT	QTI
20-29	1250	71±10.3*	84±8.4	385±27	100±4.0**
30-39	1,116	71±10.6*	83±8.5	384±28**	100±4.2**
40-49	2533	69±10.2*	89±9.4	400±28**	103±4.7**
50-59	4750	69±10.3*	90±9.4	404±30**	104±4.9**
60-74	1340	68±11.3*	87±10.0	401±33	103±5.2**
75+	263	67±11.4*	90±8.6	413±30	105±5.4**

* p < 0.001; ** p < 0.005, for sex difference (independent t-test)

The mean heart rate remained relatively unchanged in men until the age of 75 years with a mean value of 64 beats/min. In females, the mean value of heart rate decreased from 72 beats/min at age group 30-39 years to 67 beats/min. at the oldest age groups 75 years or older. Although the trend towards the decreasing heart rate with age was non-significant both in men and in women, as expected, the heart rate values of men were significantly lower than in women in all age groups ($p < 0.001$ for all).

There were significant sex differences ($p < 0.0005$) in the absolute QT values in the younger adults aged 30 to 59 years old. The assessment of age trends in the QTI revealed an interesting result. The rate-corrected QT values in females were significantly longer than in males, as has been known for decades [18]. In Table 4.4 the mean values of the QTI in women were a significantly longer QTI ($P < 0.005$) than that in men in all age groups. The QT Prolongation Index values (QTI) tended to be about 3 percent longer in females than in males in spite of the fact that the QRS duration was about 6 ms longer in males than in females. Although there were sex differences in the mean values of QTI, the age trends in QTI were non-significant in both men and women, as shown in Figure 4.1.
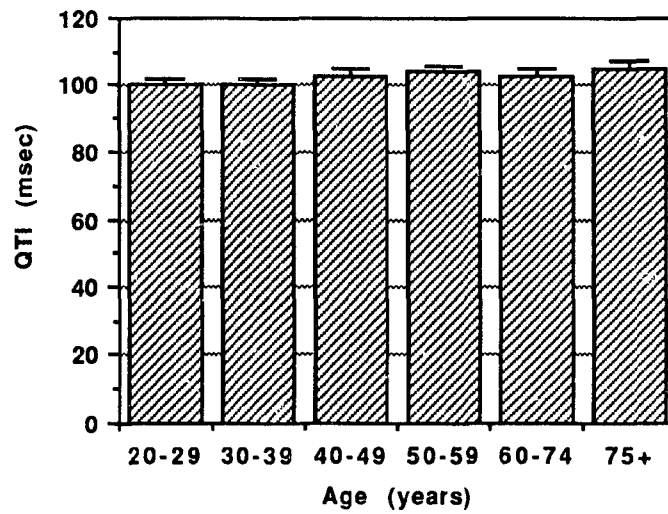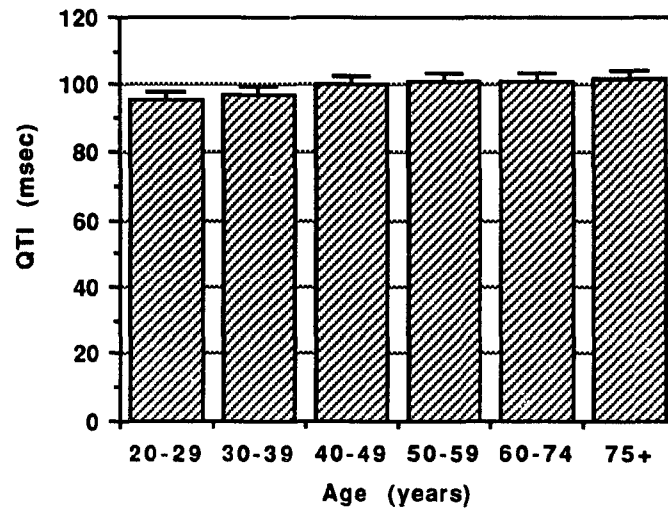
Figure 4.1: Mean values and standard deviations of QTI by age in men (top) and in women (bottom)

$$QTI = (QT/QTp) \times 100. \quad QTp = 656/(1 + 0.01HR)$$

4.2.3. Regression of QT and JT on rate correction factor

The regression of QT and JT on RF without QRS duration were determined in a combined normal population of males and females in Table 4.5. The changes in R^2 values were used to judge the relative contribution of the RF on the accuracy of the QT prediction. The results showed that RF alone explained from 57% to 65% of the total QT variance. Similarly, RF alone accounted for 51% to 60% of the total JT variance in the various age groups. In these regression formulas, α_1 and $\gamma_1 = QT_{max}$ and α_2 and $\gamma_2 = JT_{max}$, i.e. maximum asymptotic values of QT and JT respectively, when the heart rate approaches 0.

Table 4.5. Regression coefficients and R^2 values for regression of QT and JT on rate factor (RF) without the inclusion of QRS duration in the prediction models in a combined normal population of males and females by age (N = 20,565)

		Model 1 $QT = \alpha_1 RF + \gamma_1$			Model 2 $JT = \alpha_2 RF + \gamma_2$		
Age	N	α_1	γ_1	R^2	α_2	γ_2	R^2
20-29	1934	583	30.4	0.63	583	-24	0.53
30-39	1835	603	26.2	0.64	603	-27	0.56
40-49	4756	590	47.7	0.57	590	-10	0.51
50-64	8919	616	27.4	0.59	616	-29	0.54
65-75	2511	675	-1.23	0.65	675	-50	0.60
75+	610	583	49.8	0.58	580	-12	0.57

4.2.4. Regression of QT and JT on rate correction factor and QRS duration

Table 4.6: Regression of QT and JT on rate factor (RF), R-square, and increment in R-square value with the inclusion of QRS duration in a combined normal population of males and females by age (N = 20,565)

	Model 1 $QT = \alpha_1 RF + \beta_1 QRS + \gamma_1$					Model 2 $JT = \alpha_2 RF + \beta_2 QRS + \gamma_2$				
Age	α_1	β_1	γ_1	$*R^2$	ΔR^2	α_2	β_2	γ_2	$*R^2$	ΔR^2
20-29	577	0.14	28	0.63	0	577	-0.86	28	0.61	0.08
30-39	596	0.15	17	0.64	0	596	-0.85	17	0.63	0.07
40-49	564	0.42	20	0.59	0.02	564	-0.58	20	0.55	0.04
50-64	590	0.53	0.7	0.62	0.03	590	-0.47	0.7	0.57	0.03
65-75	629	0.60	-33	0.68	0.03	629	-0.39	-33	0.62	0.02
75+	577	0.55	11	0.61	0.03	577	-0.44	11	0.59	0.02

* $p < 0.001$

RF = $1/(1+0.01HR)$

β_1 = regression coefficient of QRS on QT

β_2 = regression coefficient of QRS on JT

γ_1 & γ_2 = counterpart of the intercept in linear univariate regression

R^2 = squared multiple correlation coefficient

ΔR^2 = increment in R^2 values with the inclusion of QRS duration in QT and JT prediction equations

QRS, QT and JT intervals in msec

The regression of the QT on rate-factor (RF) with the inclusion of the QRS duration in a combined normal population of males and females, indicated a significant positive contribution by QRS duration to rate-corrected QT (F < 0.001) in all age groups. The values for the QRS duration regression coefficient (β_1) ranged from 0.14 in the youngest to 0.60 for the oldest groups. The rate correction factor and the QRS duration combined, explained from 59% in the groups of 40-49 to 68% in the 65-75 age group of the total QT variance, as seen from the R-square values for the QT regression equation. QRS duration had a minimal but significant effect on QT (P <0.001) in the older age groups, but had no effect on QT in the youngest age group from 20 to 39 years, as indicated by zero incremental values of R^2 in these two age groups.

For JT regression on QRS, the negative values of the QRS regression coefficient (β_2) decreased from -0.86 in the youngest group to -0.39 in the 65-75 age group. The changes of R-square values with the inclusion of QRS duration in the multiple regression model for JT (Model 2) showed that the influence of QRS duration on JT decreased significantly (P < 0.001) from 8% to 2% with age.

4.2.5. Regression of QT and JT on rate factor and QRS duration by age and gender

Table 4.7 shows the coefficient estimates for the regression of QT and JT on QRS duration in multiple regression models together with the correction term for HR stratified by gender and age. It was noted that QRS duration made a relatively small contribution on QT interval in the two younger age groups, with regression coefficient 0.29 in males and 0.43 in females in the age group of 20 to 39 years. However, QRS duration made a progressively increasing contribution to QT interval with advancing age. Values of the QRS regression coefficient for QT increased to 0.65 in males of 65-75 years old and to 0.93 in the 75+ age group of females. There was a considerable jump in value of the QRS regression coefficient in the age group of 30 -39 years old in both sexes and remained approximately constant in the old age groups. As for JT in Model 2, the negative values of the QRS regression coefficient decreased with age from -0.71 to -0.48 in males, and from -0.57 to -0.07 in females.

Table 4.7: Regression of QT and JT on rate factor (RF) and QRS duration by age and gender

	Model 1 $QT = \alpha_1 RF + \beta_1 QRS + \gamma_1$					Model 2 $JT = \alpha_2 RF + \beta_2 QRS + \gamma_2$			

Males

Age	N	α_1	β_1	γ_1	R^2*	α_2	β_2	γ_2	R^2*
20-29	684	593	0.29	-5.0	0.67	593	-0.71	-6.80	0.67
30-39	717	588	0.35	2.8	0.69	588	-0.65	1.22	0.67
40-49	1559	554	0.62	-0.7	0.66	554	-0.38	1.68	0.61
50-64	3425	592	0.64	5.3	0.68	592	-0.36	-18.3	0.63
65-75	839	625	0.65	-10.7	0.73	625	-0.35	-36.6	0.69
75+	147	508	0.52	-1.8	0.58	508	-0.48	-22.5	0.57
All	7371	583	0.66	-19.2	0.67	583	-0.34	-18.7	0.56

Females

Age	N	α_1	β_1	γ_1	R^2*	α_2	β_2	γ_2	R^2*
20-29	1250	625	0.43	-18.8	0.68	625	-0.57	-16.8	0.66
30-39	1115	634	0.41	-16.6	0.69	634	-0.59	-25.6	0.67
40-49	2533	590	0.64	-8.9	0.64	590	-0.36	-6.9	0.58
50-64	4750	619	0.77	-34.3	0.65	619	-0.23	-32.3	0.59
65-74	1340	653	0.71	-46.4	0.69	653	-0.28	-49.4	0.62
75+	263	559	0.93	-11.4	0.62	559	-0.07	-3.4	0.58
All	11,251	623	0.76	-36.6	0.66	623	-0.24	-4.6	0.34

*p < 0.001

β_1 = regression coefficient of QRS on QT
β_2 = regression coefficient of QRS on JT
γ_1 = counterpart of the intercept in linear univariate regression
R^2 = squared multiple correlation coefficient
QRS, QT and JT in ms

Comparatively, the values of the QRS duration regression coefficient (β_1) after rate correction in females were higher than those in males in all age groups. To test whether the values of the QRS regression coefficients in the QT regression model in men were significantly different from those in women after adjusting for heart rate, comparisons were made between these two groups on changes of the slopes by means of an analysis of variance. No significant difference could be shown in individual age groups except for the 50 to 64 age group ($P < 0.001$). When data were analyzed for the total group, a statistically significant difference between men and women ($P < 0.001$) was obtained.

Coefficients for QRS duration from the regression of QT (β_1) and JT (β_2) from the multiple linear regression model containing a heart rate correction term in Figure 4.2 revealed a progressively increasing contribution of QRS duration on QT (β_1) with advancing age, and a parallel decrease in the inverse (negative) association between QRS duration and JT interval with age, in such way that for all age groups $\beta_2 = \beta_1 - 1$. This relationship was strictly due to the fact that a linear multiple regression model for QT and JT predictions was used in this analysis, and JT = QT - QRS duration. This relationship is summarized in Figure 4.2.
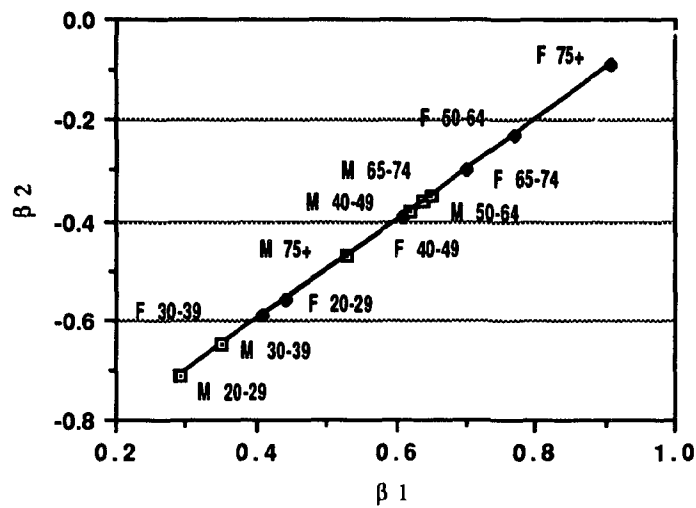
Figure 4.2: Coefficients for QRS from regression of QT (β_1) and JT (β_2) on QRS, from the multiple regression models containing the heart rate correction term as a covariate with QRS for females and males stratified by age

Age trend and sex differences must be taken into consideration before the QT prediction becomes sufficiently accurate. This was achieved by introducing a correction term for age and sex in the QT prediction equation (Table 4.8). When data were analyzed as a total group in men and in women, the multiple regression equation was derived with RF, QRS duration, and age. All these variables were statistically significant predictors ($P < 0.001$) for both men and women. However, among all variables included in the model, RF remained highly significant, independent of QRS duration and age.

Table 4.8. QT regression on RF, QRS duration and age in males and females

Males

Regression Model	R^2 values
(1) QT = 10.44 + 0.95RF	0 63
(2) QT = -19.40 + 0.89RF + 0.65QRS	0.67
(3) QT = -30.27 + 0.88RF + 0.61QRS + 0.38Age	0.70

Females

Regression Model	R^2 values
(1) QT = 5.86 + 1.01RF	0 61
(2) QT = -36.70 + 0.94RF + 0.76QRS	0.66
(3) QT = -40.48 + 0.93RF + 0.72QRS + 0.23Age	0.67

4.3. Association between ventricular excitation time and QT and JT intervals in ventricular conduction defects

Das [7] evaluated the relationship of QRS duration and QT and JT intervals in a small group of patients with ventricular conduction defects and observed that QT prolonged in direct proportion to QRS prolongation. He concluded that the prolongation of rate-corrected QT in complete bundle branch blocks was entirely secondary to a prolonged depolarization time.

In view of the practical as well as theoretical importance of this issue, the associations of excitation time with QT and JT intervals were investigated in a large ECG data file composed of various categories of complete and incomplete bundle branch blocks (Table 4.9).

Several linear regression models were introduced to assess the contribution of QRS duration to QT and JT intervals in various study groups. The two primary regression equations used in this study were:

$$QT = \alpha_1 RF + \beta_1 QRS + \gamma_1 \qquad \text{(Model 1)}$$

$$\text{and}$$

$$JT = \alpha_2 RF + \beta_2 QRS + \gamma_2 \qquad \text{(Model 2)}$$

where : $RF = 1/(1 + 0.01 \, HR)$.

QT, JT and QRS intervals were expressed in milliseconds

Two additional regression models were subsequently used to evaluate JT prediction

accuracy without the inclusion of QRS duration as a covariate.

$$JT = \alpha_3 RF + \gamma_3 \qquad \text{(Model 3)}$$

and the same formula without intercept

$$JT = \alpha_4 RF \qquad \text{(Model 4)}$$

R-square values were determined to evaluate what fraction of the total QT or JT

variance could be accounted for by each prediction formula, and root-mean square

error(RMSE) was determined to assess the overall prediction accuracy.

4.3.1. Population description

The study population for this investigation was a subset of 2,865 persons

with ventricular conduction defects, and 20,687 normal adult subjects aged 20 to 99

years, with normal ventricular conduction. The group with various categories of

ventricular conduction defects (VCD), was stratified into five subgroups of

complete and incomplete bundle branch blocks, using the Minnesota Code Criteria.

Complete bundle branch blocks include code 7.1 (left bundle branch block or

LBBB), code 7.2 (right bundle branch block or RBBB), and code 7.4 (IVCD,

complete block of unspecified type), which all require a QRS duration of 120 ms or

more. Incomplete left bundle branch block or ILBBB (code 7.6) requires QRS

duration of 100 to 120 ms, and incomplete right bundle branch block or IRBBB

(code 7.3) requires QRS duration of 100 - 120 ms with R' > R pattern in V1 or V2.

The composition of the study population is shown in Table 4.9.

Table 4.9: Composition of the study population in various categories of ventricular conduction defects classified according to the Minnesota Code Criteria

Minnesota Code	Category	Number Subjects	Mean age (year)
7.0	Normal conduction	20,687	51.4
7.1	LBBB	231	63.9
7.2	RBBB	673	63.8
7.4	IVCD	616	60.1
7.3	Incomplete RBBB	607	53.5
7.6	Incomplete LBBB	738	54.6

In one of the studies (NHANES 2), the conventional electrocardiograms were sampled in groups of three simultaneous leads, and to avoid difference in QT measurements from different lead groups [144], QT and JT measurements in these subgroups were made from Frank orthogonal X, Y and Z leads. A comparison of QT measurements in a large subset of eight simultaneously sampled components of the 12 lead electrocardiograms and the Frank leads, showed no significant difference between these two sampling and measurement procedures.

4.3.2. Mean values

Mean values of QT, JT, HR and QRS are listed in Table 4.10. These data

revealed that the mean values of HR in complete and incomplete bundle branch

blocks were comparable to those in normal conduction, ranging from 66 to 69. The

mean values of QT intervals in complete bundle branch blocks were approximately

32 ms longer than in normal conduction and in incomplete bundle branch blocks.

The prolonged QT intervals in complete bundle branch blocks were associated with

prolonged QRS durations. As expected, the mean values of QRS duration in

complete bundle branch blocks were approximately 43 ms longer than in normal

conduction, and in incomplete bundle branch blocks. Conversely, the mean values

of JT duration in normal conduction (307 ms) was comparable to that in a left

bundle branch block (302 ms), in IVCD (304 ms) and in incomplete LBBB (306

ms). Complete RBBB had the shortest JT duration with a mean value of 291 ms

Table 4.10: Mean values of QT, JT, QRS duration and correspondent standard deviation in various types of ventricular conduction defects

MC	QT	SD	HR	SD	QRS	SD	JT	SD
Normal	398	10.9	68.1	10.9	90	10.0	307	12.9
7.1 LBBB	450	18.3	68.4	12.1	149	17.3	302	10.6
7.2 RBBB	430	15.2	66.5	12.2	143	17.5	291	11.8
7.3 IRBBB	396	11.7	68.9	11.8	95	11.9	302	12.3
7.4. IVCD	408	29.4	66.6	13.5	127	15.7	304	11.9
7.6 ILBBB	400	19.9	66.0	1C 7	105	4.7	306	10.7

MC = Minnesota Code
SD = Standard Deviation
QRS, QT and JT in ms

Although these QT and JT values were not corrected for heart rate, it appeared that there were considerable differences in the relationships between the duration of ventricular excitation and repolarization.

4.3.3. Dependence of QT and JT intervals on heart rate in various categories of ventricular conduction defects

The regressions of QT on RF without QRS duration were determined in various ventricular conduction categories. The results revealed that heart rate alone explained 39% (RBBB) to 60% (IRBBB) of the total QT variance. Regression of

JT on RF without QRS duration indicated that heart rate alone explained 42% to

59% of the total JT variance.

Table 4.11: Regression of QT and JT on rate factor (RF) without QRS duration in normal conduction and in five categories of ventricular conduction defects

		Model 1 $QT=\alpha_1 RF+\gamma_1$			Model 2 $JT=\alpha_2 RF+\gamma_2$		
MC Category	N	α_1	γ_1	R^2	α_2	γ_2	R^2
7.0 Normal	20687	628	23.3	0.59	566	-30.3	0.55
7.1 LBBB	231	599	96.1	0.44	565	-32.5	0.49
7.2 RBBB	673	526	117.9	0.38	496	-7.1	0.42
7.3 IRBBB	607	623	27.6	0.62	571	-37.0	0.59
7.4 IVCD	616	545	98.8	0.39	562	-38.3	0.48
7.6 ILBBB	738	524	94.9	0.50	520	-8.3	0.49

MC = Minnesota Code

RF = 1/(1+0.01HR)

R^2 = squared multiple correlation coefficient

4.3.4. Regression of QT and JT on rate correction factor (RF) and QRS duration in various categories of ventricular conduction defects

In these analyses QRS duration was included as a covariate with th? rate factor (RF) in QT and JT prediction models. For a regression of QT on RF and QRS duration, the values of QRS regression coefficient (ß₁ in Model 1) differed

substantially between various categories of ventricular conduction defects, ranging from 0.29 in incomplete LBBB to 0.99 for IVCD. The rate correction factor and QRS duration combined, explained from 50% to 66% of the total QT variance, as seen from the R-square values for model 1. QRS duration alone accounted for about 15% of the total QT variance in complete bundle branch blocks, as seen from the incremental values of R-square with the inclusion of QRS duration in the multiple regression model. The R-square increment for normal conduction and for an incomplete right bundle branch block, was considerably less than the complete bundle branch blocks, 0.03 and 0.04 respectively, but still highly significant for both ($p < 0.001$) On the other hand, QRS duration had no significant effect on QT in incomplete left bundle branch block ($p > 0.05$).

When JT was regressed on QRS with the correction term for heart rate, the negative values of the regression coefficient β_2 (Model 2) ranged from -0.01 in IVCD to -0.71 in an incomplete left bundle branch block. The combined effects of a rate correction factor and QRS duration, explained from 43% to 62% of the total JT variance, as evidenced from R-square values for Model 2. The incremental R-square values with the inclusion of QRS duration in the multiple regression model for JT in Table 4.12 revealed that QRS duration influence on JT was practically negligible in complete bundle branch blocks ($p > 0.05$). However, QRS duration retained its significant association with JT in normal conduction and in incomplete RBBB ($p < 0.001$ for both), and although still significant ($p < 0.001$), was in practical terms nearly negligible for incomplete LBBB ($\Delta R^2 = 0.01$).

Table 4.12.-Coefficient estimates for QRS from regression of QT (β_1 in Model 1) and JT (β_2 in Model 2) on the rate factor and QRS in normal ventricular conduction and in five categories of ventricular conduction defects. The rate correction was performed by determining the regression coefficients α_1 and α_2, for the rate correction factor (RF), with RF = $1/(1 + 0.01$ HR). R^2 = squared multiple correlation coefficient and ΔR^2 indicates the increment in R^2 values with the inclusion of QRS duration in QT and JT prediction formulas. QRS , QT and JT intervals are in ms.

ECG Category	Model 1 $QT = \alpha_1 RF + \beta_1 QRS + \gamma_1$					Model 2 $JT = \alpha_2 RF + \beta_2 QRS + \gamma_2$				
	α_1	β_1	γ_1	R^2	ΔR^2	α_2	β_2	γ_2	R^2	ΔR^2
Normal	596	0.55	-7	0.62	0.03*	596	-0.45	-6	0.62	0.07*
LBBB	577	0.87	-20	0.60	0.16	577	-0.13	-20	0.50	0
RBBB	503	0.77	20	0.54	0.16	503	-0.23	20	0.43	0.01
IVCD	563	0.99	-38	0.54	0.15	563	-0.01	-38	0.48	0
IRBBB	591	0.56	-7	0.66	0.04*	591	-0.44	-7	0.62	0.03*
ILBBB	523	0.29	65	0.50	0	523	-0.71	65	0.50	0.01*

*p < 0.001
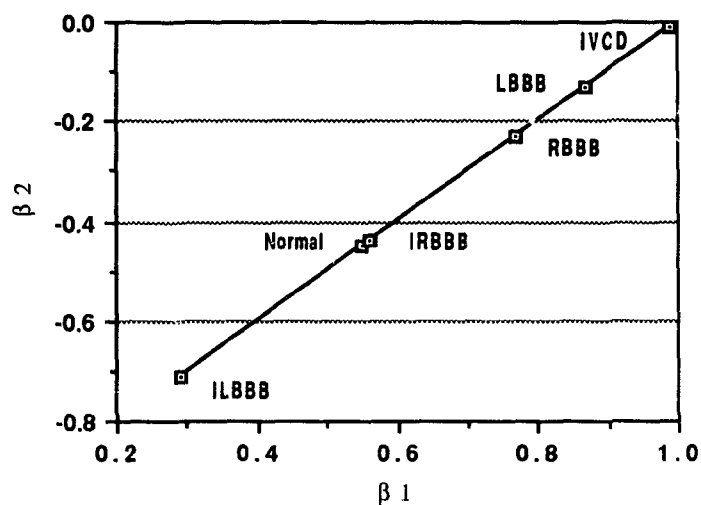
Figure 4.3: Coefficients for QRS from regression of QT (β_1) and JT (β_2) on QRS from multiple regression models containing a heart rate correction term as a covariate with QRS (Model 1 and 2) for various categories of conduction defects

Figure 4.3 summarizes the relationship between regression coefficients β_1 and β_2 for QRS regression on QT and JT. It was noted that as the values of QRS regression coefficient for QT progressively increased from 0.29 to incomplete LBBB to near unity for IVCD, the values of QRS regression coefficient for JT decreased from -0.71 for incomplete LBBB to near zero for IVCD, in such a fashion that for all categories $\beta_2 = \beta_1 - 1$. This result was due to a functional relationship between the statistical models chosen for the analysis, as will be pointed out in the discussion section.

4.3.5. Comparison of QT and JT prediction accuracy

In comparing the performance of various statistical models for QT and JT prediction, R-square values do not reveal all information needed for comparative evaluation. Furthermore, in view of the relatively small influence of QRS duration on the JT interval, a new set of JT prediction formulas was deemed necessary. Root-mean-square errors (RMSE) for all four statistical models listed in Table 4.13 was used to determine prediction accuracy. It was seen that the root-mean-square error (RMSE) for JT in model 4, ranged from 19 to 28 for various ventricular conduction defects categories, with 19 for normal conduction. This finding was almost identical to that in other models. Thus the single-parameter model for the JT prediction model (4) containing only the correction factor for heart rate, performs as well as the other more complex models, for instance, the three-parameter model used for the QT prediction (model 1).

Table 4.13. - Comparison of JT prediction accuracy of a single-parameter formula (Model 4 and same formula with intercept (Model 3), with three-parameter QT and JT prediction formulas (Models 1 and 2 from Table 4.12). RMSE (ms) is the root-mean-square error of prediction. RF is the rate correction factor defined in Table 4.12

	Model 3 $QT=\alpha_3RF+\gamma_3$			Model 4 $JT=\alpha_4RF$		Model 1 $QT=\alpha_1RF+\beta_1QRS+\gamma_1$	Model 2 $JT=\alpha_2RF+\beta_2QRS+\gamma_2$
MC	α_3	γ_3	RMSE	α_4	RMSE	RMSE	RMSE
Normal	564	-30	20	518	19	19	19
LBBB	571	-36	25	511	25	25	25
RBBB	499	-7	24	485	24	24	24
IVCD	563	-39	28	498	28	28	28
IRBBB	568	-35	19	509	19	18	18
ILBBB	519	-8	20	507	20	20	20

4.4. Excitation-repolarization relationship in normal conduction and in ventricular conduction defects

The temporal and spatial relationships of left ventricular excitation and repolarization in various phases of excitation and repolarization were examined in this section by means of vectorcardiograms derived from instantaneous QRS and T vectors and QRS - T correlation maps constructed for orthogonal X, Y and Z leads.

4.4.1. Population description

The study population for this investigation was a subset of 5828 normal subjects and 807 with ventricular conduction defects. The group with various categories of ventricular conduction defects was stratified into five subgroups of complete and incomplete bundle branch blocks by definitions of the Minnesota Code.

4.4.2. The vectorcardiograms of QRS and T vectors in horizontal, frontal and sagittal plane projections

Data for spatial vector loops are summarized in Tables 4.14 to 4.16.

Vectorcardiographic data will be presented first.

a). Normal conduction

The vectorcardiograms of QRS and T vectors in horizontal, frontal, and sagittal, plane projections for 5828 subjects with normal ventricular conduction, are shown in Figures 4.4 to 4.6.The initial QRS vectors (phases 1 to 5) represent mostly the septal and paraseptal activation, and they were directed mainly anteriorly and slightly superiorly. The body of the loop represents dominantly left ventricular excitation, with the increasing phase of the main activation vector (3 to 10) representing the excitation of the apex and anterior/lateral free wall of the left ventricle, directed to the left, inferiorly and anteriorly, and the decreasing phase (8 to 16) displaced inferiorly, posteriorly, and to the left. These vectors of the decreasing phase represent mainly the excitation of the posterior wall of left ventricle The terminal vectors (16 to 20) were directed posteriorly, superiorly, and to the right. These vectors represent the activation of the posterobasal portion of the ventricles and interventricular septum.

The spatial direction of the T vectors was remarkably uniform, and all these vectors from phases seven on, were directed to the left, inferiorly, and forward. The first seven T vectors were relatively small regarding their spatial magnitude, and they were directed mainly forward and up. These observations indicated that

with the exception of the initial phase, the spatial direction of the normal

repolarization was quite uniformly from left to right, upwards, and from the front to

back. The spatial direction of the early initial repolarization was also from front to

back, but downwards rather than up (Table 4.14).

NORMAL QRS LOOP

Frontal plane

X 100
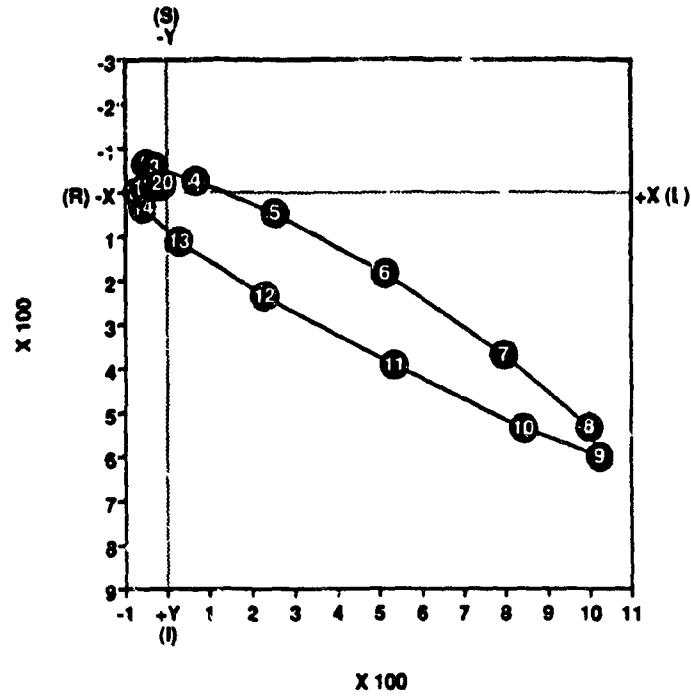
NORMAL T LOOP

Frontal plane

X 100

Figure 4.4. Frontal plane projection of the orthogonal QRS and T vectors at 20 instances of the time-normalized excitation (QRS) and repolarization (T) periods in normal conduction.

NORMAL QRS LOOP

Horizontal plane

X 100

NORMAL T LOOP

Horizontal plane

X 100

Figure 4.5. Horizontal plane projection of the orthogonal QRS and T vectors at 20 instances of the time-normalized excitation (QRS) and repolarization (T) periods in normal conduction.

Figure 4.6. Sagittal plane projection of the orthogonal QRS andT vectors at 20 instances of the time-normalized excitation (QRS) and repolarization (T) periods in normal conduction.

b). IRBBB (Incomplete right bundle branch block)

A perusal of the vectorcardiograms of QRS and T vectors in frontal, horizontal, and sagittal, plane projections for 319 patients with an incomplete right bundle branch block (Figures 4.7 to 4.9), revealed that the initial QRS vectors (phases 1-6) were directed to the right, superiorly, and anteriorly. The main spatial QRS vectors (phases 3-12) were oriented to the left and anteriorly. Like normal conduction, the main temporal contributions to these vectors come from the left ventricular free wall (Table 4.14). The terminal vectors (phases 16-20) were directed to the right, superiorly and posteriorly. The main T vectors were quite uniformly directed to the left, inferiorly and anteriorly. This evidence indicated that the repolarization direction was predominantly from left to right, upward and from the front to the back.

Figure 4.7. Frontal plane projection of the orthogonal QRS and T vectors at 20 instances of the time-normalized excitation (QRS) and repolarization (T) periods in IRBBB.

Incomplete RBBB QRS LOOP

Horizontal plane

Incomplete RBBB T LOOP

Horizontal plane
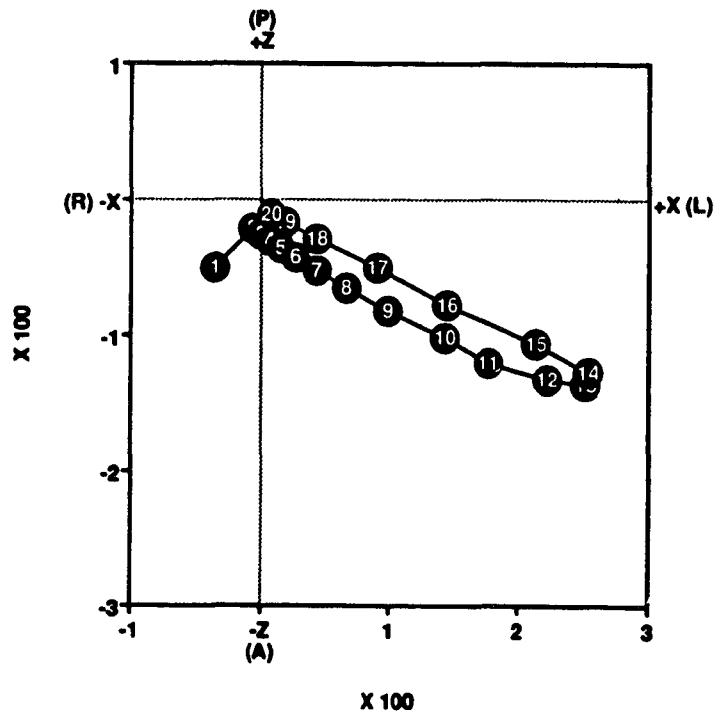
Figure 4.8. Horizontal plane projection of the orthogonal QRS and T vectors at 20 instances of the time-normalized excitation (QRS) and repolarization (T) periods in IRBBB.

Incomplete RBBB QRS LOOP

Sagittal plane

X 100
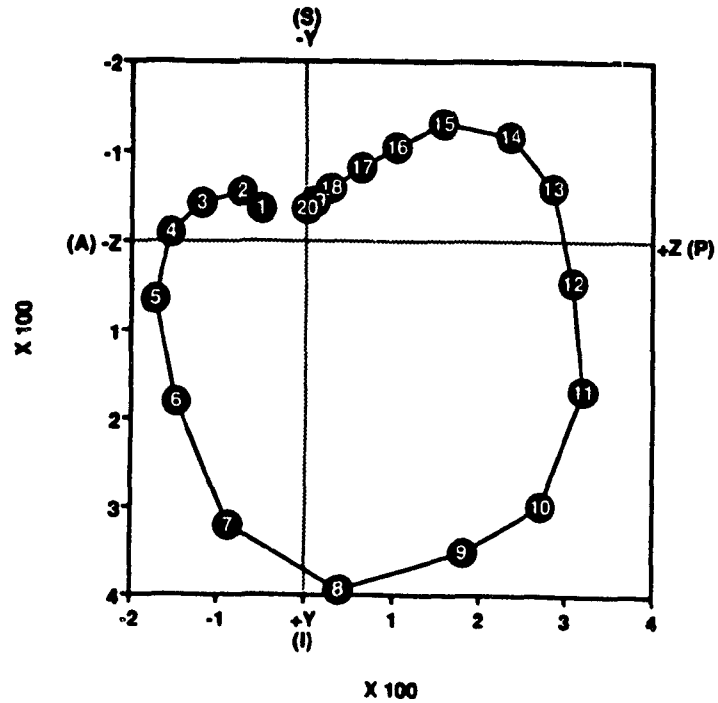
Incomplete RBBB T LOOP
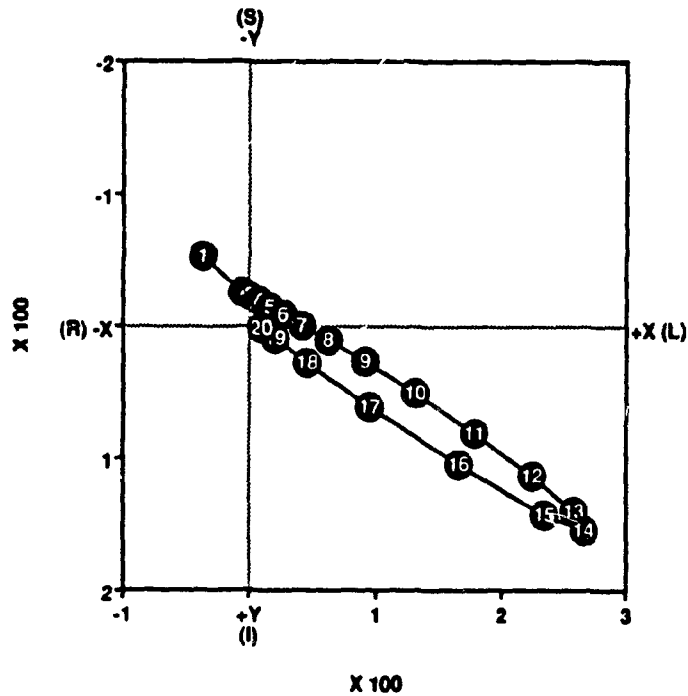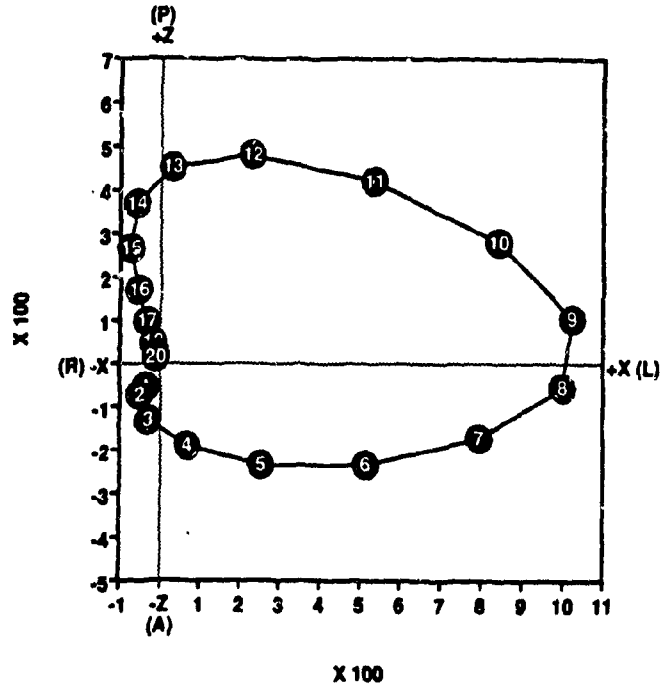
Sagittal plane

X 10
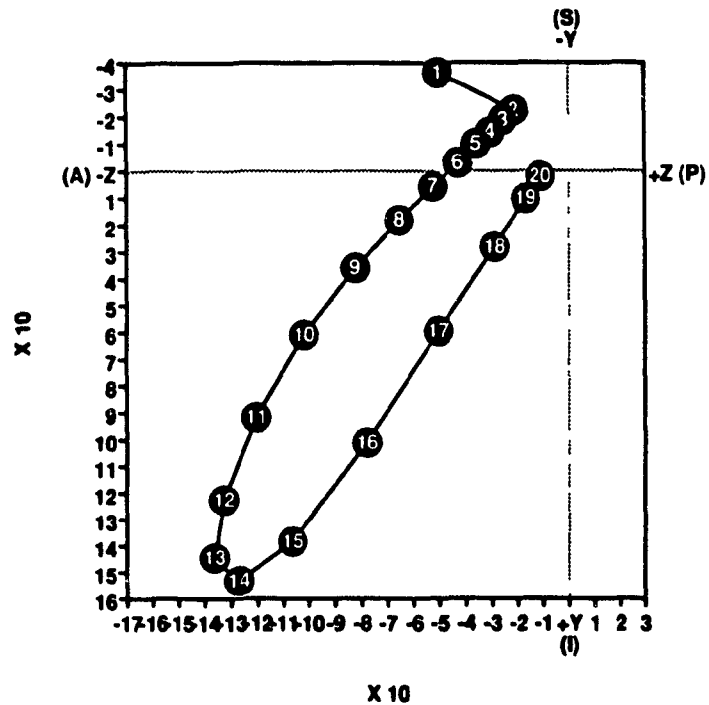
Figure 4.9. Sagittal plane projection of the orthogonal QRS and T vectors at 20 instances of the time-normalized excitation (QRS) and repolarization (T) periods in IRBBB

c). ILBBB (Incomplete left bundle branch block)

In Figures 4.10 to 4.12, the initial QRS vectors (1-5) were directed anteriorly and to the left. The main activation (6-12) was uniformly oriented to the left and posteriorly, with the terminal QRS vectors (12-20) located in right, posterior, and superior direction. With the exception of the initial T vectors (phases 1-6), the spatial directions of the T vectors were remarkably uniform, directed to the left, anteriorly, and inferiorly. Thus the dominant direction of repolarization v. as from left to right, upward, and to the back (Table 4.14).

Incomplete LBBB QRS LOOP

Frontal plane

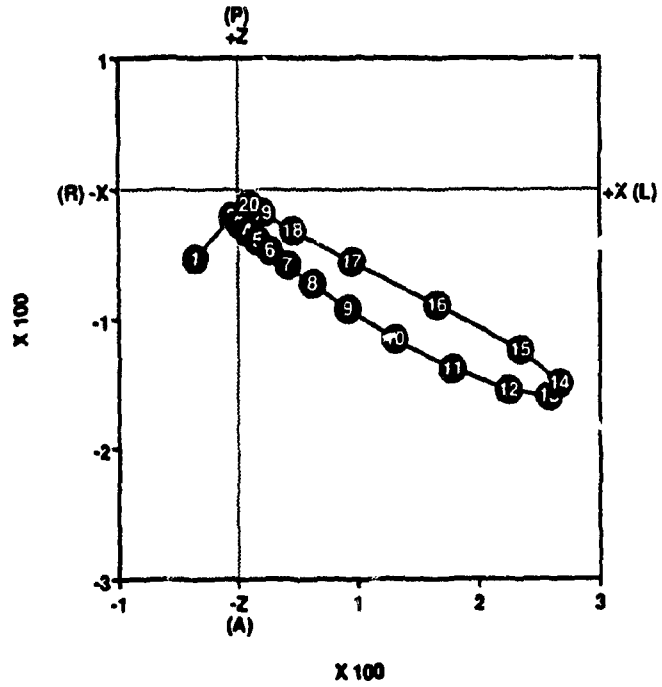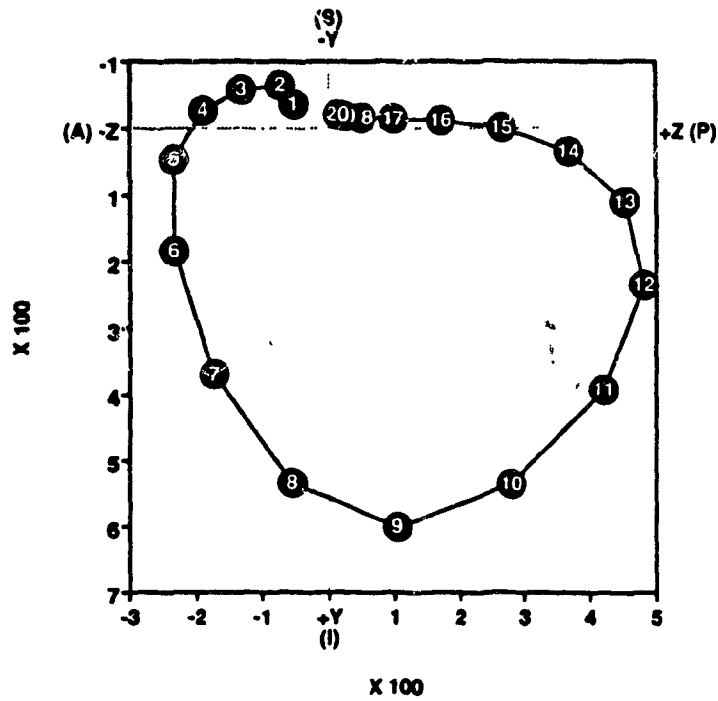X 100

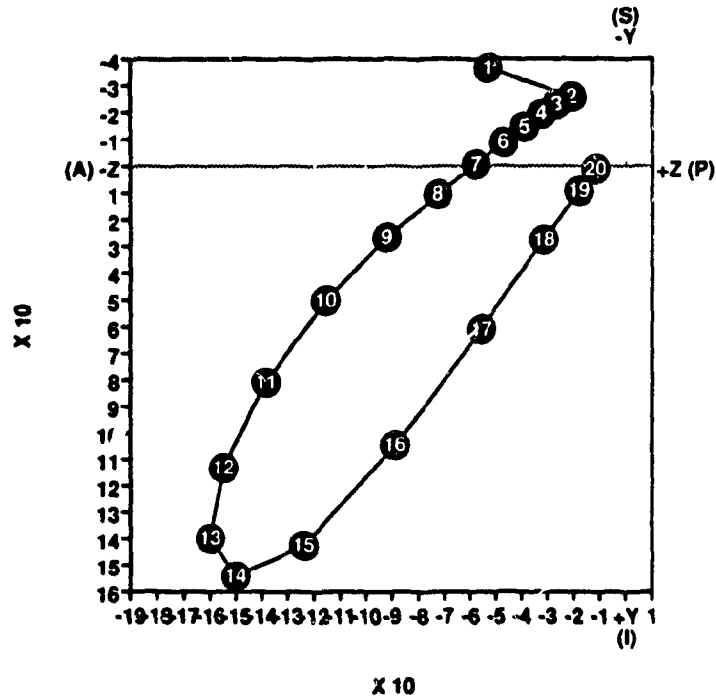**Incomplete LBBB T LOOP**

Frontal plane

X 10

Figure 4.10. Frontal plane projection of the orthogonal QRS and T vectors at 20 instances of the time-normalized excitation (QRS) and repolarization (T) periods in ILBBB.

Incomplete LBBB QRS LOOP

Horizontal plane

X 100

Incomplete LBBB T LOOP

Horizontal plane

X 100

Figure 4.11. Horizontal plane projection of the orthogonal QRS and T vectors at 20 instances of the time-normalized excitation (QRS) and repolarization (T) periods in ILBBB.
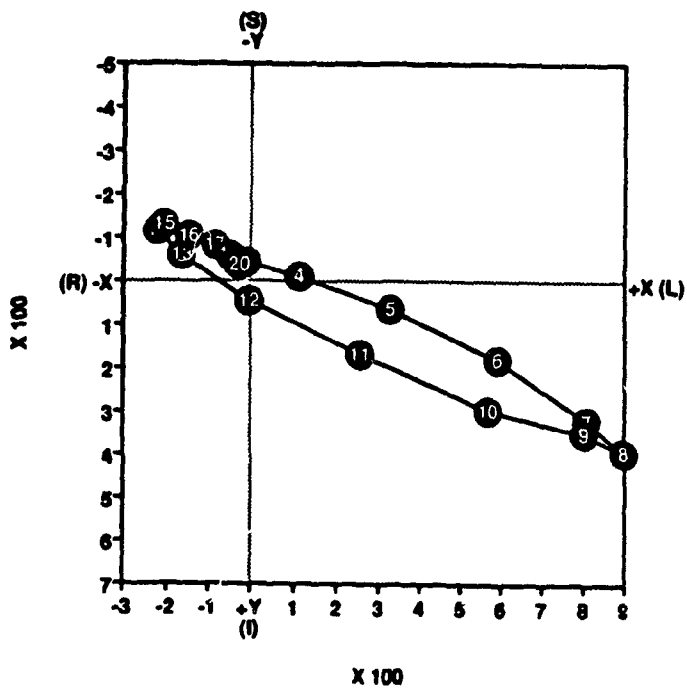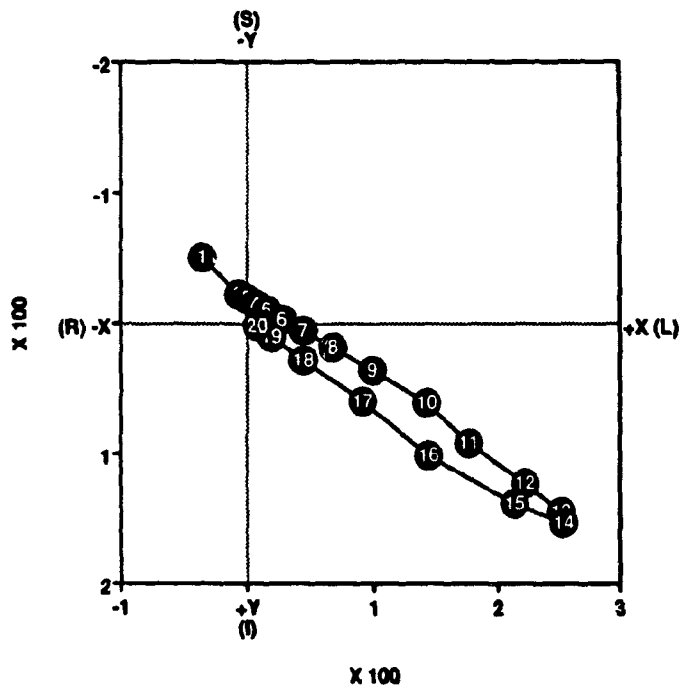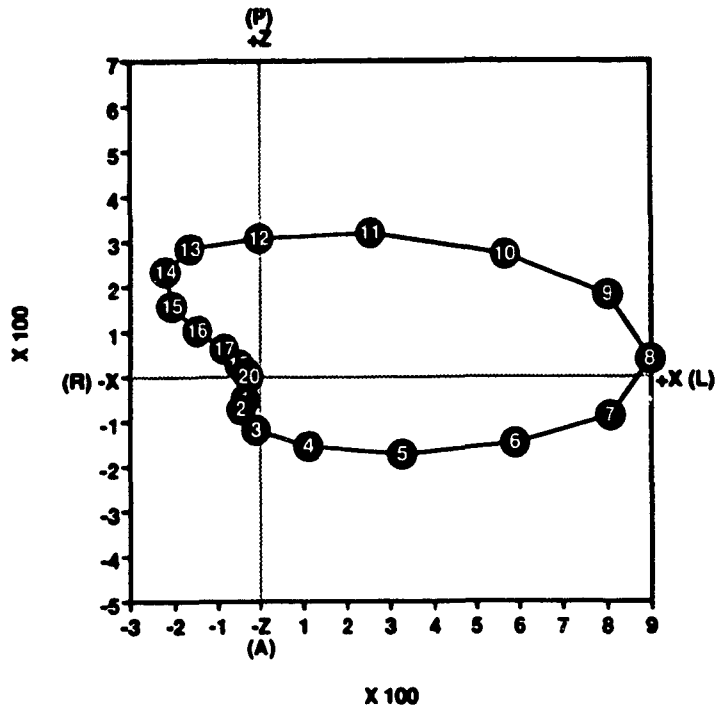
Figure 4.12. Sagittal plane projection of the orthogonal QRS and T vectors at 20 instances of the time-normalized excitation (QRS) and repolarization (T) periods in ILBBB.

Table 4.14. Temporal regional sequence of the left ventricular depolarization process and dominant spatial direction of the corresponding QRS vectors, assumed temporal correspondence of the T vectors reflecting repolarization in these same regions, T vector spatial directions and the likely dominant directions of the repolarization process in normal conduction, IRBBB and ILBBB. It is assumed that the left ventricular influence on the surface ECGs dominates and that the right ventricular influence can be ignored as a first approximation

	Region Sequence	Depolarization			Repolarization					
		Temporal sequence	QRS vector	Dominant direction	Assumed temporal sequence	T vector	Dominant direction	Repolarization direction	Ø	
Normal	LV septum	1	1-5	A	2	9-14	LAI	RPS	69	Semi-reverse
	Anterior/lat wall	2	3-10	LIA	1	1-7	AS	PI	82	Intermediate
						8-16	LAI	RPS	25	Reverse
	posterior wall	3	8-18	LPI	4	14-20	LAI	RPS	42	Semi-reverse
	Base	4	16-20	RPS	3	12-18	LAI	RPS	144	Concordant
IRBBB	LV septum	1	1-4	RSA	?	?	?	?		
	Apex LV antero/	1	3-8	LIA	2	9-17	LI	RS	41	Semi-reverse
	lateral wall	2	8-12	L	1	1-9	L	R	84	Intermediate
	Posterior wall	3	8-16	LP	4	16-20	LA	RSP	71	Semi-reverse
	Base	4	16-20	RSP	3	14-18	LIA	RSP	170	Concordant

Table 4.14. Temporal regional sequence of the left ventricular depolarization process and dominant spatial direction of the corresponding QRS vectors, assumed temporal correspondence of the T vectors reflecting repolarization in these same regions, T vector spatial directions and the likely dominant directions of the repolarization process in normal conduction, IRBBB and ILBBB. It is assumed that the left ventricular influence on the surface ECGs dominates and that the right ventricular influence can be ignored as a first approximation (Continued)

	Region	Depolarization			Repolarization				
		Temporal sequence	QRS vector	Dominant direction	Assumed temporal sequence	T vector	Dominant direction	Repolarization direction	Sequence
								$\emptyset$	
ILBBB	Septum	1	1-5	LA	?	?	?	?	
	Apex	2	6-11	LIP	2	5-12	LA	RP	81	Intermediate
	Anterolateral free wall	1	1-12	L	1	1-10	LSA	RIP	106	Intermediate
	Posterior wall	3	7-11	LP	4	10-20	LIA	RSP	99	Intermediate
	Base	4	12-20	RPS	3	7-16	LIA	RSP	168	Concordant

A = Anterior   S = Superior   L = Left   LV = Left ventricle   P = Posterior   I = Inferior   R = Right
RV = Right ventricle $\emptyset$ = estimated values for the QRS/T angle

d). Left bundle branch block

Figures 4.13 to 4.15 show the mean vectorcardiograms of QRS and T vectors of 45 patients with left bundle branch block. The initial QRS vectors (phases 1 to 9) represent the right ventricular septum and right ventricular lateral wall, and the spatial vectors 3 to 14 represent the left ventricular anterior and lateral walls. These vectors were directed towards the left, posteriorly and inferiorly. QRS vectors of phases 15 to 20 represented the anterobasal region of the left ventricle. They were predominantly in superior position. The spatial direction of the T vectors from phase 2 to 14 were directed to the right, superiorly and anteriorly. This indicates that the dominant repolarization direction was from right to left and from anterior to posterior, concordant with respect to depolarization. The last five T vectors were comparatively small in terms of spatial magnitude, and were primarily located to the left and inferiorly. Thus the dominant direction of repolarization was upward,and to the right. It is concordant with depolarization.

LBBB QRS LOOP

Frontal plane

X 100

LBBB T LOOP
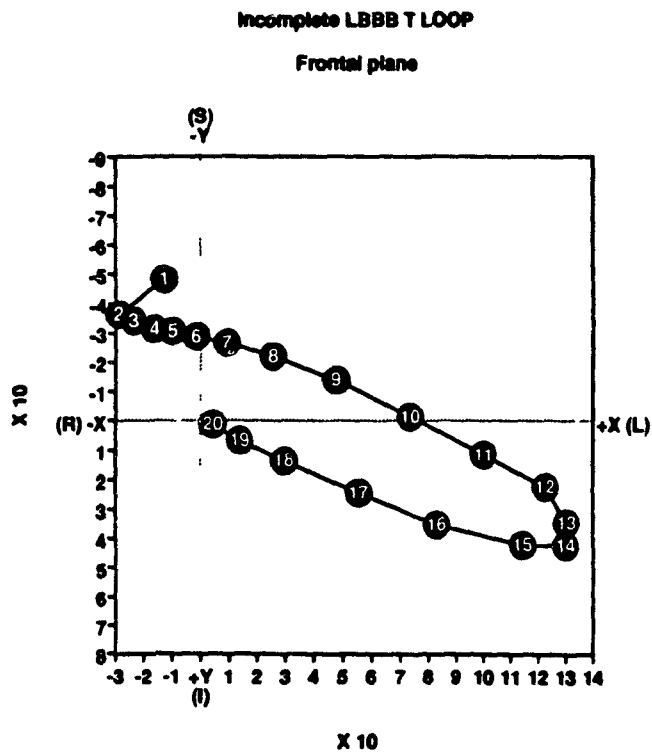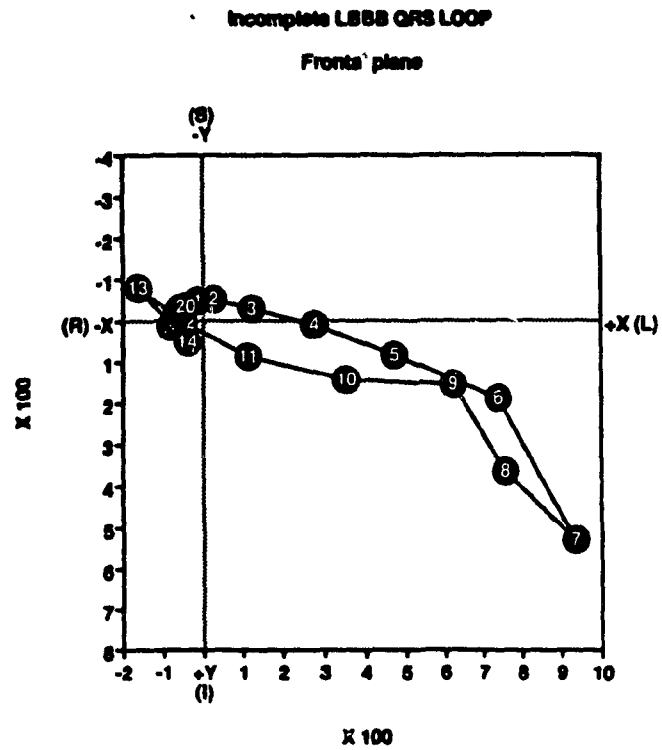
Frontal plane

X 10

Figure 4.13. Frontal plane projection of the orthogonal QRS and T vectors at 20 instances of the time-normalized excitation (QRS) and repolarization (T) periods in LBBB.
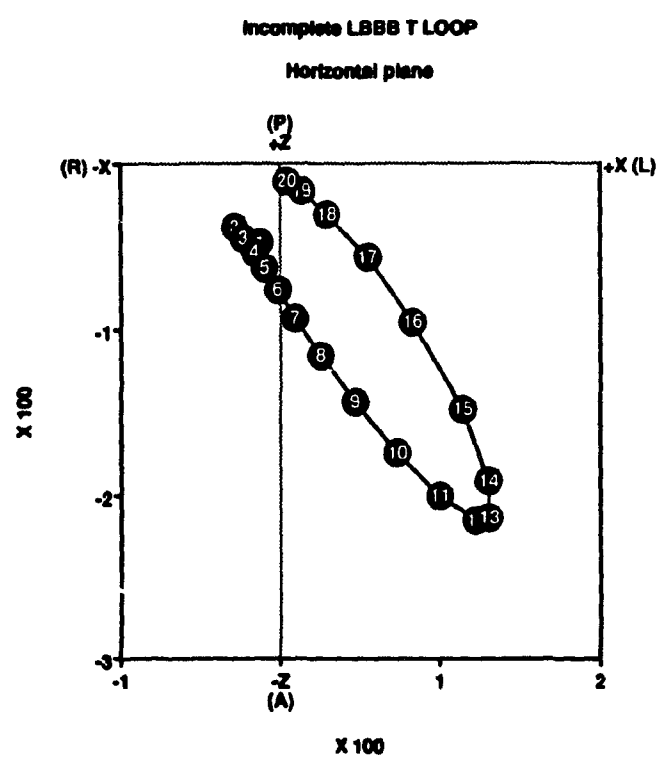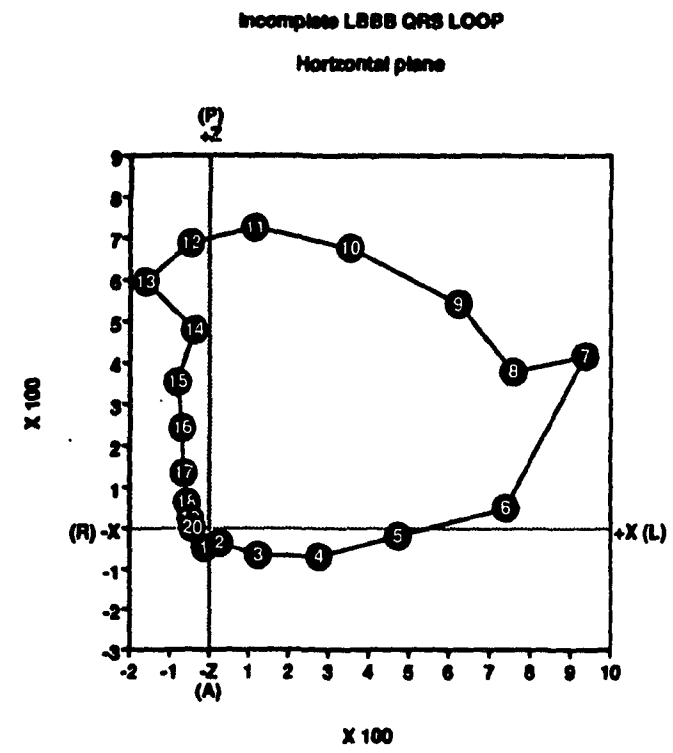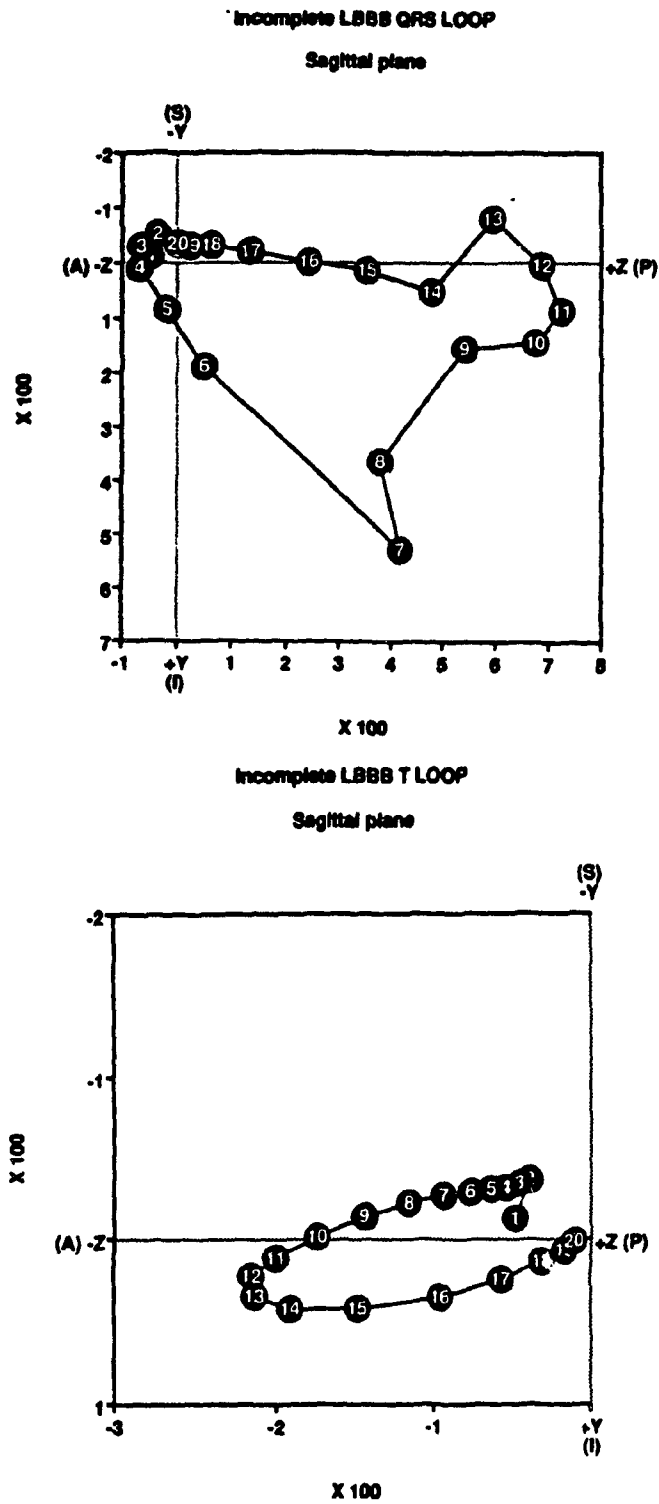
Figure 4.14. Horizontal plane projection of the orthogonal QRS and T vectors at 20 instances of the time-normalized excitation (QRS) and repolarization (T) periods in LBBB

LBBB QRS LOOP

Sagittal plane

X 100

LBBB T LOOP

Sagittal plane

X 100

Figure 4.15. Sagittal plane projection of the orthogonal QRS and T vectors at 20 instances of the time-normalized excitation (QRS) and repolarization (T) periods in LBBB.

e). Complete block of unspecified type (IVCD)

An inspection of QRS and T vectors (Figures 4.16 - 4.18) revealed that the initial QRS vectors (1 - 6) were directed to the right and forward. The main activation of the right ventricle (4 - 8) and left ventricle (7-16) was directed to the left, inferiorly, and posteriorly. The terminal QRS vectors (13-20) were in a right and superior direction. With the exception of the initial T vectors (phases 1-6), the main T vectors were directed to the left and inferiorly. Thus, the dominant direction of repolarization was from left to right, upward and from front to back, shown in Table 4.15.

IVCD QRS LOOP

Frontal plane

X 100

IVCD T LOOP

Frontal plane

X 100

Figure 4.16. Frontal plane projection of the orthogonal QRS and T vectors at 20 instances of the time-normalized excitation (QRS) and repolarization (T) periods in IVCD.

IVCD QRS LOOP

Horizontal plane

X 100

IVCD T LOOP

Horizontal plane

X 100

Figure 4.17. Horizontal plane projection of the orthogonal QRS and T vectors at 20 instances of the time-normalized excitation (QRS) and repolarization (T) periods in IVCD.

IVCD QRS LOOP

Sagittal plane

X 100

IVCD T LOOP

Sagittal plane

X 100
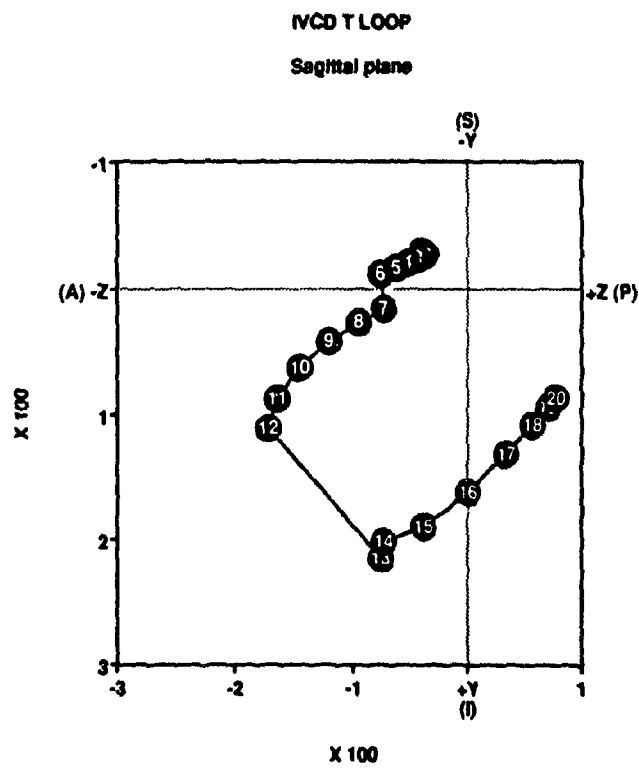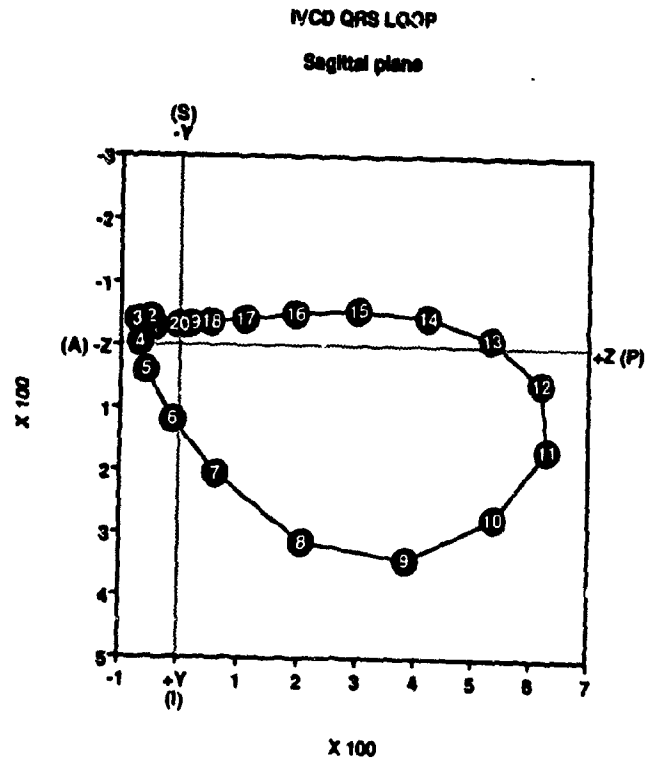
Figure 4.18. Sagittal plane projection of the orthogonal QRS and T vectors at 20 instances of the time-normalized excitation (QRS) and repolarization (T) periods in IVCD.

Table 4.15. Temporal regional sequence of the left ventricular depolarization process and dominant spatial direction of the corresponding QRS vectors, assumed temporal correspondence of the T vectors reflecting repolarization in these same regions, T vector spatial directions and the likely dominant directions of the repolarization process in LBBB and IVCD. It is assumed that the anterobasal region of left ventricle dominantly influence the surface ECGs.

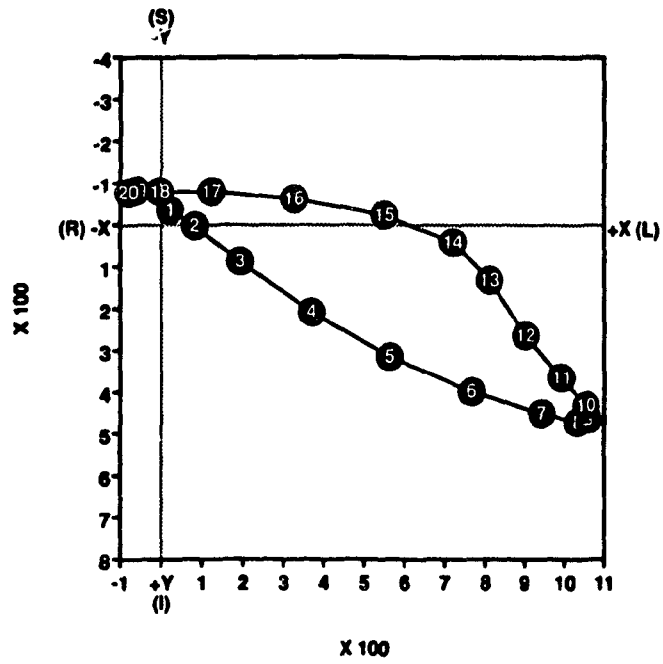|	Region	Depolarization			Repolarization					
		Temporal sequence	QRS vector	Dominant direction	Assumed temporal sequence	T vector	Dominant direction	Repolarization direction	Ø	Sequence
LBBB	Septum	1	1-9	LIP	2?	2-10	RSA	LIP	170	Concordant
	RV	1	1-9		2	6-10	RA	LP	167	Concordant
	LV free wall	2	3-14	LIP	1	1-14	RAS	LIP	175	Concordant
	Anterobasal IV	3	15-20	LSP	3	14-20	LI	RS	142	Semi-concordant
IVCD	Septum RV Lateral	1	1-6	LA	?	?	?	?	?	
	wall	1	4-8	LIA	2	10-16	LIA	RP	36	Reverse
	LV free wall	2	7-16	LIP	1	1-6	RS	LIP	145	Concordant
	Anterobasal LV	3	13-20	RSP	3	11-20	LIP	RSA	110	Semi Concordant

A = Anterior   S = Superior   L = Left   LV = Left ventricle
P = Posterior   I = Inferior   R = Right   RV = Right ventricle   Ø = estimated values for the QRS/T angle

f). **Right bundle branch block**

The mean QRS and corresponding T vectors in frontal, horizontal, and sagittal plane projections of 166 patients with a right bundle branch block are shown in Figures 4.19 to 4.21. The initial QRS vectors (1-9) did not differ significantly from those of normal conduction. They were directed to the left and anteriorly. Like normal conduction, the main QRS vectors (2-10) were oriented to the left and anteriorly. Characteristic findings were represented by large terminal appendages (from 9 to 20). These vectors, located to the right and superiorly, represent the depolarization process in the right ventricle. All the T vectors were directed to the left and posteriorly.

Left ventricular excitation remains presumably normal in RBBB. Repolarization resembled fairly closely the normal patterns, with the exception of the right ventricle, because of the delayed activation. The dominant direction of repolarization of the right ventricle was to the right and upward. The main temporal contributions to the terminal T vectors come from the anterobasal region of the right ventricle.

RBBB QRS LOOP

Frontal plane

X 100
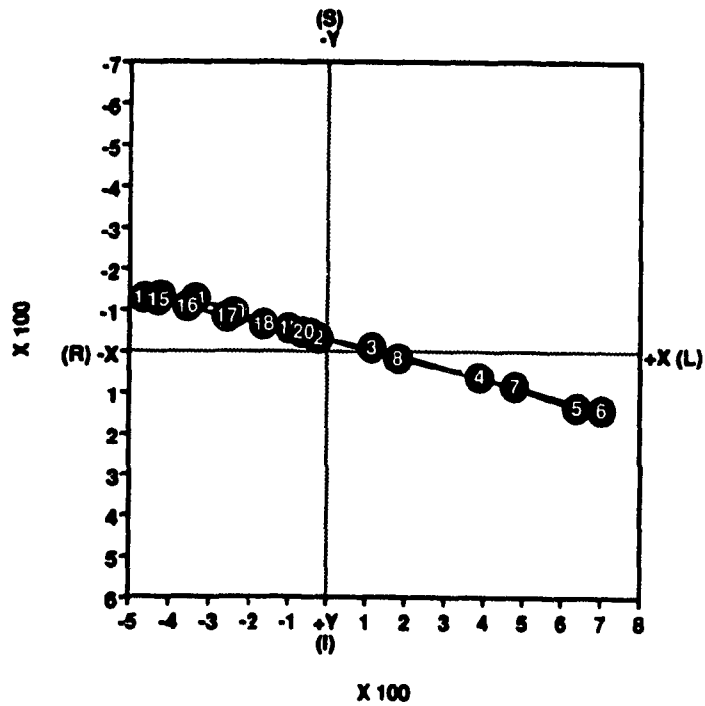
RBBB T LOOP

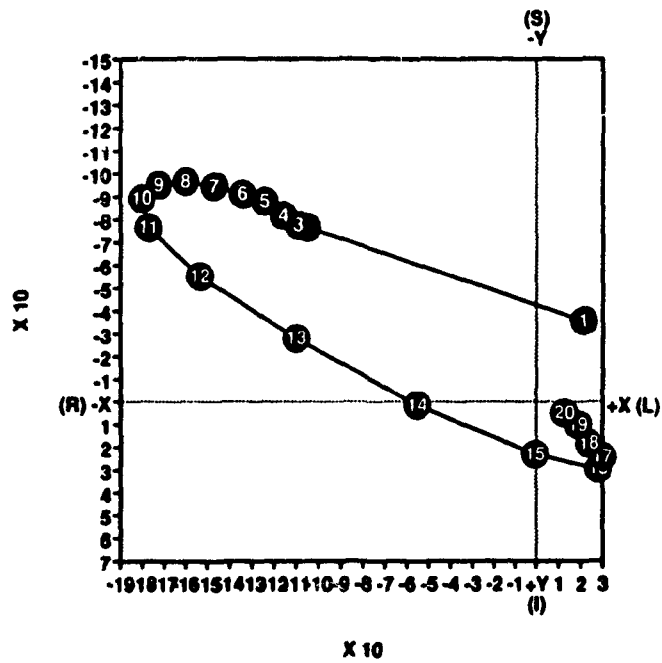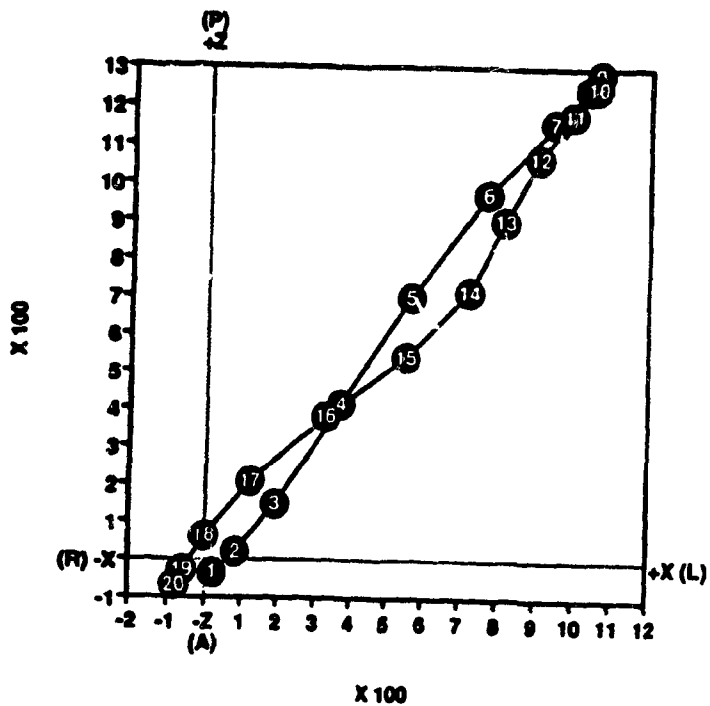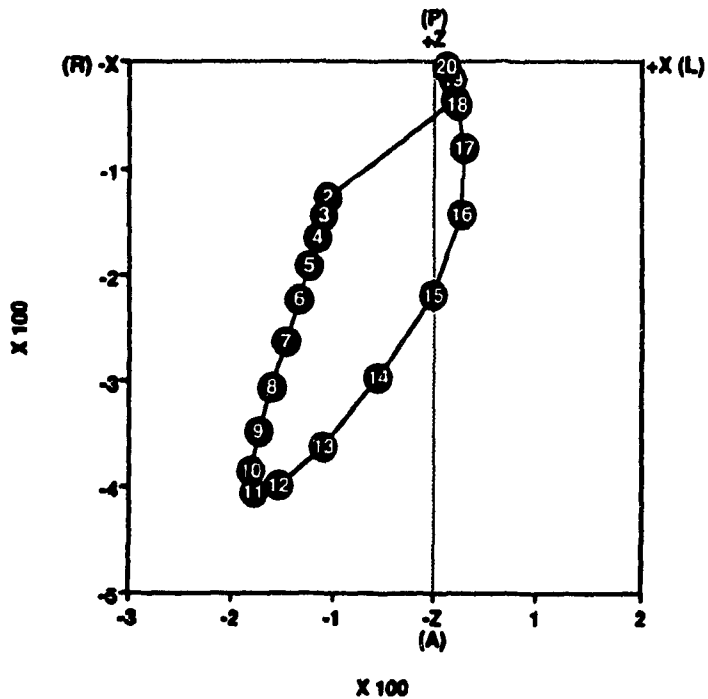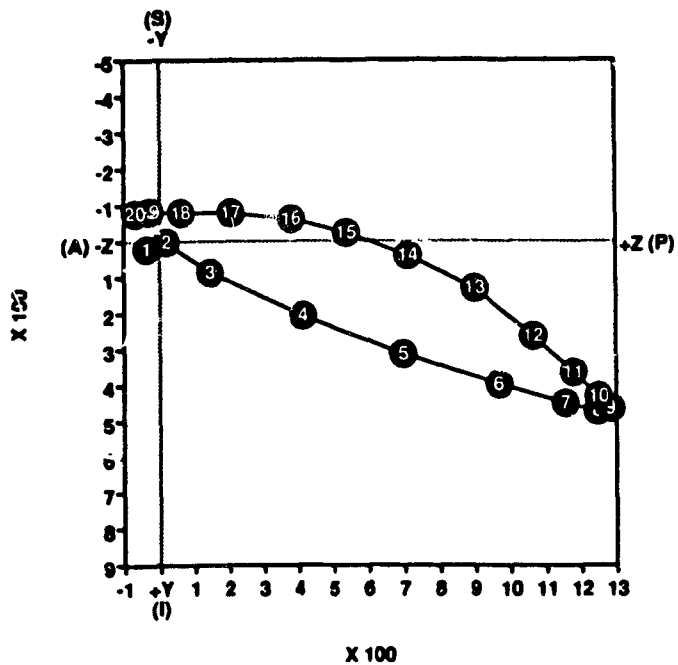**Frontal plane**

X 100
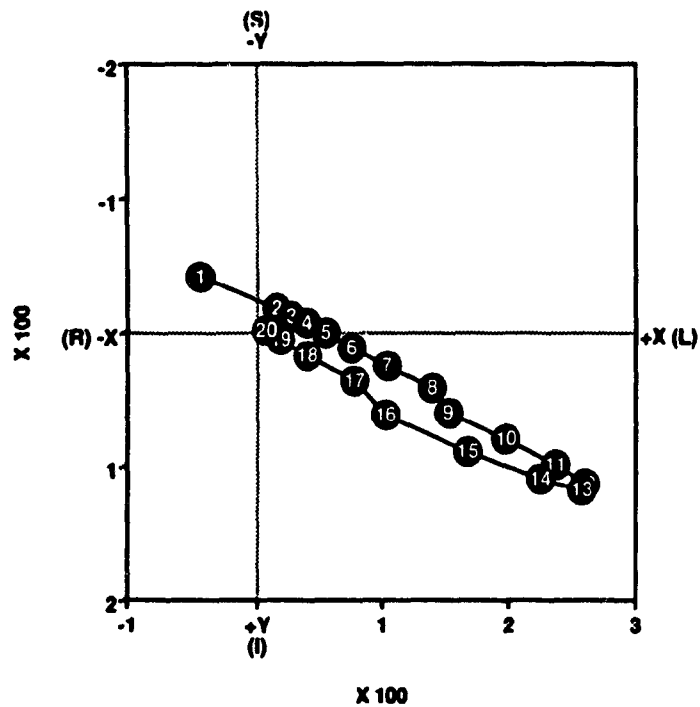
Figure 4.19. Frontal plane projection of the orthogonal QRS and to T vectors at 20 instances of the time-normalized excitation (QRS) and repolarization (T) periods in RBBB.

RBBB QRS LOOP

Horizontal plane

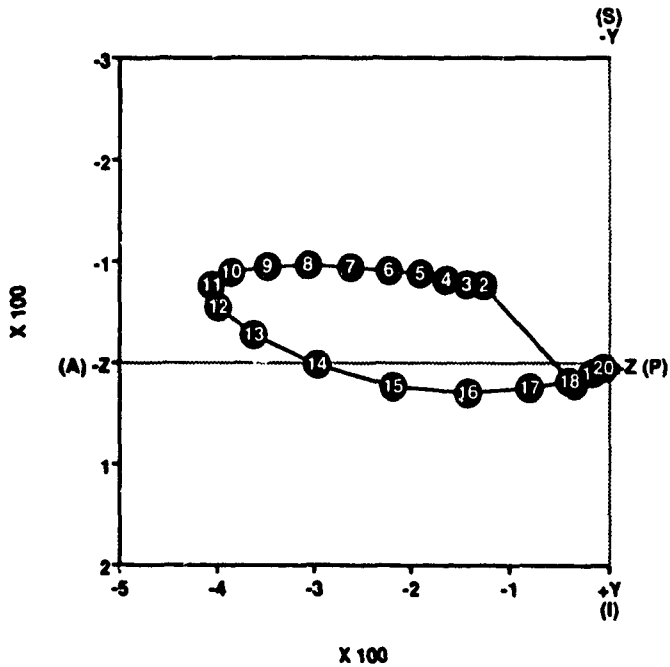**RBBB T LOOP**
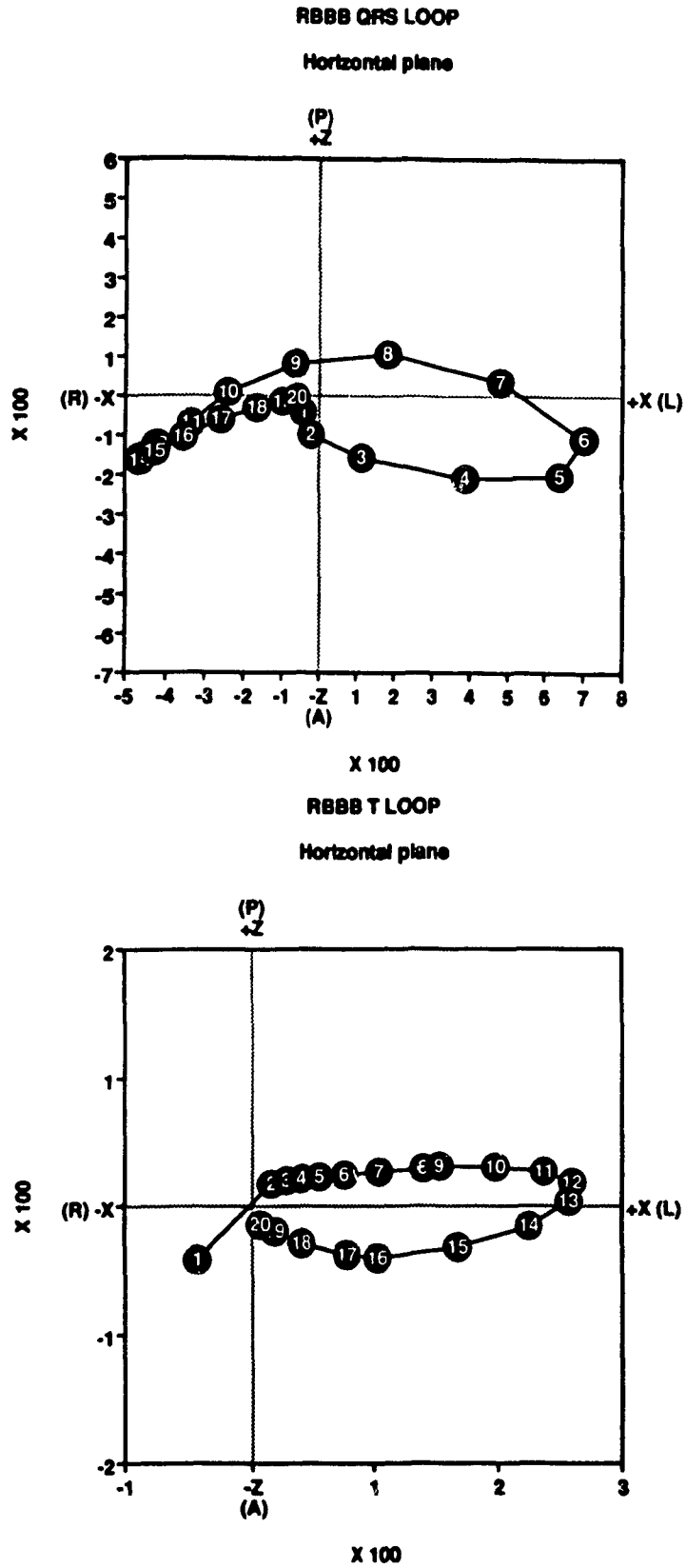
Horizontal plane

Figure 4.20. Horizontal plane projection of the orthogonal QRS and T vectors at 20 instances of the time-normalized excitation (QRS) and repolarization (T) periods in RBBB.

RBBB QRS LOOP

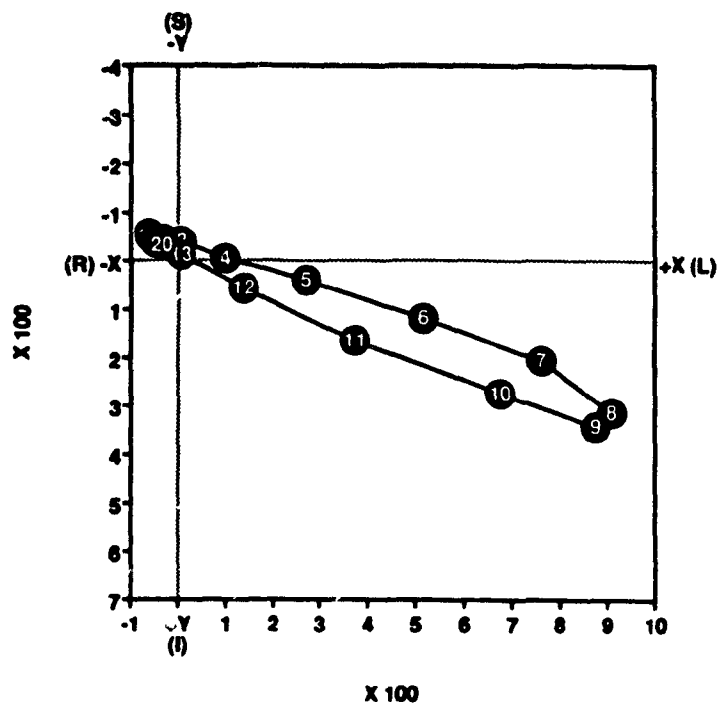**Sagittal plane**
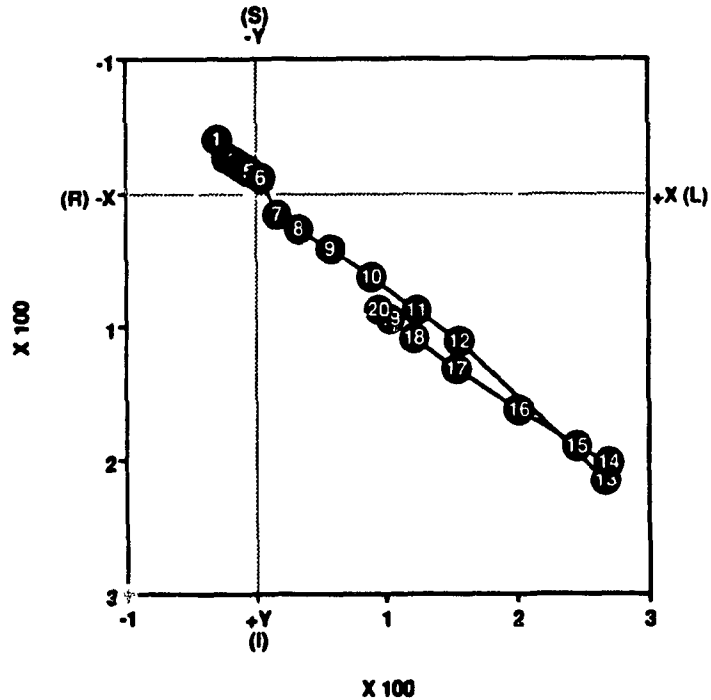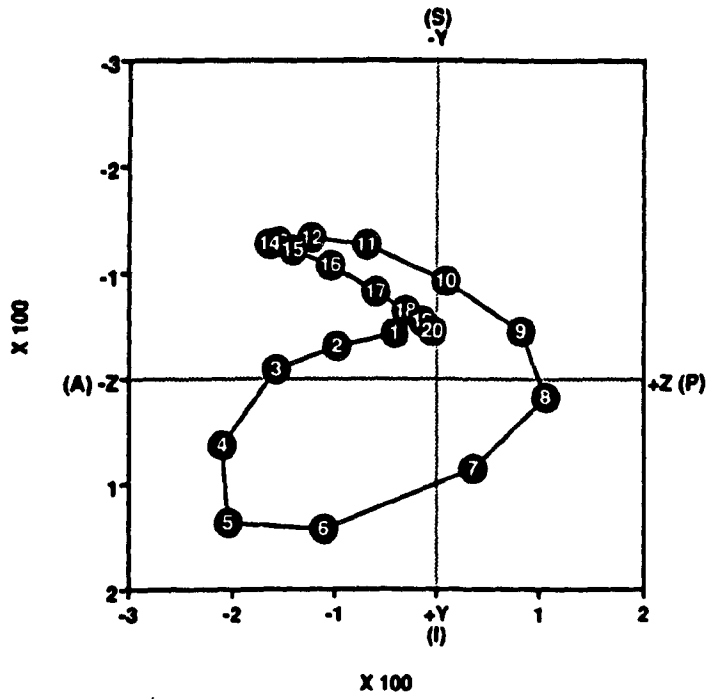

RBBB T LOOP

Sagittal plane
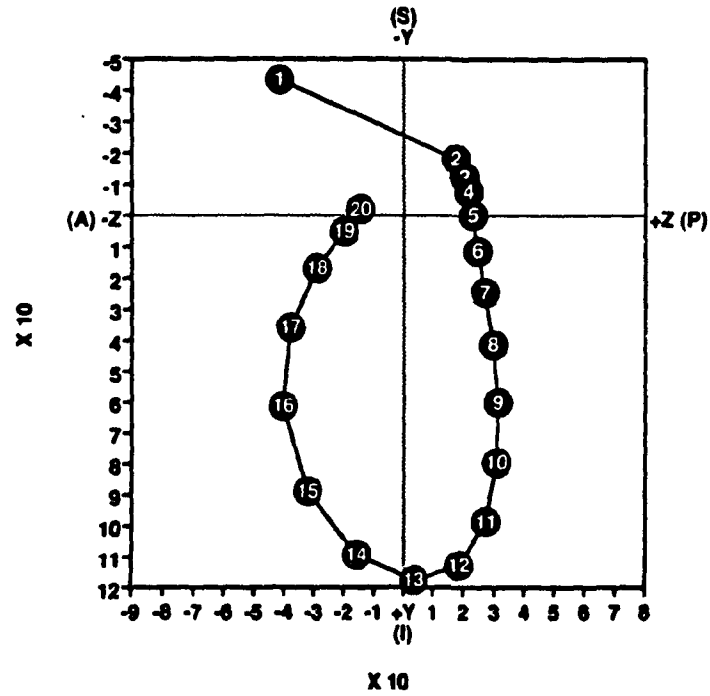
Figure 4.21 Sagittal plane projection of the orthogonal QRS and T vectors at 20 instances of the time-normalized excitation (QRS) and repolarization (T) periods in RBBB.
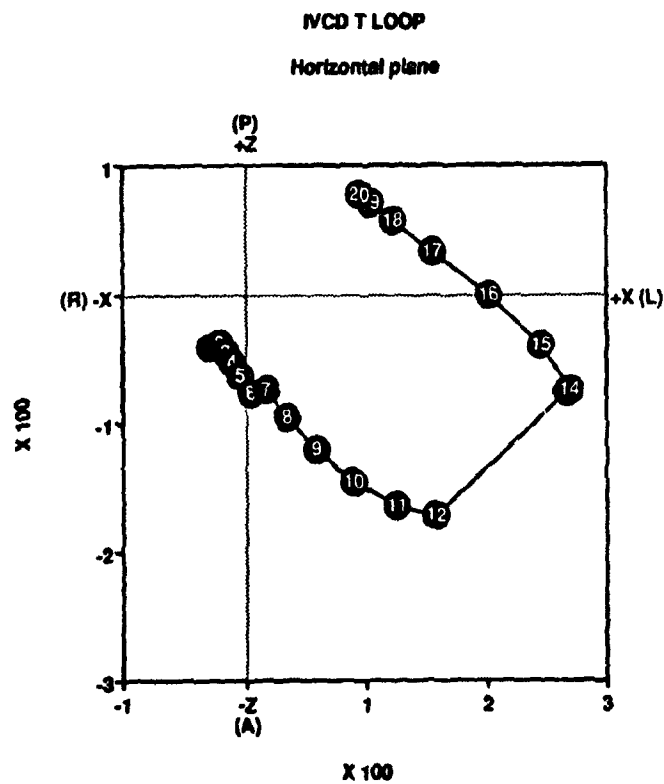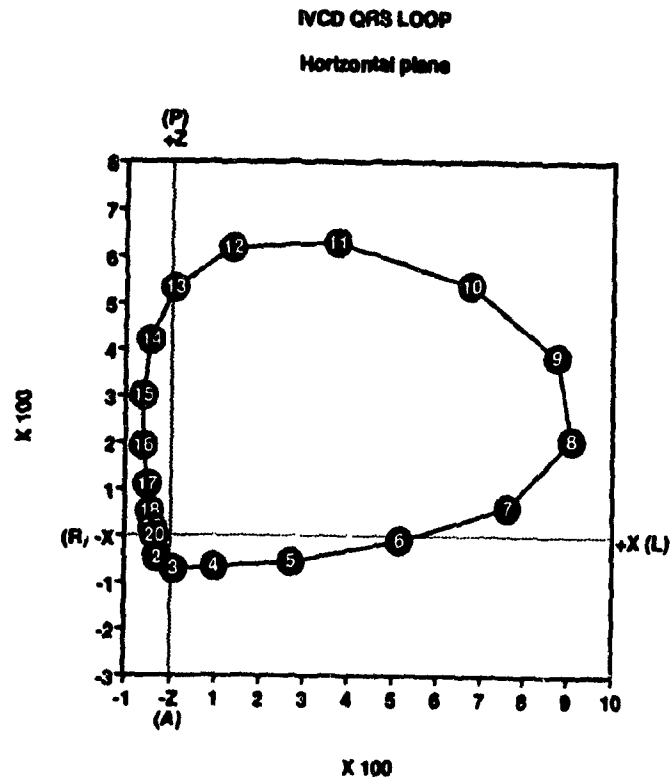
Table 4.16. Temporal regional sequence of the left ventricular depolarization process and dominant spatial direction of the corresponding QRS vectors, assumed temporal correspondence of the T vectors reflecting repolarization in these same regions, T vector spatial directions and the likely dominant directions of the repolarization process in RBBB. It is assumed that the anterobasal region of right ventricle dominantly influence the surface ECGs.

	Region	Depolarization			Repolarization				
		Temporal sequence	QRS vector	Dominant direction	Assumed temporal sequence	T vector	Dominant direction	Repolarization direction	sequence
							-	Ø	
RBBB	LV septum	1	1-8	LA	?	?	?	?	?
	Anterolat.LV	1	2-8	L	1	1-10	L	R	31	Reverse
	Posterior LV	2	6-16	RA	2	5-13	LP	RA	151	Concordant
	Lateral RV	3	9-16	R	3	6-15	L	R	165	Concordant
	Anterobasal RV (pulmonary Conus)	4	9-20	RA	4	13-20	LIA	RSP	156	Concordant

A = Anterior S = Superior L = Left   LV = Left ventricle

P = Posterior I = Inferior R = Right   RV = Right ventricle   Ø = estimated values for the QRS/T angle

4.4.3. QRS-T correlation maps

It is important to distinguish between regional temporal sequence (temporal order of repolarization from region to region) and local temporal/spatial sequence of repolarization with respect to excitation sequence.

4.4.3.1. Six-segment repolarization model of the left ventricle for normal conduction

Assumptions

Assumption 1). QRS vectors associated with uncancelled excitation potential differences (E vectors) are the only ones that contribute to the QRS-T correlation maps.

Assumption 2). There is no temporal overlap between the timing of the uncancelleded E vectors.

Assumption 3). There is no temporal overlap between the timing of the repolarizing regions S1-S6. This assumption will be relaxed if it becomes evident that a substantial temporal overlap exists.

The procedure followed is first described as it applies to the frontal plane cross-section of the left ventricle. Depolarization vectors E1 to E6 were visualized in the frontal plane in a cross-section of the human heart in Figure 4.22A. These vect'rs were derived as an approximation of the mean QRS vectors in Figure 4.23.

The segments considered are the following:

Segment 1. Excitation potential differences arising from the left endocardial portion of the septum (E1, corresponding to QRS vectors R1-R3, Figure 4.7).

Segment 2. Excitation potential differences arising from the anterior wall (E2, vectors R4-R6).

Segment 3. Anterolateral wall (E3, vectors R7-R9).

Segment 4. Posterolateral wall (E4, vectors R10-R11).

Segment 5. Posterior wall (E5, vectors R12-R15).

Segment 6. Basal regions (E6, vectors R16-R20).
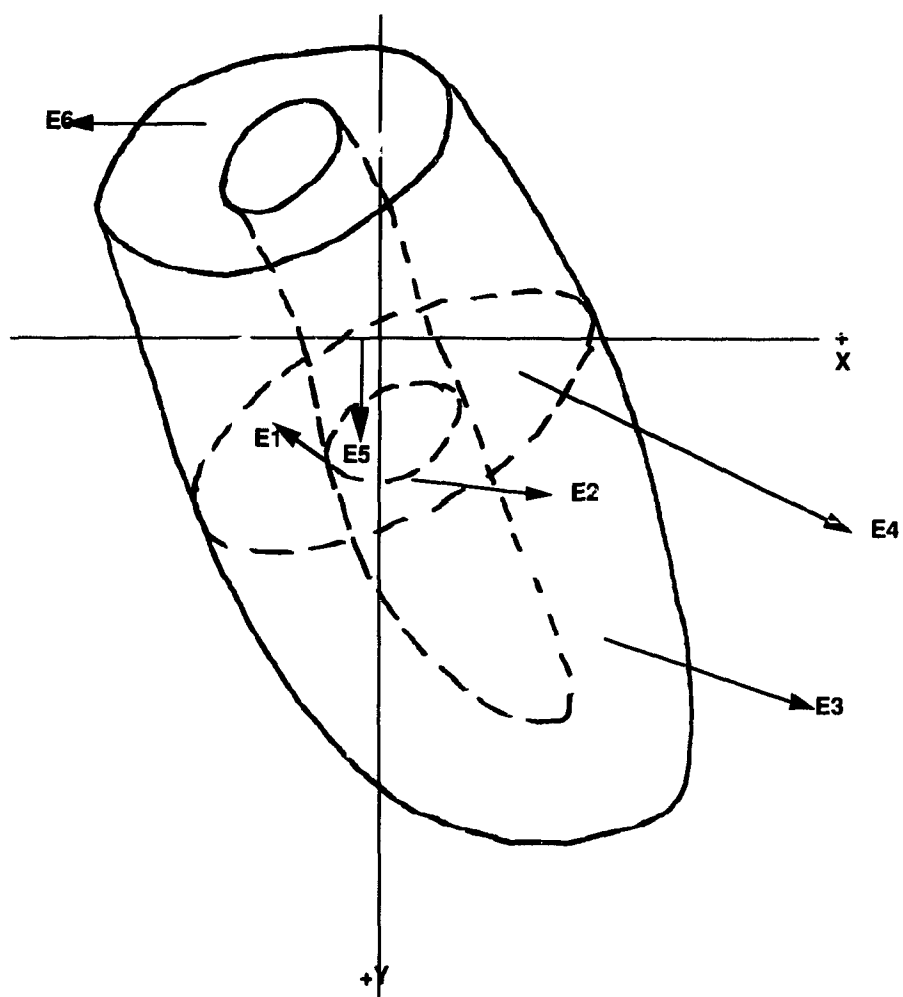
Figure 4.22A. A sketch of the frontal plane cross-section of human left ventricle with uncancelled excitation vectors E1 to E6 from six regional segments

NORMAL QRS LOOP

Frontal plane

X 100

NORMAL QRS LOOP

Sagittal plane

X 100
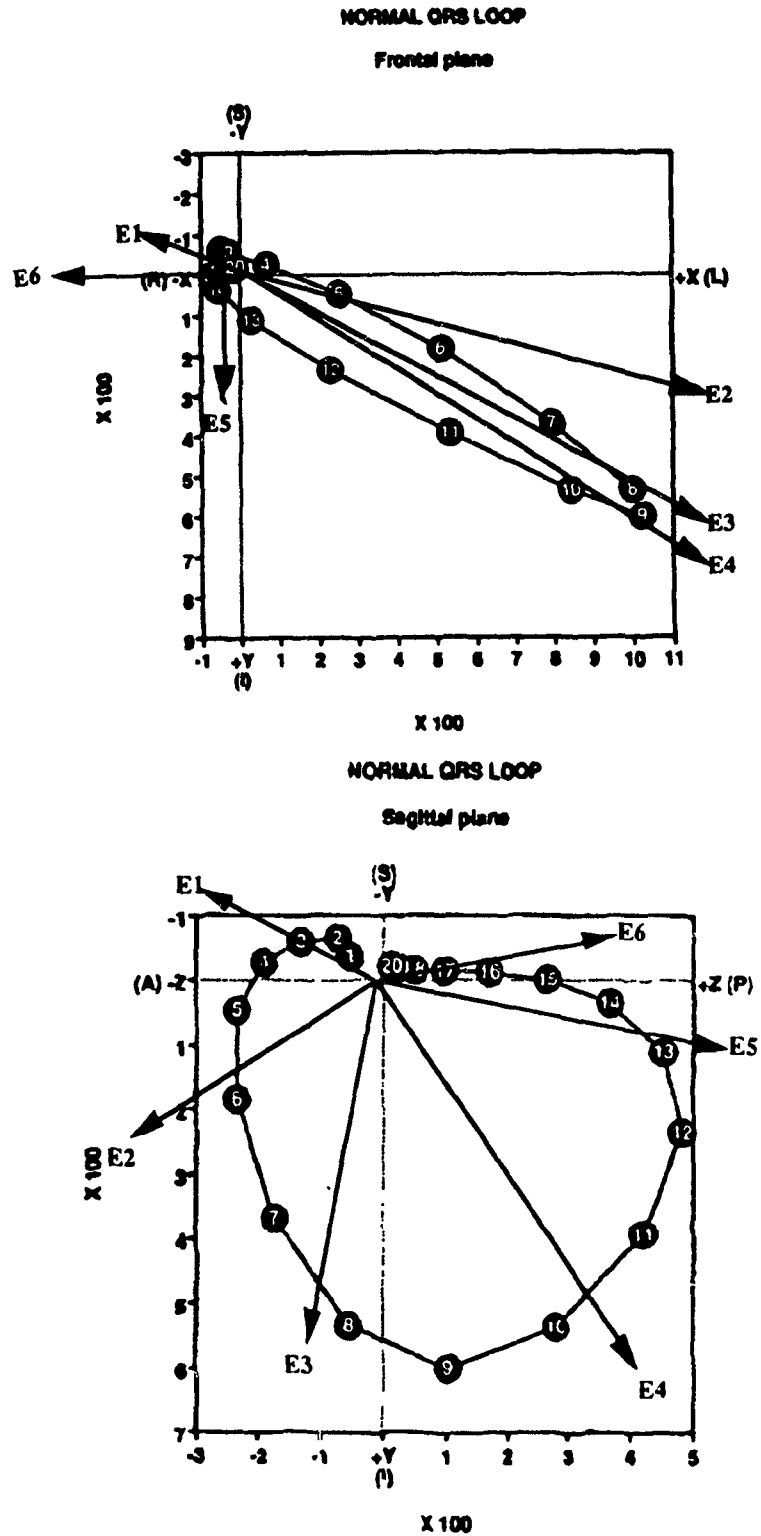
Figure 4.23. Estimated mean directions for mean QRS vectors corresponding to

E1 - E6 in the frontal plane (top) and sagittal plane (bottom) for normal conduction

The contributions of the apex are not considered separately since they are probably reasonably uniform with those of Segments 2 and 3.

Assumption 4). While the regional temporal sequence of excitation is fixed (vectors E1-E6), the regional temporal sequence of repolarization can occur in all possible permutations for Segments S1-S6, and the local spatial sequence in each region (j) can assume any of the directions depicted in Figure 4.24A in relation to the excitation vectors in each principal spatial plane considered, ranging from Sj1 (reverse) to Sj8 (concordant), and other directions from semireverse and intermediate to semiconcordant sequences.
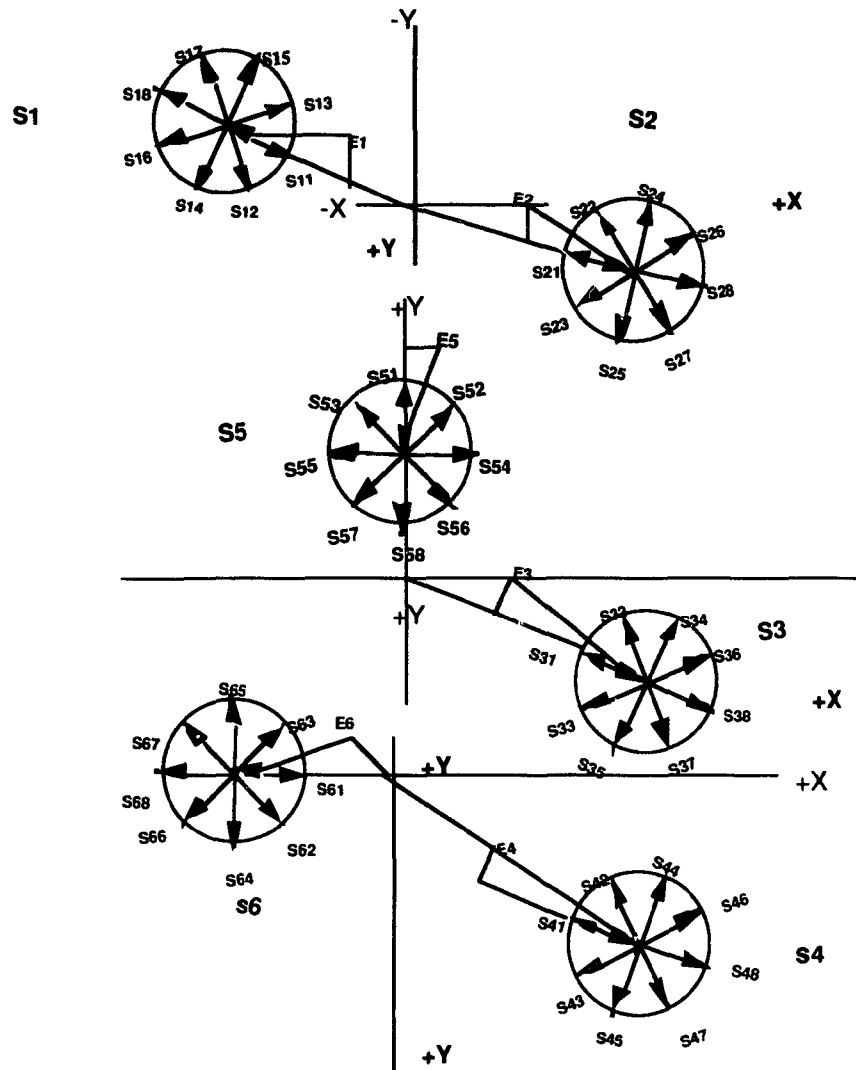
Figure 4.24A. Frontal plane projections of the directions of the uncancelled excitation vectors (E1 to E6) of six left ventricular segments (S1 to S6), and repolarization vectors (Sij, i=1-6, j=1-8) considered as alternatives to evaluate the likelihood of their contribution to the specific patterns of the correlation maps. Vector magnitudes of vectors E1 to E6 are normalized to equal length of 5 cm.

Assumption 5). The duration of the uncancelled portions of excitation (elements

E1-E6 in correlation maps) in segments S1-S6 is proportional to the regions E1-E6

shown in Figure 4.25A, and the duration of repolarization in all segments is

approximately equal (elements T1-T6 in correlation maps).
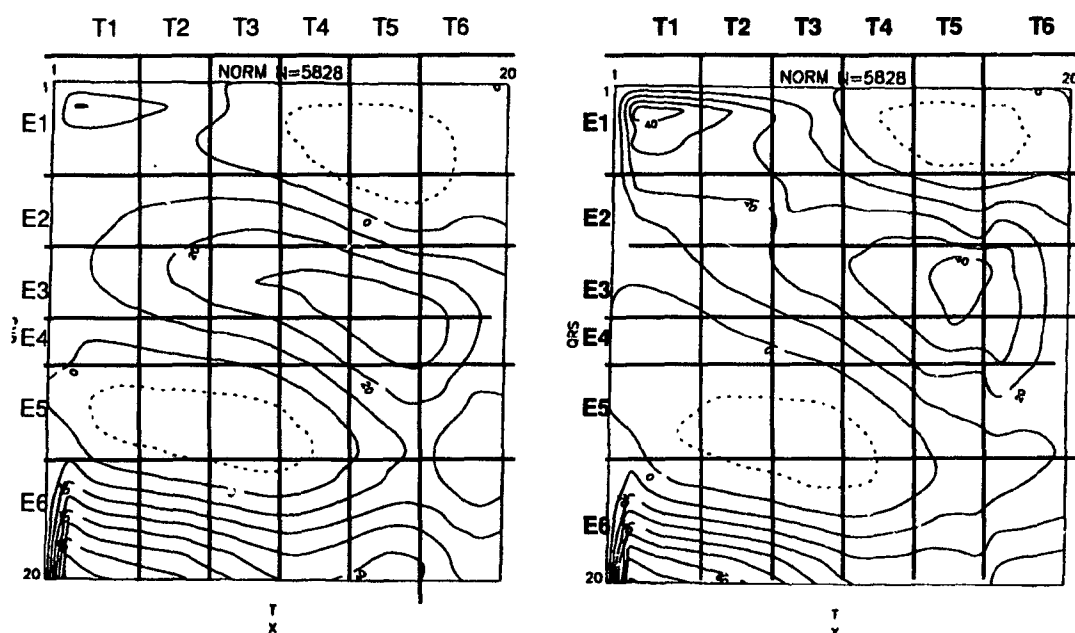
Figure 4.25A. Frontal plane components (X and Y) of QRS-T correlation maps
for normal conduction with partition lines for the six-segment regional model

Guideline: A universally reverse regional and local sequence of repolarization produces a high positive correlation with maxima along the diagonal (E6, T1) to (E1, T6). A universally concordant regional and local repolarization sequence produces a high negative correlation with minima along the diagonal (E1, T1) to (E6, T6).

There are six segments that can repolarize in any temporal order. Each segment for any given order can repolarize in eight different directions as described by the eight repolarization vectors. In view of the large number of possible combinations and permutations (N = 5,760), the selection of the most likely combinations was made on the basis of the following principles: a). for each regional segment considered as a likely candidate for repolarization during a given period (T1-T6), the repolarization vectors producing positive, negative, or near zero, correlations to match the observed correlation matrix elements for both orthogonal components in the plane considered were chosen to determine the possible local spatial repolarization sequence; b) the repolarization vector directions not agreeing with the correlation map patterns were rejected, and in cases where more than one repolarization vector matched with the correlation map patterns, the vector matching closest to the mean direction of the normal repolarization vectors was chosen from that group as the primary candidate.

The primary premise in these considerations was a realization of the fact that the spatial directional relationship of the QRS and T vectors in a population does not necessary provide sufficient information to determine whether repolarization is reverse, concordant, or whether it assumes other directions between reverse and concordant sequences. Correlation between the corresponding QRS and T vectors, on the other hand, can be assumed to reveal more information about these relationships. This expectation is based on the concept that when QRS-T correlation for a pair of vector components is positive, an increased QRS voltage at that time

point is associated with an increase in the T voltage at the time point when the segment repolarizes, suggesting a reverse repolarization sequence according to the classic theory behind the ventricular gradient concept. The same consideration can be expected to hold for negative correlation elements in the correlation maps if repolarization is concordant.

Findings

1. Frontal plane

The principal features of the QRS-T correlation maps in terms of the positivity, negativity, and approximately zero correlations in the frontal plane (X and Y components) for normal ventricular conduction are shown in Figure 4.26A. It is noted that the features or the correlation map elements match neither a universally reverse nor a universally concordant repolarization sequence. Only three of the matrix elements are consistent with the positivity along the diagonal (E6, T1) to (E1, T6) for both the X and Y components. Similarly, none of the matrix elements along the diagonal (E1, T1) to (E6, T6) are negative, which rules out the universally concordant repolarization sequence.

X	T1	T2	T3	T4	T5	T6
E1	P	P	P	N	N	N
E2	P	P	P	0	0	0
E3	P	P	P	P	P	P
E4	0	0	P	P	P	P
E5	N	N	N	0	P	P
E6	P	P	P	P	P	P

Y	T1	T2	T3	T4	T5	T6
E1	P	P	P	0	N	N
E2	P	P	P	P	P	P
E3	0	P	P	P	P	P
E4	0	0	0	P	P	P
E5	0	N	N	0	P	P
E6	P	P	P	P	P	P

Figure 4.26A. Principal patterns of correlation matrices for the frontal plane X and Y components in terms of positivity (P), and negativity (N) for normal conduction.

The results from the search for the most likely alternatives for the temporal regional and local spatial repolarization sequences are summarized in Table 4.17A.

The tabulated data reveal that the regions presented by Segments 1, 2, 3 and 4 satisfied the selection criteria for repolarization during time periods 2 and 3. Segments 3 and 4 met the selection criteria for repolarization during time periods T4, T5 and T6. This observation suggests an extensive overlap in repolarization time in these regions. The local spatial direction of repolarization in these regions fits the reverse or semireverse sequence. Segment 4 (posterolateral) together with Segments 1 (septum) and 2 (anterior), satisfied the criteria for repolarization during the first period (T1). The septum, anterolateral, and posterior walls were the regions qualifying as the candidates for the last regions to repolarize with a concordant sequence, with respect to the spatial direction of E1 representing the initial, uncancelled portion of depolarization. The local spatial direction of repolarization in the anterolateral and posterior wall fit a reverse sequence. Segment 6 (basal portions) did not meet the correlation matrix criteria for any of the repolarization vectors in any of the time periods considered.

Table 4.17A. Segments meeting correlation map criteria for repolarization in normal conduction, at defined time periods, corresponding repolarization vectors, local spatial sequence and direction of repolarization, and the direction of the T wave component produced in the frontal plane.

<u>**Frontal Plane**</u>

Period	Segment	Vector	Local Sequence	Direction of Repolarization	Direction of T wave
T1	S1, Septum	S11	Reverse	Right to Left	T1, Right
	S2, Anterior	S21	Reverse	Left to Right	T1, Left Inferior
	S4, Posterolateral	S48	Concordant	Right to Left Superior to Inferior	T1, Right Superior
T2	S1, Septum	S11	Reverse	Right to Left	T2, Right
	S2, Anterior	S21	Reverse	Left to Right Inferior to Superior	T2, Left Inferior
	S3, Anterolateral	S31	Reverse	Left to Right Superior to Inferior	T2, Left Inferior
	S4, Posterolateral	S43	Semi-reverse	Left to Right	T2, Left
T3	S1, Septum	S11	Reverse	Right to Left	T3, Right
	S2, Anterior	S21	Semi-reverse	Inferior to Superior Left to Right	T3, Inferior Left
	S3, Anterolateral	S31	Reverse	Left to Right Superior to Inferior	T3, Left Superior
	S4, Posterolateral	S41	Reverse	Left to Right Inferior to Superior	T3, Left Inferior
T4	S2, Anterior	S21	Semi-reverse	Left to Right Inferior to Superior	T4, Left Inferior
	S3, Anterolateral	S31	Reverse	Left to Right Superior to Inferior	T4, Left Inferior
	S4, Posterolateral	S41	Reverse	Left to Right Inferior to Superior	T4, Left Inferior

Table 4.17A. Segments meeting correlation map criteria for repolarization in normal conduction, at defined time periods, corresponding repolarization vectors, local spatial sequence and direction of repolarization, and the direction of the T wave component produced in the frontal plane (Continued).

<u>Frontal Plane</u>

Period	Segment	Vector	Local Sequence	Direction of Repolarization	Direction of T wave
T5	S1, Septum	S18	Concordant	Left to Right Inferior to Superior	T5, Left Inferior
	S3, Anterolateral	S31	Reverse	Left to Right Superior to Inferior	T5, Left Inferior
	S4, Posterolateral	S41	Reverse	Inferior to Superior Left to Right	T5, Inferior Left
	S5, Posterior	S53	Semi-reverse	Inferior to Superior Left to Right	T5, Inferior Left
T6	S1, Septum	S18	Concordant	Left to Right Inferior to Superior	T6, Left Inferior
	S3, Anterolateral	S31	Reverse	Left to Right Superior to Inferior	T6, Left Inferior
	S4, Posterolateral	S41	Reverse	Inferior to Superior Left to Right	T6, Inferior Left

2. Sagittal plane

Similar considerations and assumptions as to those for the frontal plane were used in deductive reasoning for the repolarization sequence in the sagittal plane. Depolarization vectors E1 to E6 were visualized in the sagittal plane cross-section of the human heart in Figure 4.22B. These vectors were derived as an approximation of the mean QRS vectors in Figure 4.23. Repolarization vectors considered in association with each excitation vector in the sagittal plane are shown in Figure 4.24B. The correlation matrices for the Y and Z components produced in Figure 4.25B, and the main features of the 6-by-6 elements in terms of positivity, negativity, and approximately zero correlation are shown in Figure 4.26B.
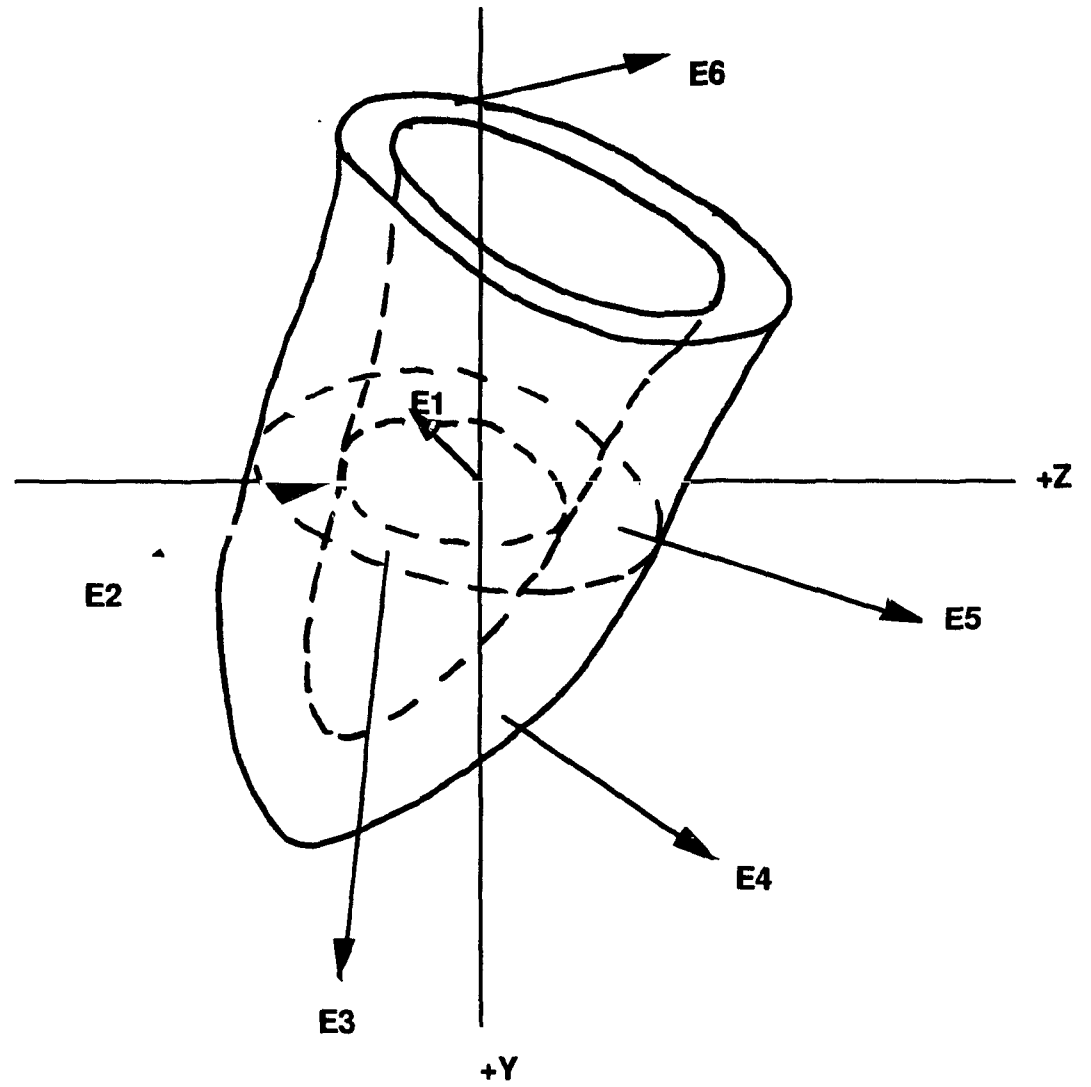
Figure 4.22B. A sketch of the sagittal plane cross-section of human left

ventricle with uncancelled excitation vectors E1 to E6 from six regional segments.
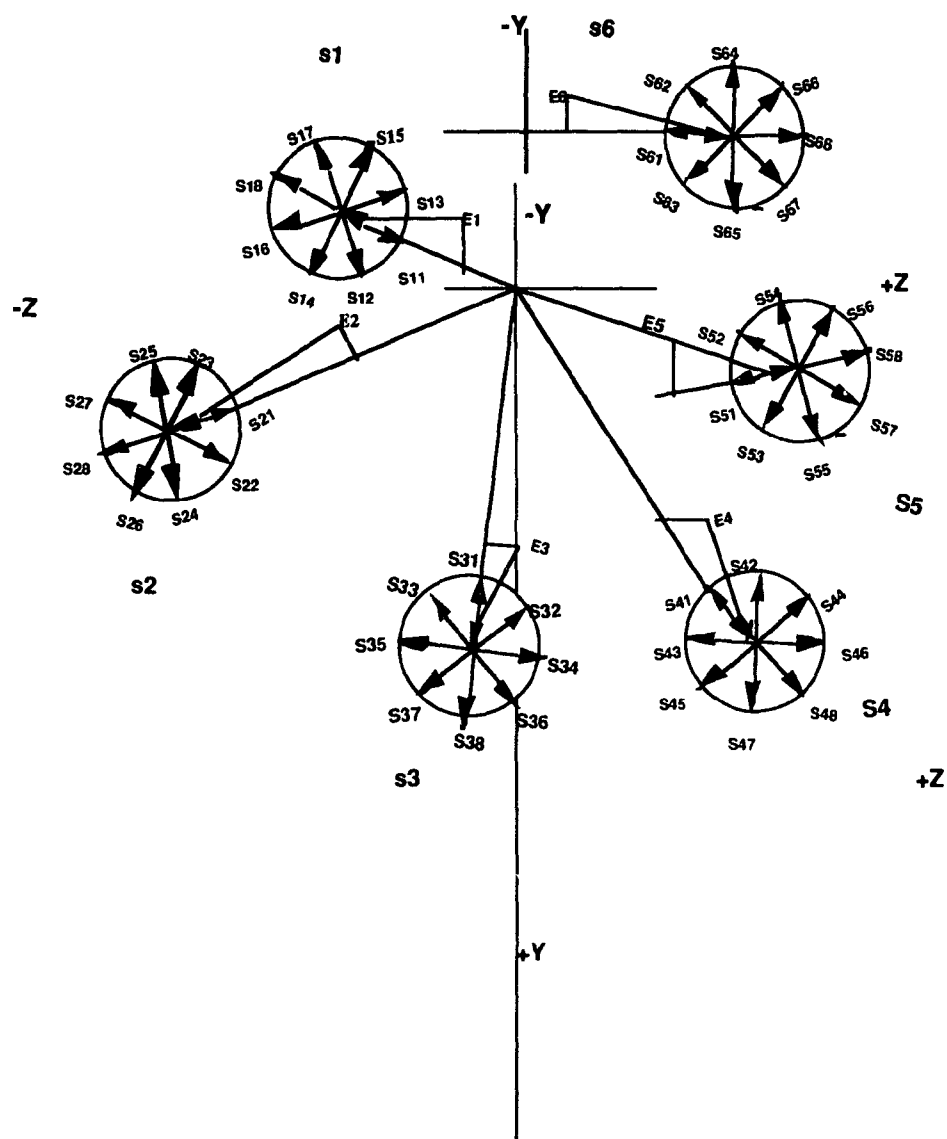
Figure 4.24B. Sagittal plane projections of the directions of the uncancelled excitation vectors (E1 to E6) of six left ventricular segments (S1 to S6), and repolarization vectors (Sij, i=1-6, j=1-8) considered as alternatives to evaluate the likelihood of their contribution to the specific patterns of the correlation maps. Vectors magnitudes of vectors E1 to E6 are normalized to equal length of 5 cm.
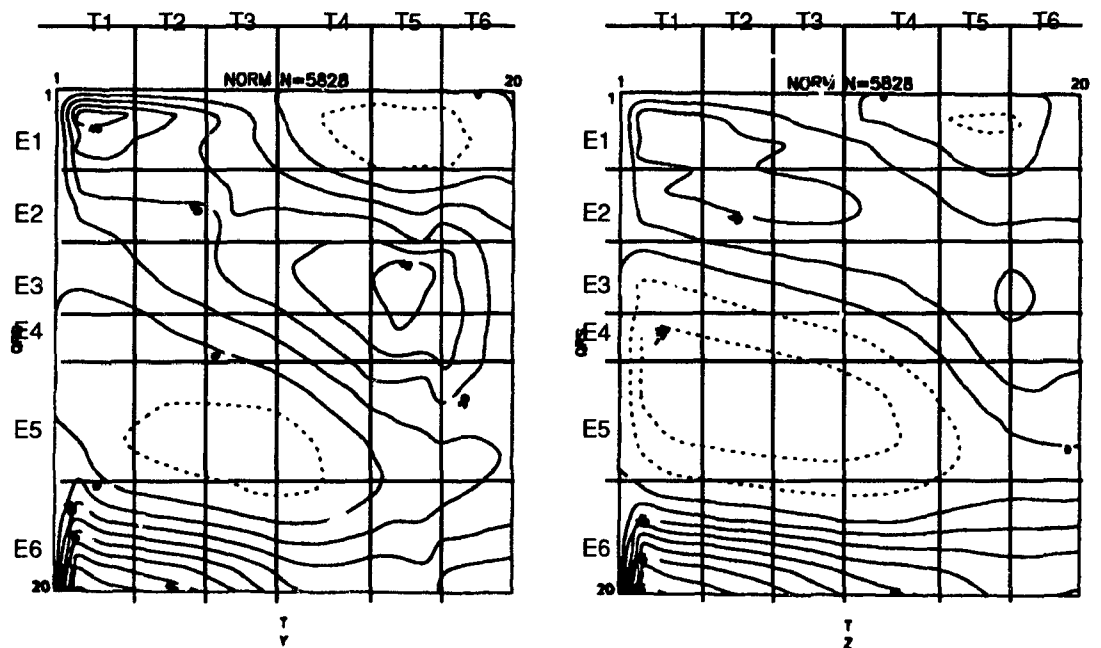
Figure 4.25B. Sagittal plane components (Y and Z) of QRS-T correlation maps for normal conduction with partition lines for the six-segment regional model.

Y						
	T1	T2	T3	T4	T5	T6
E1	P	P	P	0	N	N
E2	P	P	P	P	P	P
E3	0	P	P	P	P	P
E4	0	0	0	P	P	P
E5	0	N	N	0	P	P
E6	P	P	P	P	P	P

Z						
	T1	T2	T3	T4	T5	T6
E1	P	P	P	P	N	0
E2	P	P	P	P	P	P
E3	N	N	0	P	P	P
E4	N	N	N	N	0	P
E5	N	N	N	N	N	0
E6	P	P	P	P	P	P

Figure 4.26B. Principal patterns of correlation matrices for the sagittal plane Y and Z components in terms of positivity (P) and negativity (N) for normal conduction.

The results from the search for candidates for likely combinations of regional temporal, and local, spatial repolarization sequences are summarized in Table 4.17B. As for the frontal plane patterns, Segments 1(septum), 2 (anterior) and 3 (anterolateral) met the criteria for the last regions to repolarize, with an apex to base and anterior to posterior spatial direction with reverse sequence.

Four segments satisfied criteria for being the first to repolarize in the sagittal plane, namely, Segment 1 (reverse), Segment 3 (intermediate), Segment 4 (semiconcordant) and Segment 5 (concordant). All these combinations would produce repolarization in an anterior to posterior direction during the initial repolarization. Among the primary candidates for repolarization during the middle periods were Segments 1, 2, and 4 for periods T3, T4 and T5, with a semireverse and semiconcordant sequence. S1 met the selection criteria for repolarization for any of the periods considered, with a predominant semireverse and reverse sequence. Segment 3 (anterolateral) also met criteria for repolarization during periods T5 and T6, with a semireverse sequence in an apex to base direction. As for the frontal plane, segment 6 (base) did not meet the criteria for any of the repolarziation vectors for any of the periods considered.

Table 4.17B. Segments meeting correlation map criteria for repolarization in normal conduction, at defined time periods, corresponding repolarization vectors, local spatial sequence and direction of repolarization, and the direction of the T wave component produced in the sagittal plane.

<u>**Sagittal Plane**</u>

Period	Segment	Vector	Local Sequence	Direction of Repolarization	Direction of T wave
T1	S1, Septum	S11	Reverse	Anterior to Posterior	T1, Anterior
	S3, Anterolateral	S34	Intermediate	Anterior to Posterior Superior to Inferior	T1, Anterior Superior
	S4, Posterolateral	S46	Semiconcordant	Anterior to Posterior Superior to Inferior	T1, Anterior Superior
	S5, Posterior	S58	Concordant	Anterior to Posterior Superior to Inferior	T1, Anterior superior
T2	S1, Septum	S11	Reverse	Anterior to Posterior	T2, Anterior
	S4, Posterolateral	S46	Semiconcordant	Anterior to Posterior Superior to Inferior	T2, Anterior Superior
	S5, Posterior	S56	Semiconcordant	Superior to Inferior Anterior to Posterior	T2, Superior Anterior
T3	S1, Septum	S11	Reverse	Anterior to Posterior	T3, Anterior
	S2, Anterior	S22	Semi-reverse	Inferior to Superior Anterior to Posterior	T3, Inferior Anterior
	S4, Posterolateral	S46	Semiconcordant	Anterior to Posterior Superior to Inferior	T3, Anterior Superior
T4	S1, Septum	S13	Semi-reverse	Anterior to Posterior	T4, A· .rior
	S2, Anterior	S21	Semi-reverse	Inferior to Superior Anterior to Posterior	T4, Inferior Anterior
	S4, Posterolateral	S44	Intermediate	Inferior to Superior Anterior to Posterior	T4, Inferior Anterior
	S5, Posterior	S56	Semiconcordant	Anterior to Posterior Inferior to Superior	T4, Inferior Anterior

Table 4.17B. Segments meeting correlation map criteria for repolarization in normal conduction, at defined time periods, corresponding repolarization vectors, local spatial sequence and direction of repolarization, and the direction of the T wave component produced in the sagittal plane (Continued).

<u>Sagittal Plane</u>

Period	Segment	Vector	Local Sequence	Direction of Repolarization	Direction of T wave
T5	S1, Septum	S18	Concordant	Posterior to Anterior Superior to Inferior	T5, Posterior Superior
	S2, Anterior	S23	Semi-reverse	Inferior to Superior Anterior to Posterior	T5, Inferior Anterior
	S3, Anterolateral	S33	Semi-reverse	Inferior to Superior Anterior to Posterior	T5, Inferior Anterior
	S4, Posterolateral	S46	Semiconcordant	Inferior to Superior Anterior to Posterior	T5, Inferior Anterior
T6	S1, Septum	S15	Intermediate	Inferior to Superior Anterior to Posterior	T6, Inferior Anterior
	S2 Anterior	S21	Reverse	Anterior to posterior Superior to Inferior	T6, Anterior Inferior
	S3, Anterolateral	S33	semi-reverse	Inferior to Superior Anterior to Posterior	T6, Inferior Anterior

4.4.3.2. QRS-T correlation maps for complete and incomplete bundle branch blocks

Similar procedures for the interpretation of QRS-T correlation maps of normal conduction also apply to those of ventricular conduction defects. They are summarized as follows:

1. An approximation of depolarization vectors E1 to E6 from the mean QRS vectors in the frontal and sagittal plane;

2. Consideration of repolarization vectors in association with each excitation vector in the frontal and sagittal plane;

3. Construction of the main features of the 6-by-6 elements in terms of positivity, negativity, and approximately zero correlation;

4. Deduction for the regional temporal and local spatial repolarization sequence in the frontal and sagittal plane.

Not all of the tables and figures are reproduced here.

Left bundle branch block (LBBB)

Depolarization vectors E1 - E6 in the frontal plane and sagittal plane were derived as an approximation of the mean QRS vectors in Figure 4.27. As the temporal and spatial excitation sequence in the left ventricle are altered in LBBB, the myocardial regions (S1 - S6) are therefore considered to be different from those in normal conduction:

Segment 1 - Septum, with E1 corresponding to QRS vectors R1 - R3.

Segment 2 - Paraseptal, with E2 corresponding to QRS vectors R4 - R6.

Segment 3 - Anterior and posterior paraseptal, and apex, with E3 corresponding to QRS vectors R7 - R9.

Segment 4 - Anterolateral and posterior walls, with E4 corresponding to R10 - R 11.

Segment 5 - Posterolateral, with E5 corresponding to R 12 - R15.

Segment 6 - Base, with E6 corresponding to R16 - R20.
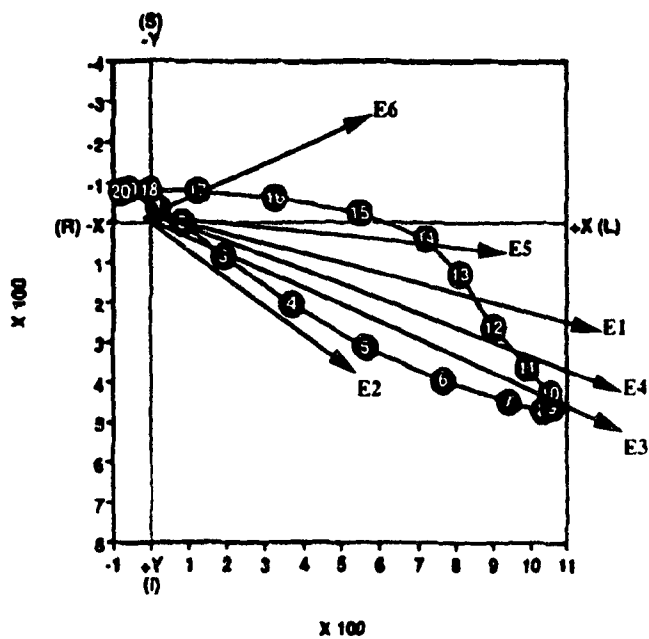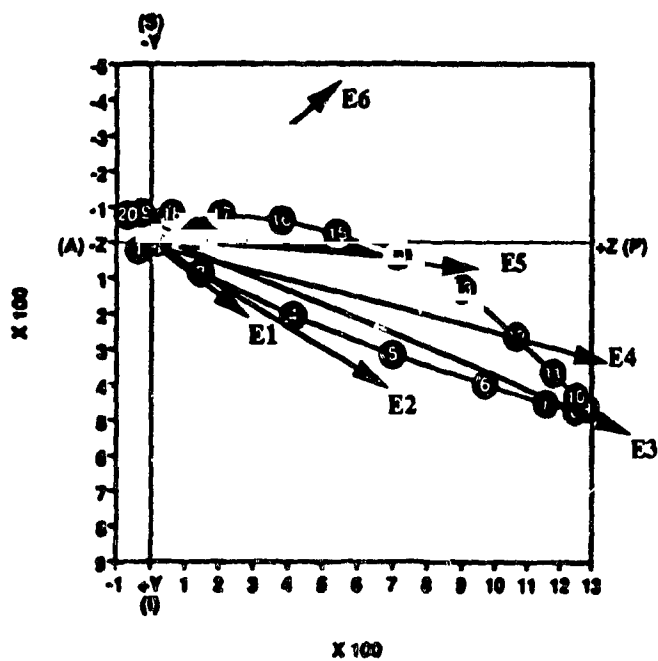
Figure 4.27. Estimated mean directions for QRS mean vectors corresponding to

E1 - E6 in the frontal plane (top) and sagittal plane (bottom) for LBBB.

The visualization of the correlation patterns in Figure 4.28 shows that the correlation map elements match a universally concordant repolarization sequence as many matrix elements are consistent with the negativity along the diagonal (E1, T1) to (E6, T6). Figures 4.29A and 4.29B present the frontal and sagittal plane projections of the directions of the uncancelled excitation vectors of the left ventricle.
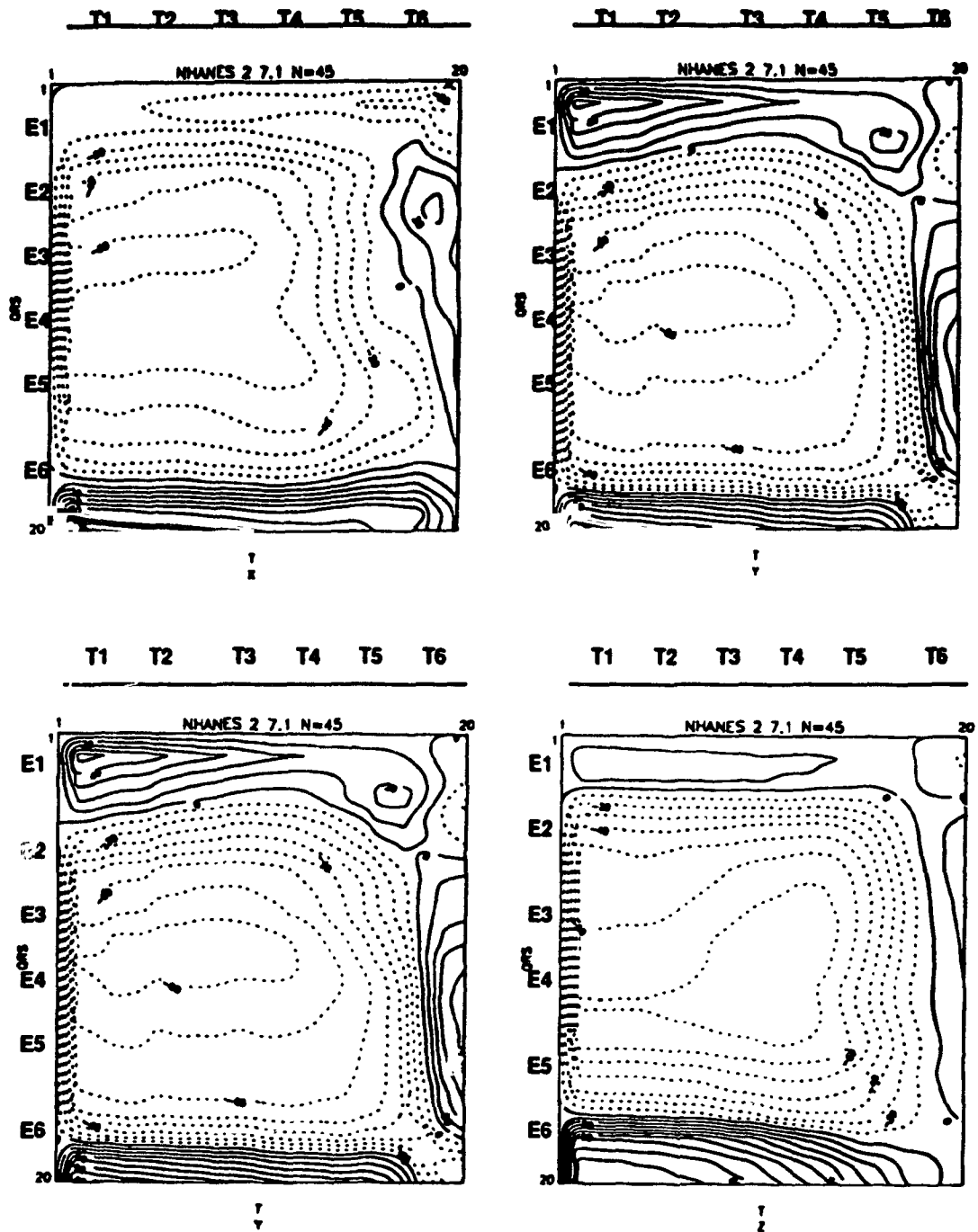
Figure 4.28. Frontal plane components (X and Y) (top) and sagittal plane components (Y and Z) (bottom) of QRS-T correlation maps for LBBB.
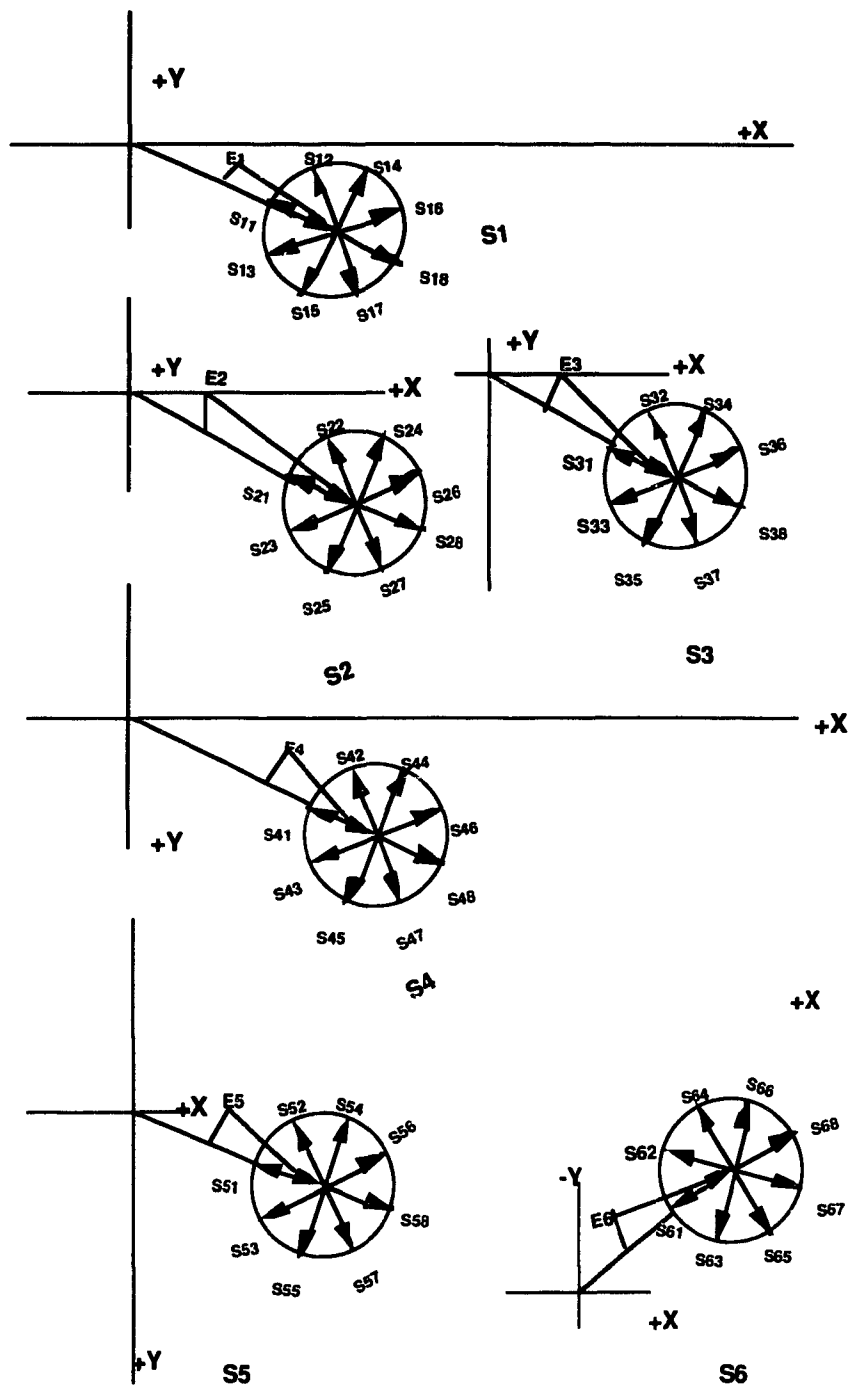
Figure 4.29A. Frontal plane projections of the directions of the uncancelled excitation vectors (E1 to E6) of six left ventricular segments (S1 to S6), and repolarization vectors considered as alternatives to evaluate the likelihood of their contribution to the specific patterns of the correlation maps in LBBB. Vector magnitudes of vectors E1 to E6 are normalized to equal length of 5 cm.
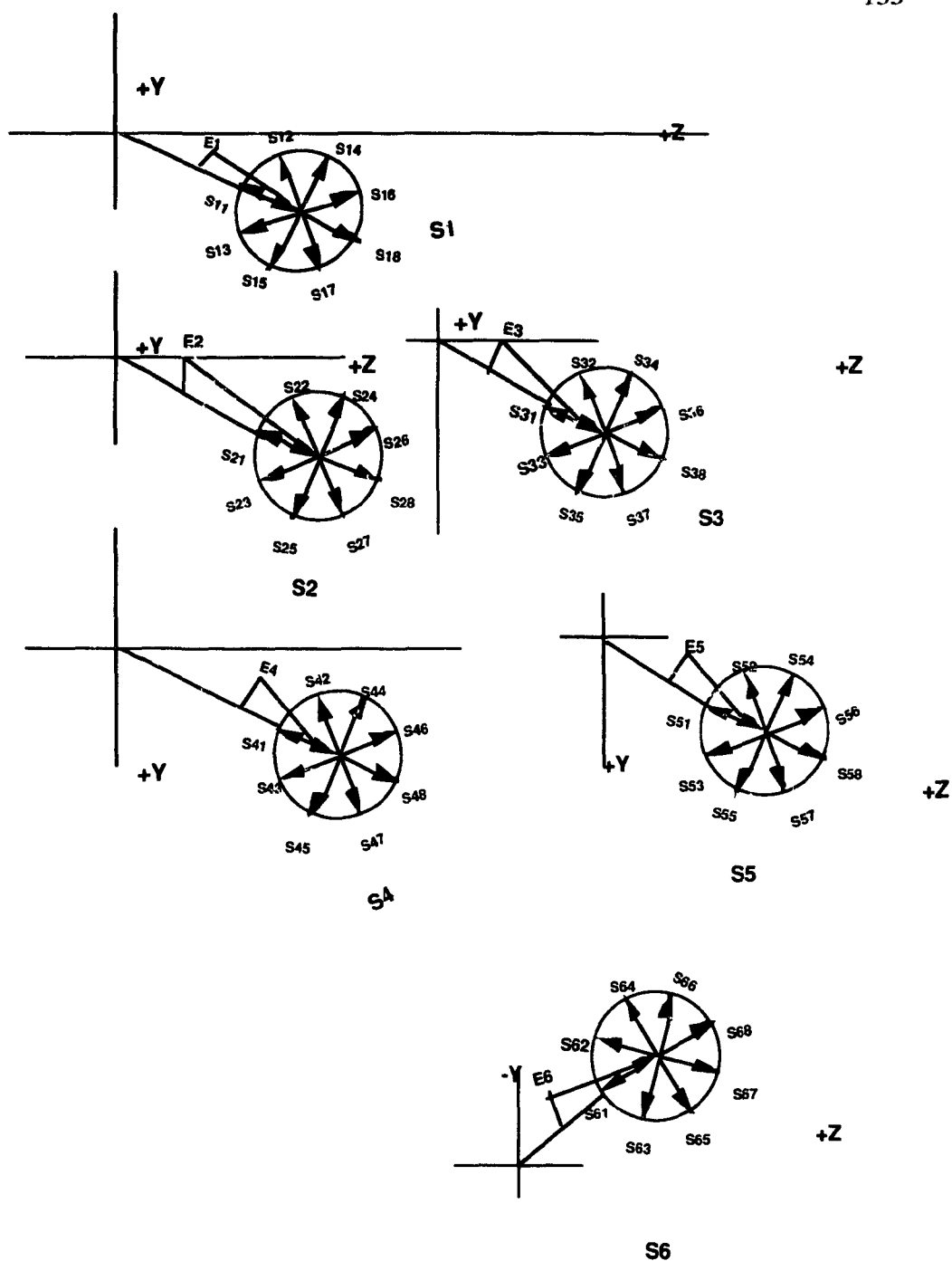
Figure 4.29B. Sagittal plane projections of the directions of the uncancelled excitation vectors (E1 to E6) of six left ventricular segments (S1 to S6), and repolarization vectors considered as alternatives to evaluate the likelihood of their contribution to the specific patterns of the correlation maps in LBBB. Vectors magnitudes of vectors E1 to E6 are normalized to equal length of 5 cm.

The tabulated data in Table 4.18A and 4.18B reveal that there was an extensive overlap of repolarization in all the regions for time periods T2 - T5, in the frontal and sagittal plane. The local spatial direction of repolarization in these regions primarily fits the concordant or semiconcordant sequence. It is interesting to note that septal repolarization varied from semi-reverse sequence for T1 in the frontal plane to semi-concordant sequence for T6 in the sagittal plane. All the segments satisfied criteria for being the last to repolarize in the frontal and sagittal plane. With the exception of S1 (septum) and S2 (anteroparaseptal), four segments (S3-anterior posterior paraseptal, S4 - anterolateral posterior wall, S5 - posterolateral and S6 - base) in the sagittal plane fit semiconcordant or concordant sequence. All these combinations would produce repolarization in an anterior to posterior and apex to base spatial direction.

Table 4.18A. Segments meeting correlation map criteria for repolarization in LBBB, at defined time periods, corresponding repolarization vectors, local spatial sequence and direction of repolarization, and the direction of the T wave component produced in the frontal plane.

<u>Frontal Plane</u>

Period	Segment	Vector	Local Sequence	Direction of Repolarization	Direction of T wave
T1	S1, Septum	S13	Semi-reverse	Left to Right	T1 Left
	S2, Anterior paraseptal, Apex	S28	Concordant	Right to left Superior to Inferior	T1 Right Superior
	S3, Anterior, posterior paraseptal	S38	Concordant	Right to Left Superior to Inferior	T1 Right Superior
	S4, Anterolateral, posterior walls	S48	Concordant	Right to Left Superior to Inferior	T1 Right Superior
	S5, Posterolateral	S58	Concordant	Right to Left Superior to Inferior	T1 Right Superior
	S6, Base	S66	Semi-concordant	Right to Left Inferior to Superior	T1 Right Inferior
T2, T3, T4, T5	S1, Septum	S15	Intermediate	Right to Left	T1 - T5 Right
	S2, Anterior paraseptal, Apex	S28	Concordant	Right to left Superior to Inferior	T1 - T5 Right Superior
	S3, Anterior, posterior paraseptal regions	S38	Concordant	Right to Left Superior to Inferior	T1 - T5 Right Superior
	S4, Anterolateral, posterior walls	S48	Concordant	Right to Left Superior to Inferior	T1 - T5 Right Superior
	S5, Posterolateral wall	S58	Concordant	Right to Left Superior to Inferior	T1 - T5 Right Superior
	S6, Base	S66	Semi-concordant	Right to Left Inferior to Superior	T1 - T5 Right Inferior
T6	S1, Septum	S15	Intermediate	Right to Left	T6 Right
	S2, Anterior paraseptal, Apex	S21	Reverse	Left to Right Inferior to Superior	T6 Left Inferior
	S3, Anterior, posterior paraseptal regions	S36	Semi-concordant	Right to Left Superior to Inferior	T6 Right Superior
	S4, Anterolateral posterior walls	S46	Semi-concordant	Right to Left Superior to Inferior	T6 Right Superior
	S5, Posterolateral	S58	Concordant	Right to Left Superior to Inferior	T6 Right Superior
	S6, Base	S66	Semi-concordant	Right to Left Inferior to Superior	T6 Right Inferior

Table 4.18B. Segments meeting correlation map criteria for repolarization in LBBB, at defined time periods, corresponding repolarization vectors, local spatial sequence and direction of repolarization, and the direction of the T wave component produced in the sagittal plane.

<u>Sagittal Plane</u>

Period	Segment	Vector	Local Sequence	Direction of Repolarization	Direction of T wave
T1, T2, T3, T4, T5	S1, Septum	S13	Semi-reverse	Posterior to Anterior	T1 - T5 Posterior
	S2, Anterior paraseptal, Apex	S28	Concordant	Anterior to Posterior Superior to Inferior	T1 - T5 Anterior Superior
	S3, Anterior, posterior paraseptal	S38	Concordant	Anterior to Posterior Superior to Inferior	T1 - T5 Anterior Superior
	S4, Anterolateral, posterior walls	S48	Concordant	Anterior to Posterior Superior to Inferior	T1 - T5 Anterior Superior
	S5, Posterolateral	S58	Concordant	Anterior to Posterior Superior to Inferior	T1 - T5 Anterior Superior
	S6, Base	S66	Semi-concordant	Anterior to Posterior Inferior to Superior	T1 - T5 Anterior Inferior
T6	S1, Septum	S16	Semi-concordant	Anterior to Posterior	T6 Anterior
	S2, Anterior paraseptal, Apex	S26	Semi-concordant	Anterior to Posterior Superior to Inferior	T6 Anterior Superior
	S3, Anterior, posterior paraseptal regions	S38	Concordant	Anterior to Posterior Superior to Inferior	T6 Anterior Superior
	S4, Anterolateral posterior walls	S46	Semi-concordant	Anterior to Posterior Superior to Inferior	T6 Anterior Superior
	S5, Posterolateral wall	S58	Concordant	Anterior to Posterior Superior to Inferior	T6 Anterior Superior
	S6, Base	S68	Concordant	Anterior to Posterior Inferior to Superior	T6 Anterior Inferior

138

Complete block of unspecified type (IVCD)

The correlation patterns in Figure 4.30 are considerably more complex than in LBBB. The correlations between excitation vectors E1 - E5 with the initial few vectors negative while the correlations with the remaining T vectors was positive. Thus, it is substantially more difficult to draw dedective conclusions about excitation-repolarization relationships in IVCD from these simple conceptual models, and this will not be comtemplated here.
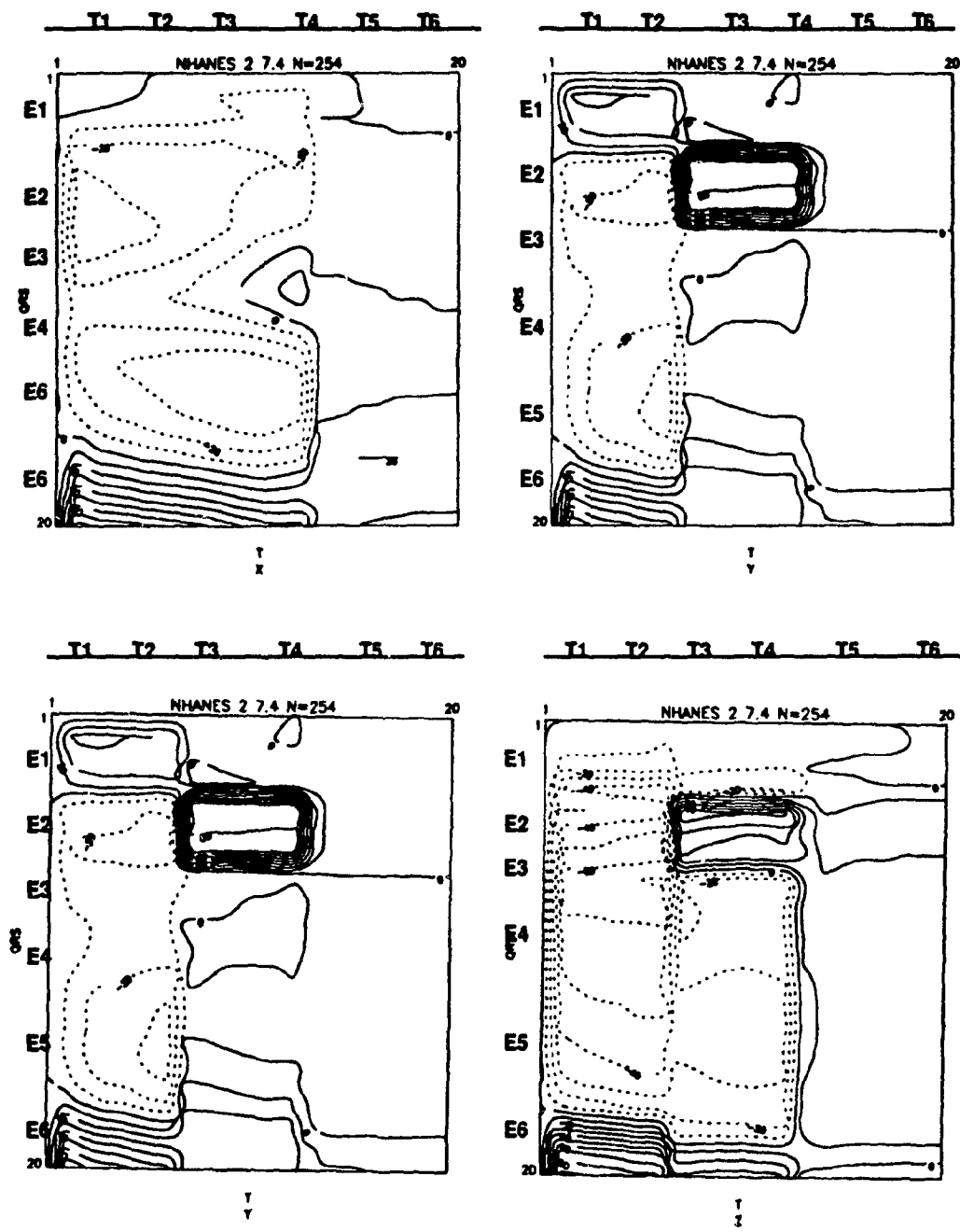
Figure 4.30. Frontal plane components (X and Y) (top) and sagittal plane components (Y and Z) (bottom) of QRS-T correlation maps for IVCD.

Right bundle branch block (RBBB)

Left ventricular excitation remains normal in RBBB. The estimated mean directions for mean QRS vectors in Figure 4.31 and the correlation patterns in Figure 4.32 resembled fairly closely the normal pattern in X and Y components, with the exception of late QRS vectors (Y and Z components) because of delayed activation of the right ventricle. The segments corresponding to excitation periods (E1 - E6) are considered as following:

Segment 1 - Septum, with E1 corresponding to QRS vectors R1 - R3.

Segment 2 - Anterolateral LV, with E2 corresponding to QRS vectors R4 - R6.

Segment 3 - Posterior LV, with E3 corresponding to QRS vectors R7 - R9.

Segment 4 - Lateral RV, with E4 corresponding to QRS vectors R10 - R11.

Segment 5 - Posterior RV, with E5 corresponding to QRS vectors R12 - R15

Segment 6 - Anterobasal RV or Pulmonary conus, with E6 corresponding to QRS vectors R16 - 20.

RBBB QRS LOOP

Frontal plane

(S)
-Y

+X (L)
E1
E2
E3
E4
E5
E6
(R) -X
+Y
(I)

X 100

X 100

RBBB QRS LOOP

Sagittal plane

(S)
-Y

E5
E4
E6
E1
E2
E3
+Z (P)
(A) -Z
+Y
(I)

X 100

X 100

Figure 4.31. Estimated mean directions for QRS mean vectors corresponding to
E1 - E6 in the frontal plane (top) and sagittal plane (bottom) for RBBB.

Figure 4.32. Frontal plane components (X and Y) (top) and sagittal plane components (Y and Z) (bottom) of QRS-T correlation maps for RBBB.
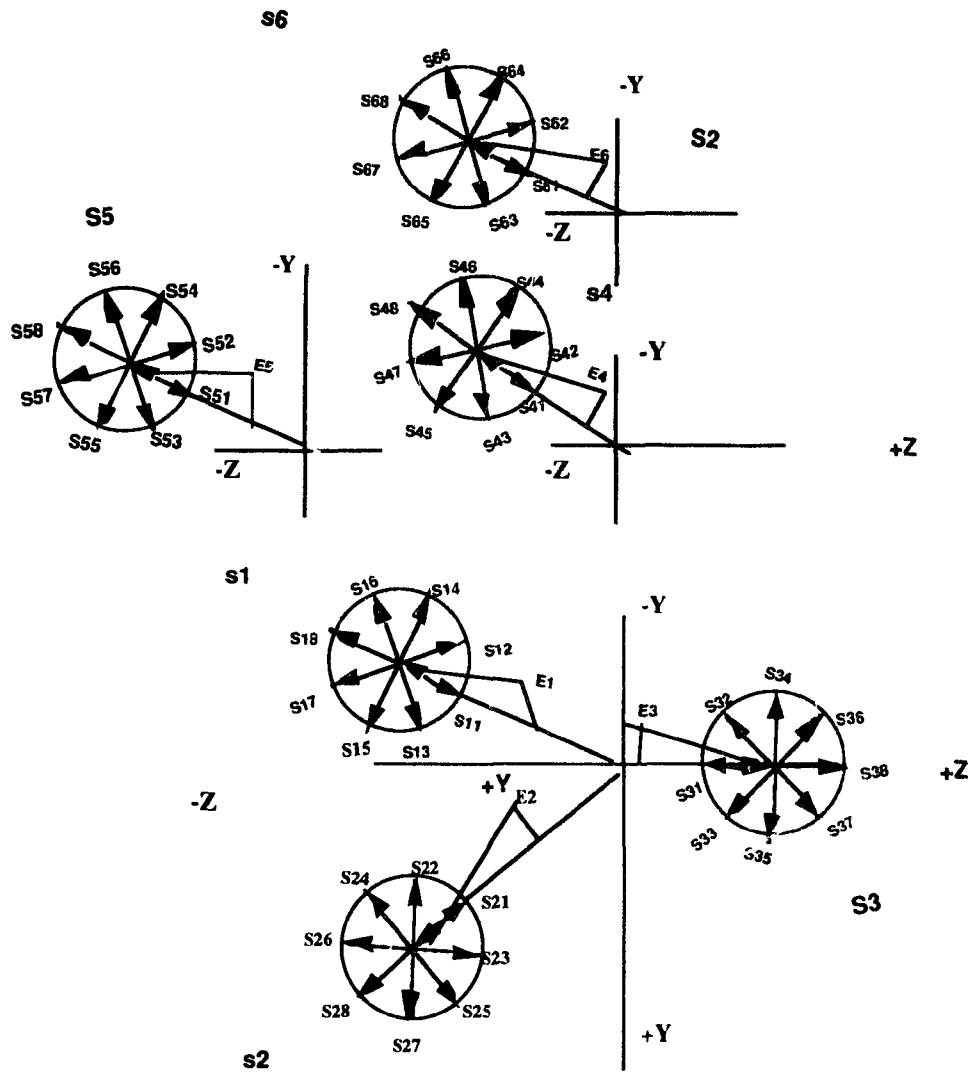
Figure 4.33. Sagittal plane projections of the directions of the uncancelled excitation vectors (E1 to E6) of six left ventricular segments (S1 to S6), and repolarization vectors considered as alternatives to evaluate the likelihood of their contribution to the specific patterns of the correlation maps in RBBB.

The results from the search for the candidates for likely combinations of a regional temporal, and local, spatial repolarization sequence in the sagittal plane are summarized in Table 4.19 after deductive reasoning from Figures 4.32 and 4.33.

Table 4.19 shows that S4 (lateral RV) and S5 (posterior RV) met the selection criteria for repolarization during time periods T1 to T5, with a concordant sequence. This observation indicates the extensive overlap in repolarization time in these regions. Segment 2, anterolateral LV fits reverse sequence during time periods T5 and T6. Segment 5 (posterior RV) and segment 6 (anterobasal or pulmonary conus) produce a posterior to anterior, and apex to base direction of repolarization.

e

e

Table 4.19. Segments meeting correlation map criteria for repolarization in RBBB, at defined time periods, corresponding repolarization vectors, local spatial sequence and direction of repolarization, and the direction of the T wave component produced in the sagittal plane.

Sagittal Plane

Period	Segment	Vector	Local Sequence	Direction of Repolarization	Direction of T wave
T1	S1, Septum	S13	Semi-reverse	Anterior to Posterior	T1, Anterior
	S2, Anterolateral LV	S23	Semi-reverse	Anterior to Superior Superior to Inferior	T1, Anterior Superior
	S4, Lateral RV	S48	Concordant	Posterior to Anterior Inferior to Superior	T1, Posterior Inferior
	S5, Posterior RV	S58	Concordant	Posterior to Anterior Inferior to Superior	T1, Posterior Inferior
	S6, Anterobasal RV (Pulmonary conus)	S61	Reverse	Anterior to Posterior Superior to Inferior	T1, Anterior Superior
T2	S1, Septum	S13	Semi-reverse	Anterior to Posterior	T2, Anterior
	S4, Lateral RV	S48	Concordant	Posterior to Anterior Inferior to Superior	T2, Posterior Inferior
	S5, Posterior RV	S58	Concordant	Posterior to Anterior Inferior to Superior	T2, Posterior Inferior
	S6, Anterobasal RV (Pulmonary conus)	S68	Concordant	Posterior to Anterior Inferior to Superior	T2, Posterior Inferior
T3, T4	S1, Septum	S11	Reverse	Anterior to Posterior	T3 - T5, Anterior
	S4, Lateral RV	S48	Concordant	Posterior to Anterior Inferior to Superior	T3 - T5, Posterior Inferior
	S5, Posterior RV	S58	Concordant	Posterior to Anterior Inferior to Superior	T3 - T5, Posterior Inferior
	S6, Anterobasal RV	S68	Concordant	Posterior to Anterior Inferior to Superior	T3 - T5, Posterior Inferior
T5	S1, Septum	S11	Reverse	Anterior to Posterior	T3 - T5, Anterior
	S2, Anterolateral LV	S21	Reverse	Anterior to Posterior Inferior to Posterior	T5 - T5, Anterior Inferior
	S4, Lateral RV	S48	Concordant	Posterior to Anterior Inferior to Superior	T3 - T5, Posterior Inferior
	S5, Posterior RV	S58	Concordant	Posterior to Anterior Inferior to Superior	T3 - T5, Posterior Inferior

e

Table 4.19. Segments meeting correlation map criteria for repolarization in RBBB, at defined time periods, corresponding repolarization vectors, local spatial sequence and direction of repolarization, and the direction of the T wave component produced in the sagittal plane (Continued).

Sagittal Plane

Period	Segment	Vector	Local Sequence	Direction of Repolarization	Direction of T wave
T6	S1, Septum	S15	Intermediate	Anterior to Posterior	T6, Anterior
	S2, Anterolateral LV	S21	Reverse	Anterior to Posterior Superior to Inferior	T6, Anterior Superior
	S4, Lateral RV	S41	Reverse	Anterior to Superior Superior to Inferior	T6, Anterior Superior
	S5, Posterior RV	S56	Semi-concordant	Posterior to Inferior Inferior to Superior	T6, Posterior Inferior
	S6, Anterobasal RV (Pulmonary conus)	S68	Concordant	Posterior to Anterior Inferior to Superior	T6, Posterior Inferior

Incomplete right bundle branch block (IRBBB)

The estimated mean directions for mean QRS vectors in Figure 4.34 and the correlation pattern in Figure 4.35 largely resembled the normal pattern. Like normal conduction, the correlation map matrices match neither a universally reverse nor a universally concordant repolarization sequence.
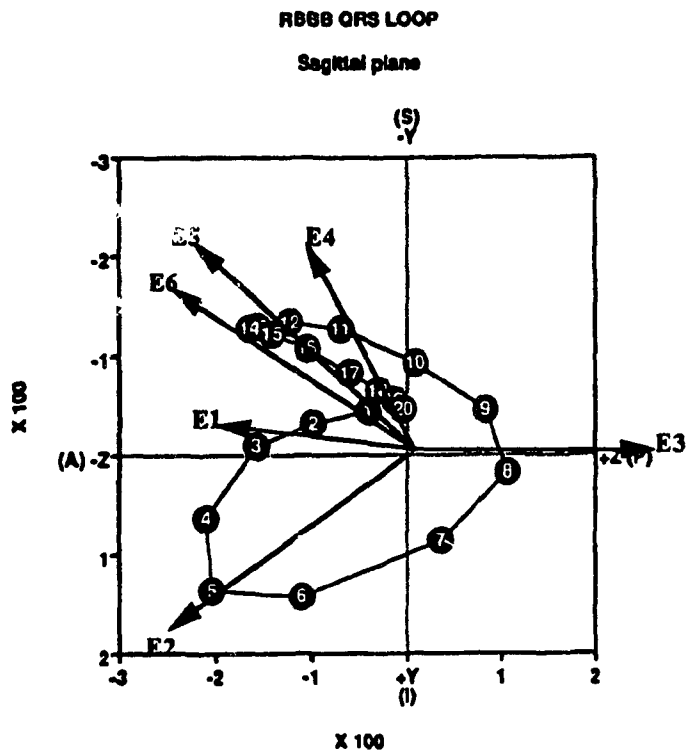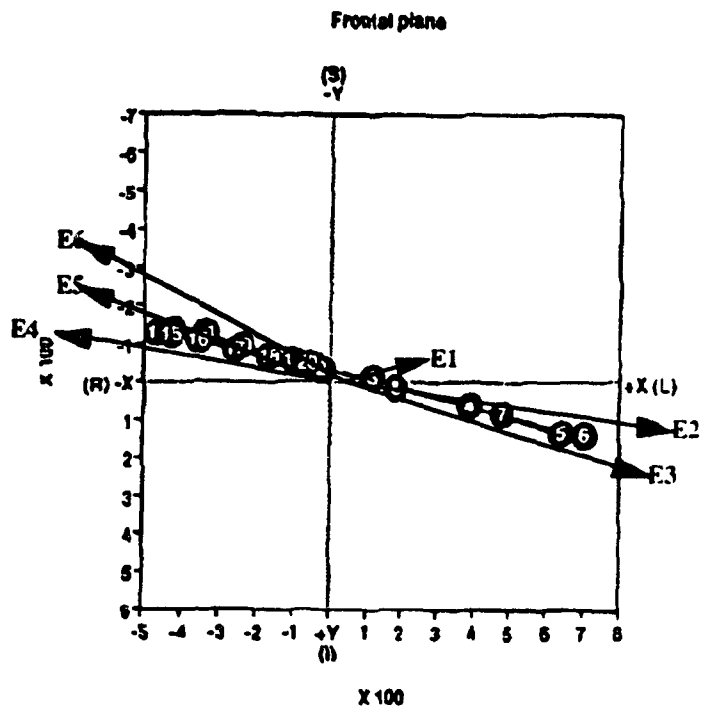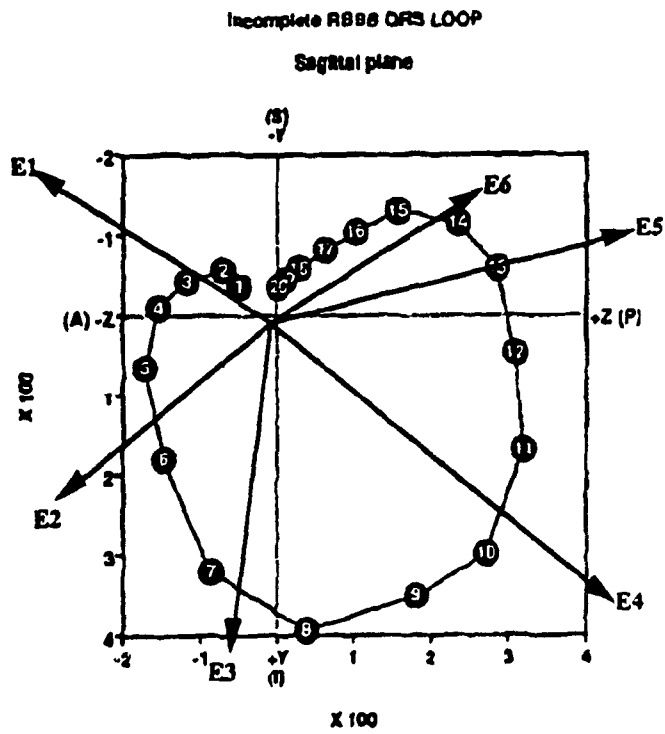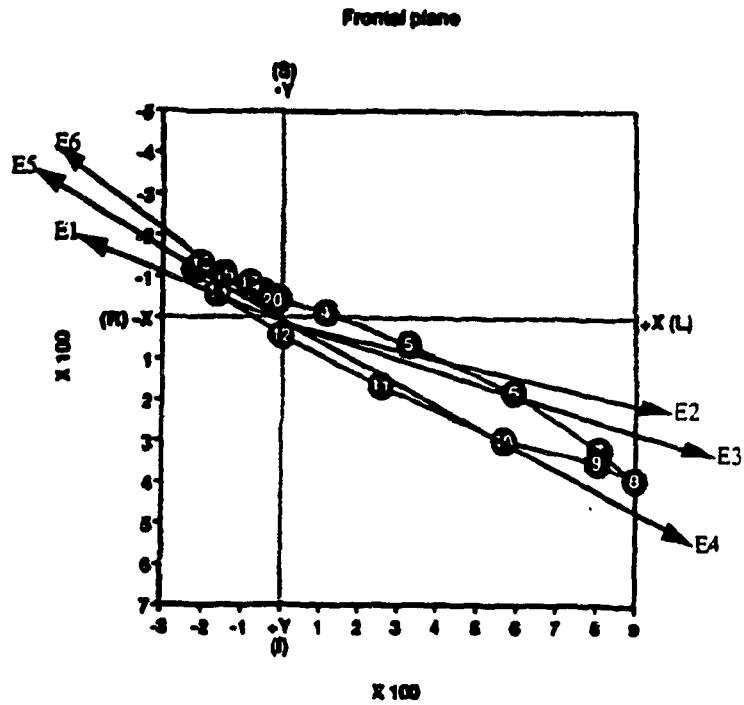
Figure 4.34. Estimated mean directions for QRS mean vectors corresponding to

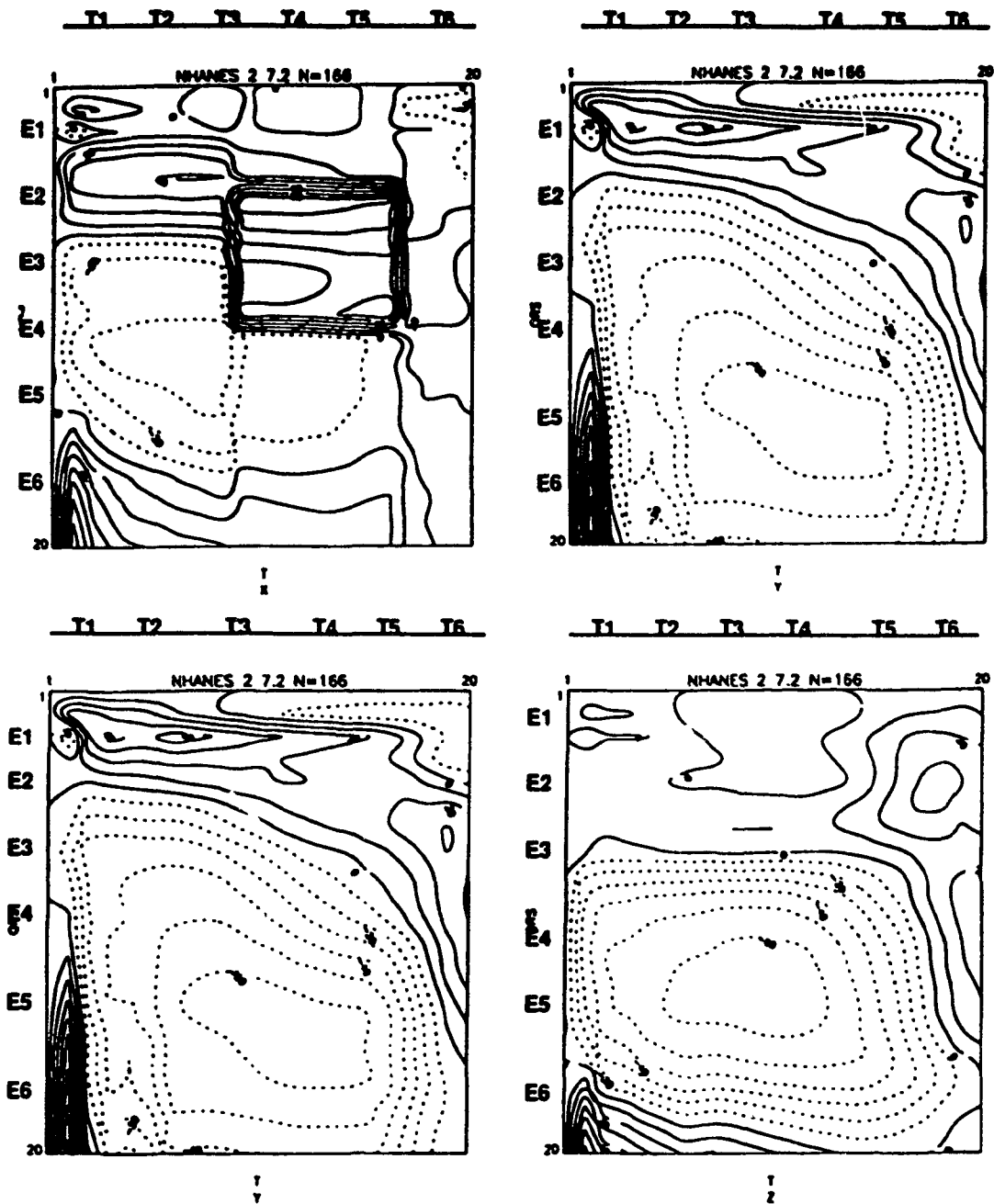E1 - E6 in the frontal plane (top) and sagittal plane (bottom) for incomplete RBBB.
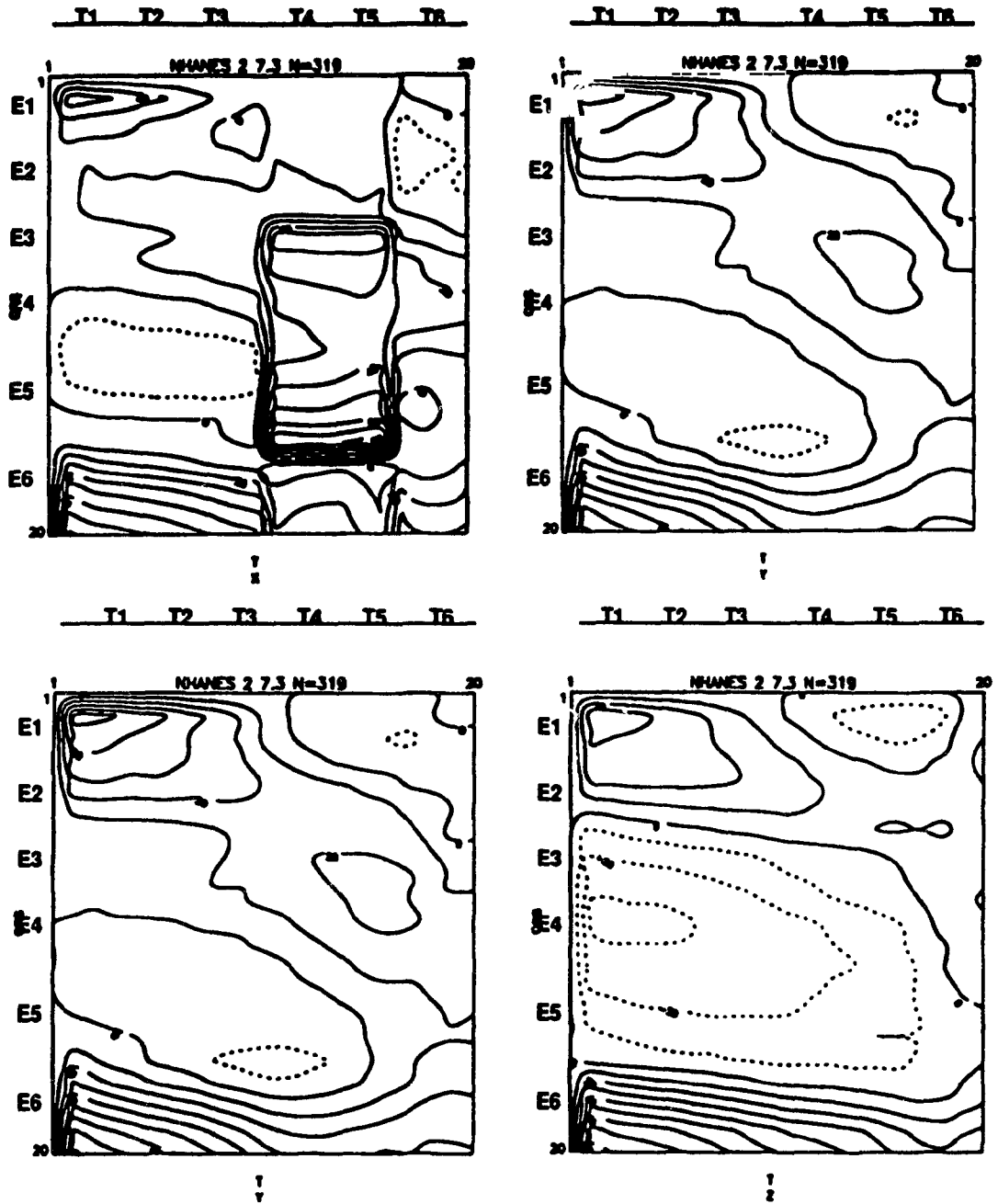
Figure 4.35. Frontal plane components (X and Y) (top) and sagittal plane (Y and Z) (bottom) of QRS-T correlation maps for incomplete right bundle branch block

Incomplete left bundle branch block (ILBBB)

In incomplete LBBB, the impulse conduction through the left bundle branch occurs at a slow rate, but depolarization of the remaining left ventricular free wall proceeds in a normal fashion. Excitation periods in the S-regions (S1 - S6) in normal conduction are assumed to be the same in ILBBB. The estimated mean directions of mean QRS vectors corresponding to E1 - E6, and the frontal and sagittal plane components of the QRS-T correlation maps are shown in Figures 4.36 and 4.37 respectively. The possible permutations of a regional and temporal sequence and a local spatial sequence of repolarization are demonstrated in Figures 4.38A (Frontal plane) and 4.38B (Sagittal plane).

Incomplete LBBB QRS LOOP

Frontal plane

X 100

Incomplete LBBB QRS LOOP

Sagittal plane

X 100
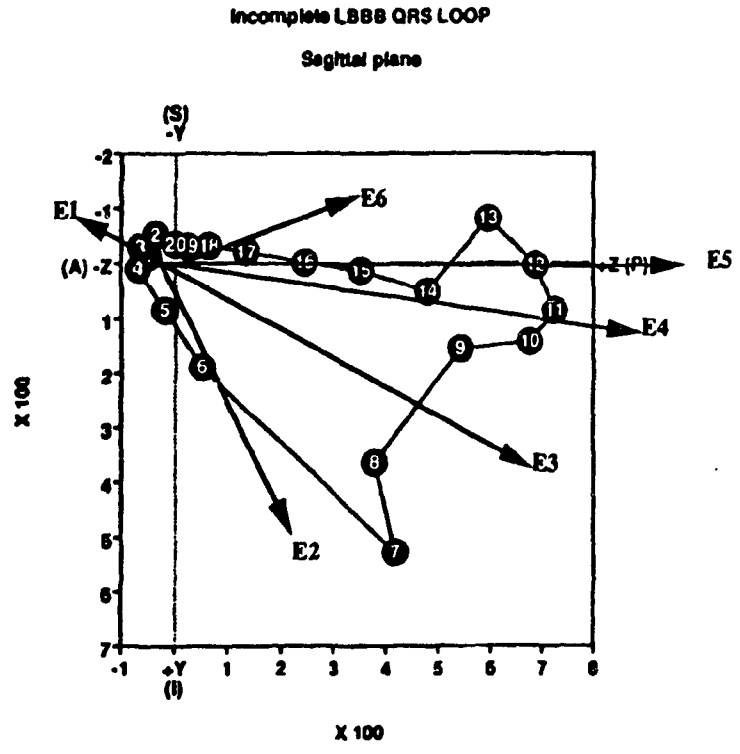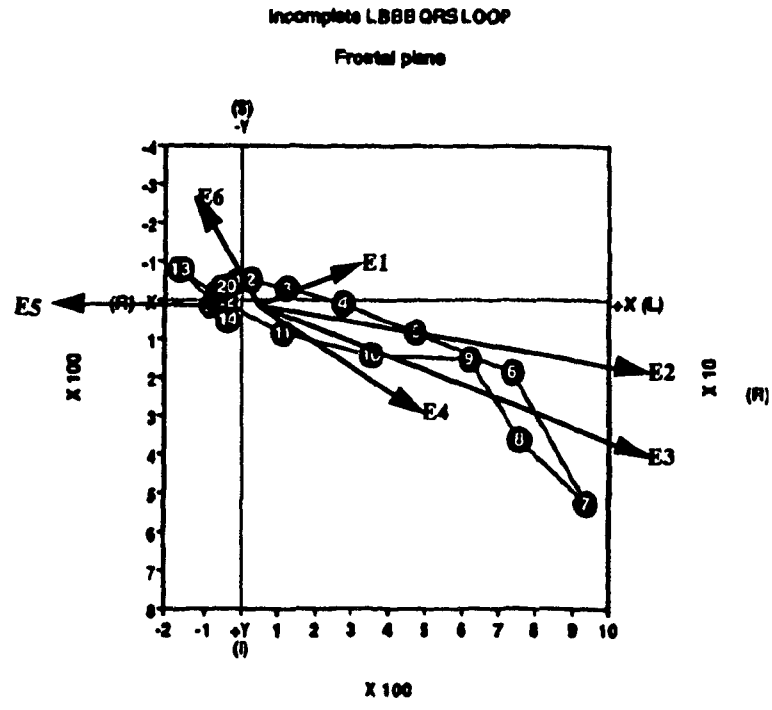
Figure 4.36. Estimated mean directions for QRS mean vectors corresponding to E1 - E6 in the frontal plane (top) and sagittal plane (bottom) for incomplete LBBB.
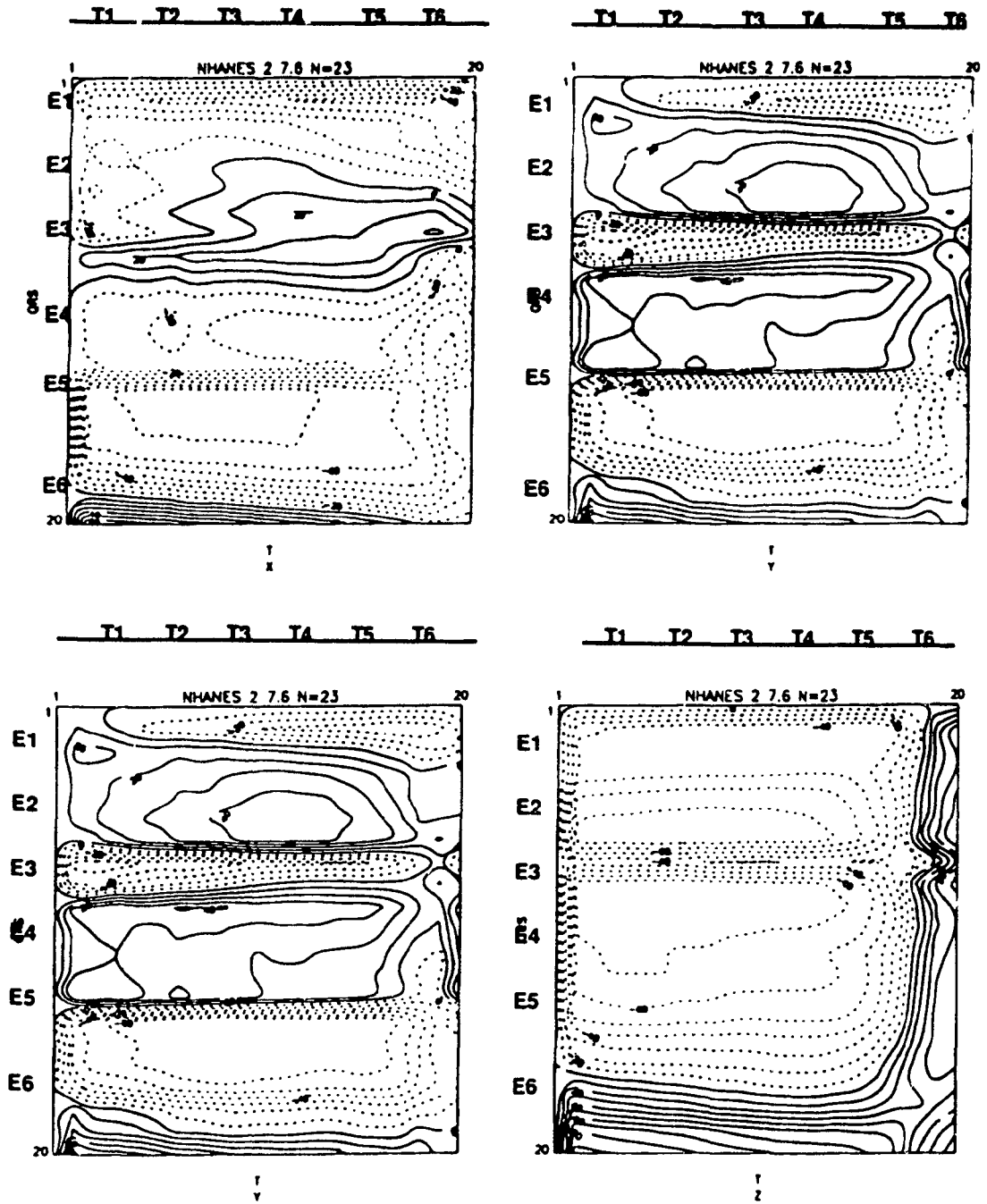
Figure 4.37. Frontal plane components (X and Y) (top) and Sagittal plane components (Y and Z) (bottom) of QRS-T correlation maps for incomplete left bundle branch block.
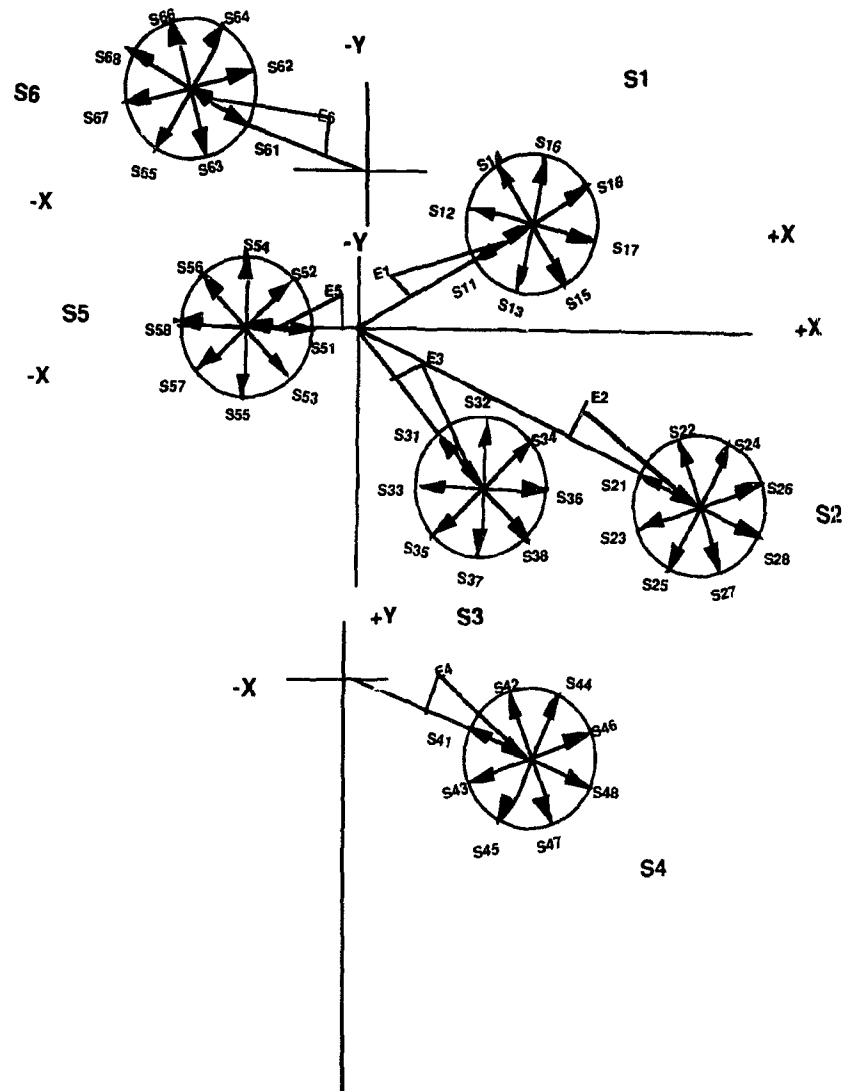
Figure 4.38A. Frontal plane projections of the directions of the uncancelled excitation vectors (E1 to E6) of six left ventricular segments (S1 to S6), and repolarization vectors considered as alternatives to evaluate the likelihood of their contribution to the specific patterns of the correlation maps in ILBBB.
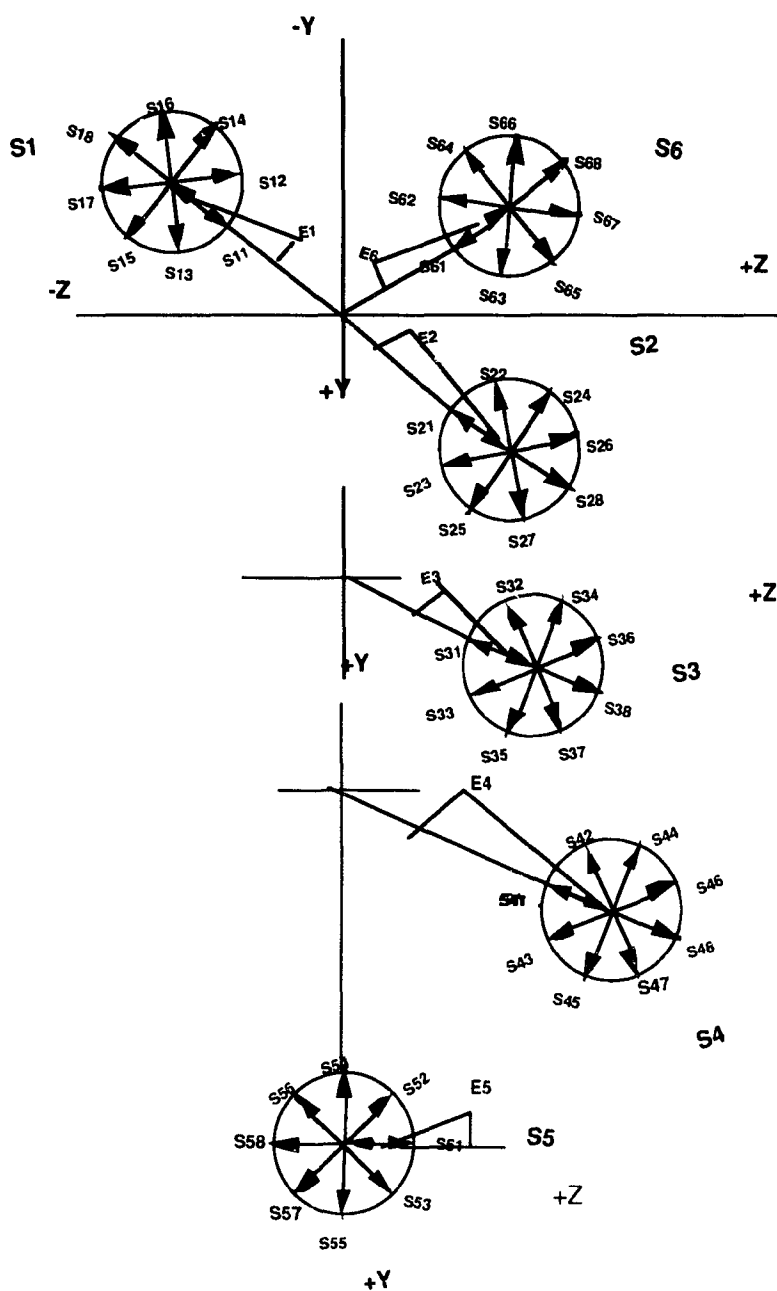
Figure 4.38B. Sagittal plane projections of the directions of the unconcelled excitation vectors (E1 to E6) of six left ventricular segments (S1 to S6), and repolarization vectors considered as alternatives to evaluate the likelihood of their contribution to the specific patterns of the correlation maps in LBBB.

The tabulated data shown in Table 4.20A (frontal plane) and 4.20B (sagittal plane) reveal an interesting pattern of repolarization. In the frontal plane, Segment 1 (septum) was only candidate to satisfy the selection criteria for repolarization during all six time periods (T1 to T6). This segment fits an intermediate sequence during the initial repolarization, but seems to become concordant during the middle and last portions of repolarization. Segments 2 (anterior), and 3 (anterolateral) were the only regions with a reverse sequence for time periods of T2 to T6. Segment 4 (posterolateral) and segment 6 (base) were the only candidates that met the correlation matrix for repolarization for all six time periods. The local spatial direction of repolarization for the posterolateral wall and the base was primarily left to right and apex to base, with an intermediate and concordant sequence respectively.

In the sagittal plane, three regions (S1 - septum, S2 - anterior, and S3 - anterolateral) met the selection criteria for repolarization for any of the time periods considered. This observation again confirms an extensive overlap of repolarization time in these regions. It is interesting to note that segment 4 (posterolateral) and segment 6 (base) fits intermediate repolarization for all six time periods considered. Segments 2 (anterior) and 3 (anterolateral) were the only regions qualifying as candidates for the last regions to repolarize, with reverse sequence with respect to the spatial direction of E6, the last uncancelled portion of depolarization.

Table 4.20A. Segments meeting correlation map criteria for repolarization in ILBBB, at defined time periods, corresponding repolarization vectors, local spatial sequence and direction of repolarization, and the direction of the T wave component produced in the frontal plane.

Frontal Plane

Period	Segment	Vector	Local Sequence	Direction of Depolarization	Direction of T wave
T1	S1, Septum	S16	Intermediate	Right to Left	T1, Right
	S3, Anterolateral	S38	Concordant	Right to Left Superior to Inferior	T1, Right Superior
	S4, Posterolateral	S46	Intermediate	Left to Right Superior to Inferior	T1, Left Superior
	S6, Base	S68	Concordant	Left to Right Inferior to Superior	T1, Left Inferior
T2	S1, Septum	S16	Intermediate	Right to Left	T2, Right
	S3, Anterolateral	S35	Semi-reverse	Left to Right Inferior to Superior	T2, Left Inferior
	S4, Posterolateral	S46	Intermediate	Left to Right Superior to Inferior	T2, Left Superior
	S6, Base	S68	Concordant	Left to Right Inferior to Superior	T2, Left Inferior
T3, T4, T5	S1, Septum	S18	Concordant	Left to Right	T3 -T5, Left
	S2, Anterior	S21	Reverse	Right to Left Superior to Inferior	T3 -T5, Right Superior
	S3, Anterolateral	S35	Semi-reverse	Right to Left Superior to Inferior	T3 - T5, Right Superior
	S4, Posterolateral	S46	Intermediate	Left to Right Superior to Inferior	T3 -T5, Left Superior
	S6, Base	S68	Concordant	Left to Right Inferior to Superior	T3 -T4, Left Inferior
T6	S1, Septum	S18	Concordant	Right to Left	T6, Right
	S3, Anterolateral	S31	Reverse	Left to Right Inferior to Superior	T6, Left Inferior
	S4, Posterolateral	S48	Concordant	Right to Left Superior to Inferior	T6, Right Superior
	S6, Base	S68	Concordant	Left to Right Inferior to Superior	T6, Left Inferior

Table 4.20B. Segments meeting correlation map criteria for repolarization in ILBBB, at defined time periods, corresponding repolarization vectors, local spatial sequence and direction of repolarization, and the direction of the T wave component produced in the Sagittal plane.

Sagittal Plane

Period	Segment	Vector	Local Sequence	Direction of Depolarization	Direction of T wave
T1, T2	S1, Septum	S16	Intermediate	Posterior to Anterior	T1 - T2, Posterior
	S2, Anterior	S26	Intermediate	Anterior to Posterior Inferior to Superior	T1 - T2, Anterior Inferior
	S3, Anterolateral	S38	Concordant	Anterior to Posterior Superior to Inferior	T1 - T2, Anterior Superior
	S4, Posterolateral	S46	Intermediate	Anterior to Posterior Inferior to Superior	T1 - T2, Anterior Inferior
	S6, Base	S66	Intermediate	Anterior to Superior Inferior to Superior	T1 - T2, Anterior Inferior
T3, T4, T5	S1, Septum	S18	Concordant	Posterior to Anterior	T3 - T5, Posterior
	S2, Anterior	S26	Intermediate	Anterior to Posterior Inferior to Superior	T3 - T5, Anterior Inferior
	S3, Anterolateral	S38	Concordant	Anterior to Posterior Superior to Inferior	T3 - T5, Anterior Superior
	S4, Posterolateral	S46	Intermediate	Anterior to Posterior Inferior to Superior	T3 - T5, Anterior Inferior
	S6, Base	S66	Intermediate	Anterior to Superior Inferior to Superior	T3 - T5, Anterior Inferior
T6	S1, Septum	S16	Intermediate	Posterior to Anterior	T6, Posterior
	S2, Anterior	S21	Reverse	Posterior to Anterior Inferior to Superior	T6 Posterior Inferior
	S3, Anterolateral	S31	Reverse	Posterior to Anterior Superior to Inferior	T6, Posterior Superior
	S4, Posterolateral	S46	Intermediate	Anterior to Posterior Inferior to Superior	T6, Anterior Inferior
	S6, Base	S66	Intermediate	Anterior to Superior Inferior to Superior	T6, Anterior Inferior

4.4.3.3. Synthesis of overall considerations

Considering repolarization sequence and QRS-T relationships in one plane or in one lead only, can produce a misleading impression of the overall repolarization process. Repolarization activity in a given region may not be apparent at some time periods in one lead or in one plane, depending on the spatial projection of the activity on different orthogonal leads. Therefore, it is necessary to consider the three dimensional aspects of the process, and the information contained in correlation maps in two principal planes. As a case in point, the schema in Figure 4.39 contains a summary of the regional repolarization sequences for segments meeting correlation map criteria in the frontal and sagittal planes in normal conduction. Figure 4.40 demonstrates the likelihood of a large degree of temporal overlap between the repolarization sequences in various regions of the left ventricle in normal ventricular conduction. Consideration of the fact that repolarization in all likelihood is not a propagated process like excitation, facilitates the understanding of the reasons behind this observation. This observation is consistent with the fact that endocardial repolarization of all segments occurs normally, and nearly simultaneously.

The fact that no match could be found for the repolarization of the basal regions in normal conduction, may be associated with a number of reasons. Repolarization of the basal region may well overlap with repolarization of other regions or may be cancelled by them. Excitation of the basal portions may take considerable interindividual variations diluting correlations. However, the correlations between Segment 6 excitation vectors and repolarization vectors at all six time periods were systematically positive for all elements (E6, T1) to (E1, T6) for all three orthogonal components. It may well be that this observation is related to the late excitation of

the right ventricle or with its repolarization which were both completely ignored in the present consideration. Thus, the basic reason for this observation remains unclear. The repolarization sequence of the left ventricular apex was also not separately considered.

The excitation/repolarization relationships and timing in this region is likely to follow the patterns of the anterior and anterolateral wall, and possibly the lower septum and even lower posterior wall.

	SEGMENT	T1	T2	T3	T4	T5	T6
Frontal	Septum	xxxx	xxxx	xxxx		xxxx	xxxx
Plane	Anterior	xxxx	xxxx	xxxx			
	Anterolateral		xxxx	xxxx	xxxx	xxxx	xxxx
	Posterolateral	xxxx	xxxx	xxxx	xxxx	xxxx	xxxx
	Posterior					xxxx	xxxx
Sagittal	Septum	xxxx	xxxx	xxxx	xxxx	xxxx	xxxx
Plane	Anterior			xxxx	xxxx	xxxx	xxxx
	Anterolateral	xxxx				xxxx	xxxx
	Posterolateral	xxxx	xxxx	xxxx	xxxx		
	Posterior	xxxx	xxxx		xxxx	xxxx	

Figure 4.39. A schema of regional repolarization sequence in normal conduction for segments meeting correlation map criteria indicated in Table 4.17A and 4.17B. x signifies X component of frontal plane

Segment	T1	T2	T3	T4	T5	T6
Septum	xxxx xxxx	xxxx xxxx		xxxx xxxx	xxxx xxxx	xxxx xxxx
Anterior		xxxx xxxx	xxxx xxxx	xxxx xxxx	xxxx xxxx	xxxx xxxx
Anterolateral	xxxx xxxx	xxxx xxxx	xxxx xxxx	xxxx xxxx	xxxx xxxx	xxxx xxxx
Posterolateral and Posterior	zzzz zzzz	zzzz zzzz	zzzz zzzz	zzzz zzzz	zzzz zzzz	

Figure 4.40. A schema of the overall regional repolarization sequence meeting correlation map criteria, demonstrating the likelihood of a large degree of temporal overlap between the repolarization sequences in various regions. x signifies the X component of frontal plane and z signifies the Z component of sagittal plane.

In LBBB, the correlation between segment 6 (base) excitation vectors and repolarization vectors at all six time periods were also systematically positive for all elements for all three orthogonal components. However, unlike normal conduction the basal region met the selection criteria for repolarization for any of the time periods considered. This region fits semiconcordant sequence of repolarization. Excitation/repolarization relationships and timing in this region are likely to follow the patterns of anterior, posterior paraseptal, and anterolateral and posterolateral regions. These regions fit concordant sequence of repolarization. This may also be the case in undetermined type of complete block.

RBBB is the only condition in which the correlation between Segment 6 (base) excitation vectors and repolarization vectors were systematically negative for all elements from (E1, T1) to (E6, T6) for all three orthogonal components. Excitation/repolarization relationship and timing in the base may be governed by the anterobasal portion of the right ventricle. This region fits concordant sequence of repolarization. In an incomplete left bundle branch block, the anterolateral wall is the only region that met the correlation matrix of repolarization in two principal planes during the last time period (T6). The local spatial direction of repolarization in this region fits reverse sequence. Intermediate overall relationships between corresponding excitation and repolarization vectors (i.e. when spatial angle approaches 90 degree) are observed in posterolateral and basal regions. Thus, excitation/repolarization relationship and timing in the anterolateral wall may reflect the last uncancelled portion of ventricular repolarization.

CHAPTER 5
DISCUSSION

5.1. The working hypothesis: The spatial sequence of left ventricular excitation has a strong influence on the spatial/temporal sequence of left ventricular repolarization, so that local spatial excitation-repolarization relationship contributes largely to concordant/discordant type of repolarization in normal conduction and ventricular conduction defects, and the inter-regional temporal excitation-repolarization relationship mainly determines the QT interval. Thus, the inclusion of QRS duration as a covariate with the heart rate correction factor will significantly improve the accuracy of QT and JT prediction.

There are relatively few reports on the temporal/spatial sequence of ventricular repolarization in ventricular conduction defects or even in normal conduction, to provide the basis for adequately understanding the relationship between the repolarization and excitation process [113, 145, 146]. Thus various subintervals of the excitation/repolarization cycle were examined, to determine how the direction of the excitation may be related to the type of repolarization, and its effect on QT and JT intervals.

163

In these deliberations, it turned out to be essential to consider both the overall regional sequence of repolarization, and the local sequence of repolarization, in terms of concordance or discordance with respect to the sequence of excitation. This critical distinction has not been adequately considered in previous publications, which is, perhaps, one of the primary reasons for the discrepancies reported and the considerable degree of confusion that tends to prevail. Consideration of QRS-T correlation maps and the general overall spatial/temporal phase relationships of the instantaneous QRS and T vectors is helpful in these considerations.

One complication in attempts to resolve these issues with simple conceptualized models, is caused by the fact that there is a considerable degree of spatial/temporal cancellation during excitation and repolarization, i.e. there are several overlapping events taking place at the same time in different regions. The excitation process is a relatively fast, and relatively high voltage, propagated process which makes it easier to predict the temporal sequence of propagation of the "isochrones". Ventricular repolarization in all likelihood is a non-propagated process and this process is slower and lower in voltage than activation. All these properties complicate the evaluation of excitation and repolarization relationships using primarily body surface ECG data. The overall considerations and assumptions for the interpretation of QRS-T correlation maps presented in chapter four are, perhaps, a reasonable first step in attempts to interpret these relatively complex relationships. Similarly, a consideration of the degree to which the QRS duration influences the QT and JT interval duration was helpful in these considerations.

5.1.1. Normal ventricular conduction and incomplete right bundle branch block

In normal conduction and incomplete RBBB, the matrix elements match neither a universally reverse nor a universally concordant repolarization sequence. Only three of the matrix elements are consistent with the positivity along the diagonal (E6, T1) to (E1 T6) (Figures 4.25A & 4.32). Similarly none of the matrix elements was present along the diagonal (E1, T1) to (E6, T6) (Figures 4.25B & 4.32). The spatial directions of local repolarization associated with the excitation sequence in the posterolateral and posterior segments indicated in Tables 4.17A and 4.17B, are consistent with a general apex to base and anterior to posterior repolarization, and they are also consistent with the spatial directions of the T vectors generated by these repolarization sequences.

QRS-T correlation maps indicate that some portions of the septum, anterior or anterolateral wall rather than the posterior wall or the base are repolarized last, as they met the criteria for the last regions to repolarize. This finding is consistent with the observation that, in normal conduction and incomplete RBBB, QRS duration has a relatively low, although significant, correlation with the QT interval. If the base (which depolarizes last) were the last region to repolarize, the correlation of QRS duration with QT interval would be very strong and the regression coeffcient on QRS (with rate correction term) would be close to 1. The value of the regression coefficient for QRS (approximately 0.55) in QT regression models suggests that certain myocardial regions repolarized approximately after 35 milliseconds from the onset of

excitation. These regions may well be in the basal parts of the septum or in the anterolateral wall.

In normal conduction, the QRS/T spatial angle between the mean QRS and T vector is normally not zero. The median values of the spatial angle between QRS and T vectors remain greater than 30° from birth to age 16 years [119]. This spatial angle increases with age as the QRS mean frontal plane axis shifts to the left by an average of 8° per decade in the North American population [147]. This is in agreement with the fact that the mean QRS/T angle in adult is about 45 degrees. Our tabulated data indicate that the mean QRS/T spatial angle for normal conduction and incomplete RBBB suggest intermediate type of repolarization. The main temporal contributions to the initial seven T vectors possibly come from the anterolateral wall and apex (Table 4.14). These vectors are in anterior, superior direction, so that the dominant direction of repolarization is likely to be posterior and inferior, i.e. neither reverse nor concordant (approximately intermediate) with respect to depolarization. These intermediate events may be due to competing or cancelling effects when more than one region is simultaneously activated. The remaining anterolateral and apical repolarization would seem to be largely reverse, whereas the posterior wall tends to be semi-reverse as the posterior component of the T vectors is concordant. Concordant repolarization with respect to depolarization is noted in the basal regions.

In incomplete RBBB, the QRS duration is only slightly prolonged, less than 120 ms [148]. In our investigation the correlation patterns resemble largely normal patterns, with the correlation maps matching neither a universally reverse nor a universally concordant sequence of repolarization.(Figure 4.35). Like normal conduction, QRS duration also has a significant but relatively low correlation with QT

(r = 0.04). The delayed activation in incomplete RBBB may result from the longer distance the wave fronts have to travel from the endocardium to epicardium in certain regions of the RV free wall caused by focal hypertrophy [92]. Late phase of excitation towards basal portions does not sufficiently alter the overall excitation-repolarization relationship to alter correlation maps.

The monophasic APD measurements at the epicardial surface of LV indicate a general apex to base direction of excitation [72, 118]. Considering the orientation of the left ventricle, the general overall repolarization sequence in LV is more closely parallel to the free LV wall (in a direction opposite to the lead vector of lead II), rather than transverse to the free LV wall (as is generally assumed by the advocates of the reverse repolarization concept). This implies that T waves in lateral leads I, V5 to V6 and in inferior lead II will be positive even if repolarization in the free wall is not strictly (or at all) reverse (Table 4.14). Even though the observed APD gradients (shorten APD at LV epicardium) are still valid, the APD shortening measured is unlikely to generate conditions for strictly reverse repolarization. It is conceivable that the lateral direction of overall repolarization in normal conduction and in incomplete RBBB, may create the condition in which the excitation time may influence QT interval.

The reverse sequence model can be true only if action potential duration values along a given excitation path, shorten more than excitation time values increase. If repolarization were strictly reverse, QRS duration would have no influence on the QT interval This is not the case, although the correlations between QRS duration and QT are relatively low in normal conduction and in incomplete RBBB (Table 4.12).

Let RT_L and ET_L denote repolarization time and excitation time (with respect to QRS onset) of the ventricular myocardial region, which repolarizes latest and thus determines the QT interval length. Denote action potential duration in this region by APD_L Thus:

$$QT = RT_L \qquad (5.1)$$

$$= ET_L + APD_L \qquad (5.2)$$

$$= f(HR, QRS) \qquad (5.3)$$

i.e. QT is a functi)n of both heart rate and Qi'S duration.

For a reverse sequence of repolarization, the action potential duration values across the free wall of the left ventricle shorten more than the excitation time values increase.

Under this condition:

$$QT = APD_0 \qquad (5.4)$$

and

$$JT = APD_0 - kQRS \qquad (5.5)$$

where $k = 1$ and APD_0 is the action poential duration of the endocardial sites excited earliest.

Compare the multiple model prediction QT and JT intervals of the forms as discussed in the QT and JT modeling studies in chapter four:

$$QT = \alpha_1 RF + \beta_1 QRS + \gamma_1 \qquad \text{(Model 1)}$$

$$JT = \alpha_2 RF + \beta_2 QRS + \gamma_2 \qquad \text{(Model 2)}$$

where

$RF = 656/(1 + 0.01\ HR)$ is a single parameter functional expression found to produce the best QT prediction out of 13 formulas evaluated in a large normal population [2]. If the reverse sequence concept were strictly valid, the regression coefficient (β_1) for QRS would be = 0 for QT prediction and $\beta_2 = -1$ for JT prediction.

In normal conduction and in an incomplete right bundle branch block, QRS duration has some influence on the QT interval. The values of the QRS duration regression coefficient on QT and JT are 0.55 and -0.45 for normal conduction, and 0.56 and -0.40 for an incomplete bundle branch block (Table 4.12). ET_L increases with increasing QRS duration. APD_L shortens with increasing QRS duration but not as much as ET_L prolongs. This is why QT tends to prolong and JT shortens with QRS duration increases. Also the J point shifts to a later time point which shorten JT interval. There is a modest but significant relationship between QRS duration and QT in normal conduction (r = 0.03), and in incomplete right bundle branch block (r = 0.04).This correlation would be zero if repolarization were strictly reverse universally in all regions.

The inclusion of QRS duration in the multiple QT regression formula, also made a significant contribution to the QT interval in the normal population ranging from 20 to 75+ years old, particularly after the age of 50 years, as indicated by a high value of β_1 ranging from 0.53 to 0.60 (Table 4.4).

There are sex differences in the mean values of QTI. However, the longer Q_i in females seems to suggest that sex differences are due to QT shortening in males rather than QT prolongation in females, as the females' QTI are still within the normal range (Table 4.4). The normal population standards for the QT index (QTI) has a mean value of 100 and 95% normal range from 90 to 100 [2].

The mean QRS duration of males becomes significantly longer than in females with an absolute difference of about 6 ms throughout adult life. The increased mean QRS duration in males probably reflects heart size in males [142]. However, this QRS duration difference does not explain the observed sex difference in QTI since longer QRS values in adult men are expected to result in QT prolongation rather than shortening.

In males the relatively unchanged heart rate and the significantly lower heart rate values may be taken to reflect higher parasympathetic tones in males compared to females. However, it does not explain the QT shortening since a higher parasympathetic tone is expected to prolong the QT rather than to shorten it, as has been reported to happen, for instance, during sleep [149]. At the present time it is best to concede that the mechanism of the QT shortening in males remains unknown.

Normal conduction and incomplete right bundle branch block are the situations that may come closest to the reality of a repolarization sequence that is mainly reverse, but concordant sequence prevails during the terminal part of repolarization in the

myocardial regions depolarized latest. Under these conditions, the main portion of QRS and T waves are concordant, but the terminal portion is not clearly concordant or discordant. The JT interval reflects action potential durations in the basal portions of the ventricles excited last.

5.1.2. Incomplete left bundle branch block (ILBBB)

The basic requirements for a reverse sequence of repolarization are that QRS duration has no influence on the QT interval and that the T wave is fully concordant with QRS. Incomplete LBBB is the only condition with a zero correlation between QRS and QT interval (Table 4.12). The correlation matrices results seem in full agreement with this observation. The anterolateral wall is the only candidate with a local reverse sequence of repolarization in two principal planes during the last time periods (T6) of repolarization. This seems to suggest that the anterolateral wall could be the region with uncancelled portion of ventricular repolarization, and therefore represents the T wave. The local spatial and temporal regional sequence of the left ventricular depolarization and repolarization in Tables 4.20 A and 4.20B suggest that the intermediate overall relationship between the corresponding excitation and repolarization vectors (i.e. when the spatial angle approaches 90 degrees) is dominant in the septum, posterolateral and basal regions of the left ventricle. This may imply major excitation and repolarization events occurring simultaneously in different regions, with an anterolateral wall repolarization making most the contribution to the T wave. The reverse sequences of repolarization in the anterolateral wall in both frontal and saggital planes may be the main contribution to X and Z leads.The QRS

regression coefficent on QT in Model 1 (Chapter 4) was small and insignificant, this

further supports the notion of reverse repolarization in incomplete LBBB. The

increased thickness of the LV wall may explain the increased QRS duration (Table

4.10). Another condition that is also relatively close to this situation is in the younger

age groups of 20 - 39 of our research study, where QRS duration has no significant

effect on QT interval (Table 4.2).

5.1.3. Complete bundle branch blocks

During complete bundle branch blocks, the time required to complete ventricular

activation exceeds the range of duration of ventricular action potentials. The QRS

duration in man is about 120 ms or more [72]. As a result, the sequence of activation

sets the sequence of repolarization and T vectors are oriented opposite to the direction

of QRS vectors. T vectors are practically always 180° discordant to the spatial QRS

vectors [93]. k < 1 when the Δ ET in a free LV wall is approximately 70 ms [75], and

the regional maximum Δ APD is 20 ms. In left bundle branch block and to some

extent in IVCD (complete block of unspecified type), the correlation matrix elements

match a universally concordant repolarization sequence, as many matrix elements are

consistent with the negativity along (E1, T1) to (E6, T6) diagonal (Figures 4.28 &

4.30). The local spatial direction of repolarization in many areas in LBBB primarily

fit the concordant or semiconcordant sequences. The combinations of all these local

repolarizations would produce regional repolarization in an anterior to posterior and

apex to base spatial direction. There is an extensive overlap of repolarization in many

regions for any of the time periods considered. The base is the last region repolarized

with a concordant sequence. Data tabulated in Table 4.15 confirmed the concordant

sequence of repolarization with respect to the excitation process in the left ventricle.

The initial vectors of ventricular activation direct to the left, posteriorly and inferiorly,

in agreement with the way the activation wave spreads from right to left to depolarize

the left septal mass (Table 4.15). The main net temporal contributions to the initial T

vectors and the terminal T vectors, come from the anterolateral left ventricular free

wall and anterobasal region respectively. These vectors are mainly in right, anterior,

and superior direction, so that the dominant direction of repolarization is likely to be

left, inferior and posterior, which is in the same direction as that of the excitation

process. The QRS/T spatial angle is close to 180 degrees as expected, for a full

concordant sequence of repolarization. In LBBB and IVCD a strong influence of

excitation duration on QT interval is evident (Table 4.12).

This predominant concordant repolarization in LBBB may possibly be

accounted for by the fact that excitation does not penetrate into the left ventricle

through the subendocardial Purkinje fiber network as normally, and tends to spread

mainly in an apex to base direction. An increase in the conduction time generally

implies an increase of the ventricular mass being activated in the same direction due to

loss of cancellation effects [136]. Thus there is a tendency for repolarization to

proceed in the same direction as that of depolarization. This may explain the

predominant feature of concordant repolarization over most of the local repolarization.

In the base, the spatial direction of regional repolarization to the excitation sequence

indicated in Table 4.18A is also consistent with a general apex to base repolarization.

This suggests the QT interval in concordant sequence of repolarization reflects the

sum of excitation time and the duration of repolarization in the basal portions of the ventricle in LBBB.

In RBBB, the early septal and paraseptal activation spreads from left to right in a normal activation sequence, since the left bundle branch is intact. The right septum and the right ventricular free wall activate last after most of the LV free wall depolarization has already occurred [88]. The septal depolarization is prolonged over 40 ms [97]. The Δ ET in the free RV lateral wall is approximately 60 - 70 ms [75]. The main fraction of excitation is unchanged from normal, and the main difference is the change in the direction of the terminal excitation of the right ventricle (pulmonary conus or basal right ventricle). The initial normal depolarization associated with abnormal repolarization in the horizontal and saggital plane projections of the orthogonal QRS and T vectors (Figures 4.20 & 4 21) may be due to predominance of concordant local repolarization of the lateral RV and posterior RV.

Data in Table 4.16 indicate that the net temporal contribution to the terminal T vectors comes from the right ventricle. These vectors are in a left and inferior direction. Thus the dominant direction of repolarization is to the right and superiorly, which is concordant with the excitation process in this region. A strong influence of QRS duration on QT and the dominant negative correlation elements in Y and Z components (Figure 4.32) suggest that spatial/temporal concoidant repolarization in the basal area of the right ventricle may contribute to the concordant pattern of repolarization and may determine the length of the QT interval.

For a concordant sequence of repolarization:

$$QT = ET_L + APD_L \qquad (5.6)$$

$$= QRS + APD_0 - k_2 QRS \qquad (5.7)$$

$$= APD_0 + (1-k_2)QRS \qquad (5.8)$$

$$= \alpha_2 RF + \beta_2 QRS \qquad (5.9)$$

$$\text{and } JT = APD_L \qquad (5.10)$$

$$= APD_0 + (1-k_2)QRS \qquad (5.11)$$

$$= \alpha_2 RF \qquad (5.12)$$

Let $ET_L = QRS$, and $APD_L = APD_0 - k_2 QRS$

where subscript L refers to a myocardial region which at some particular reference heart rate has the longest RT and thus repolarizes latest.

Comparing this model with the multiple model prediction QT and JT intervals of the forms as discussed in the QT and JT modeling studies in Chapter four, the regression coefficients (β_1) for QRS would be $\beta_1 = 1$ for QT prediction and $\beta_2 = 0$ for JT prediction.

The QRS duration has a pronounced influence on the QT interval in complete bundle branch blocks, explaining 15% of the total QT variance in these VCD categories. Contrariwise, the influence of QRS duration on JT is practically negligible in complete bundle branch blocks (Table 4.12). The excitation times of those regions where the repolarization occurs last, vary significantly due to the excitation delays

caused by various degrees of blocks. This is best seen from the wide range of the values of regression coefficients (β_1), suggesting that the contribution of QRS to QT and JT is proportional to the degree of blocks. For example, complete bundle branch blocks of unspecified types and left bundle branch block, have both delayed ET (i.e. prolonged QRS duration) and a greatest β_1, QT is increased due to the greatest value of β_1ET.

The prolonged mean QRS (i.e. delayed ET) with practically negligible influence of QRS duration on the JT interval in complete bundle branch blocks discussed in chapter four, implies that APD_L no longer shorten with ET_L, meaning that the regions with latest repolarization times are later and later in the excitation sequence. Consequently, the JT interval reflects the closest action potential durations in basal portions of the left or right ventricle or the intraventricular septum, depending on the type of excitation pattern. The QT reflects the sum of excitation time and the duration of repolarization, in the basal portion of the ventricle. Thus the dispersion of repolarization times is determined by the differences in activation times and the action potential duration differences.

The pronounced influence of QRS duration on QT (β_1 ranges from 0.62 to 0.91) in normal adults over 40 years old may also come closest to the reality of the concordant sequence of repolarization. The alteration in the ventricular excitation sequence is likely associated with an alteration in ventricular repolarization in the older age groups. Epidemiological studies [150] documented that heart weight increases due to left ventricular (LV) wall thickness between the age of 30-90 years. Left ventricular mass increase is an important determinant of the QRS axis left shift with age [147]. The gradually increased QRS duration and increasing left axis shifts

with age, may reflect alteration in the conduction properties, excitation sequence, or timing alteration. There is likely to be a gradual delay in the onset of excitation in those myocardial regions which repolarize latest and determine the duration of the QT interval. This would explain why CRS duration makes an increasingly important contribution to QT interval with advancing age. This is best seen in the increasing value of the QRS regression coefficient for QT which, for instance in females, increases from 0.44 in the youngest age group to 0.91 in the older age group, a value which is nearly as high as LBBB, a condition with a nearly concordant sequence of repolarization and depolarization [151].

Our results indicate that the single parameter model for JT prediction (Table 4.13) performs as well as the other complex models. Therefore, from a statistical point of view, it is inconsequential whether QT or JT is used in these prediction formulas as long as an adjustment is made for QRS duration in QT prediction. Inherent in this reasoning, is the assertion that QT duration is linearly dependent on the ventricular excitation time, which also implies that the JT interval is linearly and inversely dependent on QRS duration. This fact explains the observed linear inverse relationship between the coefficients for QRS in QT and JT regression on the rate factor and QRS (β_1 and β_2 in Figures 4.2 & 4.6) since a linear term was used for QRS duration as a covariate and JT = QT - QRS.

5.2. Conceptual problems in the assessment of excitation/repolarization relationship

The following considerations will help in the assessment of the conceptual problems involved in the development of models to account for excitation/repolarization relationships.

1. In the transmembrane action potential of a single fiber of a rhythmically beating ventricle, there is a plateau (Phase 2) of about 100 ms and a rapid repolarization (Phase 3) of 150 ms as the resting potential is restored [152]. The duration of the plateau (DP) is rate dependent. Let us assume that the plateau is 100 ms and the duration of rapid repolarization (PD$_3$) is 150 ms.

2. The slope of the fast phase of repolarization of different MAPs does not deviate by more than 10% from the average slope in canine hearts after bilateral upper thoracic sympathectomy was performed to slow the heart rate [109]. During the steady state, we assumed that the ventricular action potentials have the same slope as phase 3 and differ from each other in duration only because of the different duration of phase 2.

3. Monophasic APD measurements with suction electrodes at LV endocardial surface in man have demonstrated that APD values decrease progressively in direct proportion to excitation time so that the repolarization time (RT) tends to be equal at all endocardial sites [112].

Assume that in any myocardial region (segment) considered (for instance in the Selvester model) [79] Phase 3 duration is constant, although the slope may vary from region to region. Let excitation time and APD in the myocardial fibers excited earliest

(i.e. endocardial fibers), be denoted by ET_0 and APD_0 respectively. Assume further that APD shorten linearly with excitation time and that the excitation wave front propagates radially across the segment, then the start of repolarization (SR) in various layers across the segment is:

$$SR = ET + APD - DP_3 \qquad (5.13)$$

$$= ET + (APD_0 - kET) - DP_3 \qquad (5.14)$$

$$= (1 - k)ET + APD_0 - DP3 \qquad (5.15)$$

$$= (1 - k)ET + DP_0, \qquad (5.16)$$

when DP_0 = duration of the plateau at endocardium.

End of repolarization (ER) in various layers in this segment is:

$$ER = \text{start of repolarization (SR)} + DP_3 \qquad (5.17)$$

$$= (1 - k)ET + APD_0 \qquad (5.18)$$

The hypothesis of an exactly reverse repolarization sequence must fulfill the following conditions:

$$APD_{epi} < [APD_0 - (ET_{epi} - ET_0)], \qquad (5.19)$$

or

$$(APD_0 - APD_{epi}) > (ET_{epi} - ET_0) \qquad (5.20)$$
$$> \Delta ET$$

According to the assumption of linear shortening of APD with excitation time,

$$APD_{epi} = APD_0 - k \, \Delta ET \qquad (5.21)$$

thus, $k > 1$ is the condition for a reverse sequence of repolarization.

The approximate ΔET is 45 ms [79] and the reported maximum $\Delta APD = 20$ ms. The fact is that excitation time differences are just as large or larger than reported differences in APDs across the free wall, $k < 1$ as long as $\Delta ET > 20$ ms. This fact speaks against the reverse repolarization sequence concept, if this is taken to assume that repolarization proceeds exactly in the opposite direction to excitation in the free wall of the left ventricle. Alternative explanations and concepts must be considered to account for the observed concordant polarity of T waves in ECG leads oriented laterally, mainly in +X direction in the orthogonal reference frame of the body.

Experimental evidence demonstrates that in isolated canine ventricular muscles, the changes in activation patterns are affected by the anisotropic properties of cardiac muscles, and that the electrotonic effects of propagation of activation alter action potential durations [115, 145]. Therefore it becomes important to consider how the direction of excitation with respect to fiber orientation may determine concordant or discordant types of repolarization.

5.2.1. Alternative considerations for the mechanism of generation of concordant and discordant types of repolarization in normal conduction and in ventricular conduction defects

Little attention has been given to the contribution of myocardial fiber orientation to the patterns of ventricular excitation [75]. This is even more true regarding ventricular repolarization.

Armour and Randall [153] performed a structure-function analysis on the mammalian hearts of nine different species. They found that the bulk of ventricular fibers provide a principal fiber direction which is generally oblique to a vertical base to apex axis. It is known that the myocardial fibers rotate between the epicardial and endocardial surfaces [154] and that most of the endocardial surface contains a layer of Purkinje tissue electrically continuous with the myocardium [155]. The orientation of average ventricular muscle fibers is mainly tangential to the endocardial and epicardial surfaces of the ventricles, although their direction rotates by about 90 degrees from

the endocardial towards the epicardial layers, and the average fiber angle rotation in the LV lateral and posterior walls is close to 180 degrees [156]. Taᵣcardi [157] found that in an intramural spread of activation, the activation wavefronts, initiated at the epicardial surface, invariably proceed from epicardium to endocardium, and then rotate and spread from the endocardium back to the epicardium. Fiber orientation on the epicardium of the LV is parallel to the longitudinal axis of the heart during diastole [154], and these fibers assume a more horizontal position during systole [153]. It is evident that the spread of activation would be influenced by the orientation of fibers.

Both in vivo [114] and in vitro studies [115, 145] of limited numbers of sites have shown that the electrotonic effects of propagation of activation alter action potential durations. According to the concept of electrotonic interactions, the action potential duration in the site of origin of the stimulus will be longer than the distal area; whereas the action potential durations tend to be shorter in the sites where repolarization is expected to end. This phenomenon is attributed to the influence exerted by surrounding tissues which are either fully depolarized or fully repolarized [125, 133]. The magnitude of the electrotonic effect of activation on repolarization properties has been demonstrated. Toyoshima and Burgess [125] reported that the percent shortening of the refractory period is greater along the transverse than along the longitudinal axis of the heart. Consistent with this finding, Osaka [145] found that APD shortens more along the transverse (perpendicular to the long axis of the muscle fiber) than the longitudinal direction, and that the activation fronts proceed at a higher speed in the longitudinal direction (along the long axis of the muscle fiber) than in the transverse direction. He reported 11 ms differences in APDs during longitudinal and

transverse propagation [145]. This experimental evidence suggests that the difference in percent shortening of the refractory period is related to the orientation of fibers.

Our results are not in agreement with the commonly accepted concept of a reverse sequence of repolarization in the left ventricle. Instead, we found that left ventricular repolarization is not universally reverse in normal ventricular conduction, and becomes increasingly more concordant in the posterior and basal regions. However, our observations support the overall concordant apex to base sequence of repolarization, disputed by some investigators, at least in the dog heart [118]. This overall repolarization sequence in left ventricle tends to be consistent with the principal fiber direction [153]. The observation that the anterolateral wall ended up together with the septum as a region that may repolarize latest, may at first sound counterintuitive due to the general doctrine asserting that the first region to repolarize is the free lateral wall of the left ventricle (in reverse order). This line of thinking has been largely based on information manifested in one dimension and only in left lateral leads. Correlation map information suggests that although repolarization may start first at the epicardial portions of the left free lateral wall, the repolarization sequence in the anterolateral segment in the sagittal plane is semireverse, or even intermediate to excitation sequence. Recent reports of the long action potential durations of the M cells residing in intramural regions near the epicardium in the anterolateral wall [158] are also consistent with this possibility. The dominant effect of an apex to base direction of repolarization from region to region, no matter what happens within each region, regarding transmural repolarization patterns, indicates that the excitation time (QRS duration) is expected to have an influence on QT interval.

In the event of concordant repolarization with delayed excitation, particularly in LBBB, and IVCD, excitation spreads in apex to base direction, mainly parallel rather than transverse to fiber orientation. Under this condition, excitation has a more pronounced component in the direction of fiber orientation. Myocardial regions excited earliest are expected to be less likely to repolarize last. Inherent in this reasoning is the assertion that the excitation time of the regions which depolarize last (ET_L), will influence the onset time of repolarization in these regions. ET_L is likely to be a function of QRS duration, as ET_L prolongs strongly in direct proportion to QRS duration. The APD_L does not shorten more than the increased ET_L. As a result, JT becomes independent of QRS.

In incomplete LBBB, the repolarization sequence in the anterolateral segment in two principal planes is reverse to the excitation sequence, and occurs during the last time period (T6). An extensive intermediate overlap relationship between corresponding excitation and repolarization vectors in posterolateral and basal regions is observed. This information suggests that repolarization activity in the anterolateral wall may be the last uncancelled portion of repolarization, which is in a reverse sequence to depolarization, transverse to the free left ventricular wall and determines the QT interval. This explains the zero correlation between QRS duration and the QT interval. In this situation, the T duration may reflect the dispersion of the fast phase of repolarization times in the anterolateral wall of the left ventricle.

The influence of variation of fiber directions on the distribution of tension in the left ventricle has not yet been fully established, and it is possible that the changes of ventricular wall tension and pressure are a prominent determinant of the repolarization sequence. Lab [159] produced shortening of the QT interval of the ECG in an

isovolumic contracting frog ventricle as compared with the auxotonic beating heart. The plateau phase of the action potential was steeper during isovolumic than during auxotonic contraction as high tensions are associated with a short action potential. The percentage of reduction in duration in action potential at T_{75} was of the same order as the reduction in duration of the QT interval. Recently, Huang et al.[160] demonstrated in the canine hearts that the QT shortening induced by efferent sympathetic neurons is primarily associated with increased ventricular intramyocardial tension or left ventricular chamber pressure rather than heart rate.

A recent study [161] revealed that women aged ≥65 years have a significantly higher prevalence of QT prolongation than do men and are approximately three times more likely to have prolonged QT after adjustment for other factors expected to influence the QT interval, such as systolic and diastolic blood pressure, QRS duration, and the electrocardiographic estimate of the left ventricular mass indexed to body surface area. Our present study also indicated that the rate corrected QT values in women were indeed significantly longer than in men, but the age trend differences in QTI between gender groups were non-significant. A possible explanation is that we did not include blood pressure and left ventricular mass as covariate in our prediction models. It has been demonstrated that QT prolongation is significantly associated with the electrocardiographic estimate of the left ventricular mass and ischemic injuries [161]. Thus it is possible that myocardial contractility variations become a significant new factor contributing to the large unexplained QT variance not associated with heart rate variation and other known factors. The excess risk of cardiovascular disease mortality associated with even a moderate QT prolongation is

at least partially due to confounding factors and not entirely due to arrhythmogenic mechanisms associated with QT prolongation.

CHAPTER 6
LIMITATIONS OF THE STUDY, SUMMARY AND CONCLUSIONS

6.1. Limitations of the study

The present investigation has a number of limitations. The correlation maps used only consider QRS-T relationships separately in individual X, Y, Z leads, providing in essence partial autocorrelation data. Cross-correlation maps between the orthogonal X, Y, Z components seem warranted to extract more information on the nature of repolarization sequence (e.g. X (QRS) vs Y (T) or X (QRS) vs Z(T) correlation). Similarly, vector correlation maps correlating spatial vector magnitude of QRS with T vectors may be potentially valuable. Another limitation of this approach is that extracardiac factors which simultaneously attenuate or enhance both QRS and T amplitudes at all time instants are likely to produce positive or negative correlations between the segments and elements considered. It is not possible to separate or even to identify with any degree of reliability this possibility. Furthermore, the role of the right ventricle was ignored, with the exception of the right complete bundle branch block. It is clear that a more definitive answer to these rather difficult conceptual problems has to wait for comprehensive electrophysiological data, including action potential duration and repolarization time, measured not only on epicardial and endocardial surfaces but also in intramural regions. These detailed electrophysiological data will help to reach a better understanding of how the QT interval variations in various ECG leads relate to the dispersion of repolarization times in the myocardium.

187

6.2. Summary

The patterns of a mainly reverse sequence of repolarization in normal conduction, and mainly concordant repolarization in some categories of ventricular conduction defects, were analyzed by using instantaneous QRS and T vectors and QRS-T correlation maps. The effect of variations in excitation sequence and excitation time on QT and JT intervals was assessed by using several linear regression models. The working hypothesis was postulated to examine the influence of spatial sequence of left ventricular excitation on the spatial/temporal sequence of repolarization in terms of concordance and discordance and its effects on the QT interval. The local spatial repolarization in normal conduction and incomplete RBBB is mainly in reverse sequence in relation to spatial excitation sequence. The general overall spatial apex to base and anterior to posterior direction of repolarization suggests that the local repolarization process deviates from the reverse towards concordant repolarization at the posterior wall and the base of the left ventricle. If repolarization were strictly reverse, QRS duration would have no influence on the QT interval. Our data support a neither universally reverse, nor a universally concordant, sequence of repolarization in normal conduction, and in incomplete RBBB. Regions in the septum, anterior wall or anterolateral wall, rather than the base, are likely to repolarize last. The gradual increase of QRS duration and its significant contribution to the QT interval with age in the normal population suggests a shift from the predominant pattern of reverse sequence of repolarization in young adults (20 to 39 year old) to a partially concordant sequence of repolarization in some myocardial regions in older adults. This shift is possibly related to an increase excitation time associated with an

increased left ventricular mass in the older age groups. In complete bundle branch blocks, the concordant local and regional temporal repolarization dominate the left ventricle. A general spatial apex to base direction of regional temporal repolarization is consistent with an apex to base excitation direction. There is a strong influence of excitation duration on QT interval as QRS duration explains 16% of total QT variance. This may also be the case in untermined type of complete bundle branch block. In RBBB, the main fraction of excitation is unchanged from normal, and the main difference is the change in the direction of the terminal excitation of the right ventricle. The concordant repolarization in the basal area of the right ventricle during the large part of repolarization time may suggest that spatial/temporal sequence of excitation of the right ventricle has a strong influence on the temporal/spatial sequence of ventricular repolarization. The reverse sequence of local spatial repolarization in the anterolateral wall in two principal planes during last repolarization time and zero correlation between QRS duration and QT interval imply that the transmural difference in action potential durations is largely responsible for the T wave polarity in incomplete LBBB.

6.3. Future direction for the study of repolarization sequence and QT interval relationships in the body surface electrocardiogram

It is clear that further investigation in many areas of this field is desirable. Given the results and limitations of our study, we may speculate on the nature of future work to be carried out.

In the present invastigation, we evaluated several regression models on the steady state heart rate in order to obtain the best regression equations for QT and JT, and we did not consider dynamic behaviour of QT interval in different states of activity of sympathetic nervous system. A search for an optimal, physiologically meaningful QT prediction formula will be facilitated by detailed beat-to-beat analysis of QT/HR relationship from individual records of normal subjects, with a wide range of heart rate values over long time periods, particularly involving periods of exctreme bradycardia and tachycardia, and also from individual records of patients with various categories of ventricular conduction defects.

The electrocardiographic estimate of the LV mass has been demonstrated as one of the factors influencing the QT interval. A study of the influence of an increased LV mass on the spatial sequence of LV excitation and spatial/temporal sequence of repolarization would shed light on the mechanism responsible for a gradual prolongation of QT interval in left ventricular hypertrophy.

Experimental evidence indicated that different degrees of shortening or tension development of ventricular muscles are associated with varying rate of repolarization,

as indicated by the duration of action potential. Direction of excitation with respect to fiber orientation is likely to be an important determinant of the type of repolarization regarding its concordance or discordance. Therefore, direction of excitation in relation to fiber orientation needs to be considered in future studies designed to derive improved models for ventricular repolarization.

6.4. Conclusions

In conclusion, our working hypotheses provides a conceptual structure for explaining the observed absence of strictly reverse sequence of repolarization in normal conduction and for the pronounced alterations in repolarization patterns in ventricular conduction defects (VCD). It attempts to elucidate the meaning of the QT and JT intervals, repolarization duration and dispersion of repolarization time which varies depending on the types of ventricular conduction. The prolongation of QT interval in various categories of ventricular conduction defects may be either secondary to altered excitation process or due to primary repolarization abnormalities. No attempt was made in the present investigation to separate primary and secondary repolarization abnormalities. The results suggest that it is important to consider both the local spatial and the regional temporal sequence of repolarization in relation to the excitation sequence when interpreting the mechanism of the generation of QT and JT intervals.

References

1. Bourdillon, P. and J. Mulrow, *QRS duration is an independent predictor of QT duration [abstr]*, in *Computer ECG Analysis: Towards Standardization CSE. Working Conference*, J. Willems, v.B. JH, and C. Zywietz, Editors. 1985, North Holland, Amsterdam. p. 23.

2. Rautaharju, P., J. Warren, and H. Calhoun, *Estimation of QT prolongation: a persistent avoidable error in computer electrocardiography.* J Electrocardiol, 1991. **23 (suppl)**: p. 111.

3. Reynolds, E. and C. van der Ark, *Quinidine syncope and delayed repolarization syndromes.* Med Concepts Cardiovasc Dis, 1976. **55**: p. 117.

4. Thurman, J. and M. Cowan, *Relationship between the prolonged QTc interval and ventricular fibrillation.* Heart lung, 1986. **15**: p. 141.

5. Ahnve, S., E. Gilpin, and D. Madsen, *Prognostic importance of QT interval at discharge after acute myocardial infarction. A multicenter study of 865 patients.* Am Heart J, 1984. **108**: p. 395.

6. Somberg, J., *Calcium channel blockers that prolong the QT interval.* Am Heart J, 1985. **107**: p. 416.

7. Das, G., *QT interval and repolarization time in patients with intraventricular conduction defects.* J Electrocardiol, 1990. **23**: p. 49.

8. Carmeliet, E., *Influence du rythme sur la duree du potential d'action ventriculaire cardiaque.* Arch Internat Physiol Biochim, 1955. **63**: p. 222.

9.   Brooks, M., B. Hoffman, and E. Suckling, *Excitability of the Heart*. 1955, New York: Grune & Stratton.

10.   Hoffman, B. and P. Cranefield, *Electrophysiology of the Heart*. 1960, New York: McGraw Hill Book Co., Inc. p. 254.

11.   Carmeliet, E., *Repolarization and frequency in cardiac cells*. J Physiol Paris, 1977. **73**: p. 903.

12.   Elharrar, V. and B. Surawicz, *Cycle length effect on restitution of action potential duration in dog cardiac fibers*. Am J Physiol, 1983. **244**: p. H782.

13.   Lepeschkin, E., *Modern Electrocardiography*. Vol. 1. 1951, Balimore: The Williams & Wilkins Company.

14.   Mendez, C., C. Gruhzit, and G. Moe, *Influence of cycle length upon refractory period of auricles, ventricles and A-V node in the dog*. Am J Physiol, 1956. **184**: p. 287.

15.   Mines, G., *On functional analysis by the action of electrolytes*. J Physiol (London), 1913. **188**: p. 235.

16.   Franz, M., C. Swerdlow, and B. Liem, *Cycle length dependence of human action potential duration in vivo. Effects of single extra stimuli, sudden sustained rate acceleration and deceleration and different steady-state frequencies*. J Clin Invest, 1988. **82**: p. 972.

17.   Fridericia, L., *Die Systolendauer in Elekrokariediogramm bei normalen Menschen und bei Herzkranken. I und II*. Acta Med Scand, 1920. **53**: p. 489.

18. Bazett, H., *An analysis of the time-relations of electrocardiograms.* Heart, 1920. 7: p. 353.

19. Adams, W., *The normal duration of the elctrocardiographic ventricular complex.* J Clin Invest, 1936. 15: p. 335.

20. Schlamowitz, I., *An analysis of the time relationship within the cardiac cycle in electrocardiograms of normal men. 1 The duration of the QT interval and its relationship to the cycle length (R-R interval).* Am Heart J, 1946. 31: p. 329.

21. Simonson, E., L.J. Cady, and M. Woodbury, *The normal QT interval.* Am Heart J, 1962. 63: p. 747.

22. Hodges, M., D. Salerno, and D. Erlien, *Bazett's Qf correction reviewed: Evidence that a linear correction for heart rate is better (Abstr).* J Am Coll Cardiol, 1983. 1: p. 694.

23. Arhras, F. and A. Rickards, *The relationship between QT interval and heart rate during physiological exercise and pacing.* Jpn Heart J, 1981. 22: p. 345.

24. Boudoulas, H., P. Geleris, and R. Lewis, *Linear relationship between electrical systole, mechanical systole and heart rate.* Chest, 1981. 80: p. 613.

25. Kovacs, S., *The duration of the QT interval as a function of heart rate: A derivation based on physical principles and a comparison to measured values.* Am Heart J, 1985. 110: p. 872.

26. Sarma, J., R. Sarma, and M. Bilitch, *An exponential formula for heart rate dependence of QT interval during exercise and cardiac pacing in humans: Reevaluation of Bazett's formula.* Am J Cardiol, 1984. 54: p. 103.

27.   Puddu, P., R. Jouve, and S. Mariotti, *Evaluation of 10 QT prediction formulas in 881 middle-aged men from the seven countries study: Emphasis on the cubic root Fridericia' equation.* J Electrocardiol, 1988. **21**: p. 219.

28.   Dickhuth, H., E. Bluemner, and W. Auchschwelk, *The relationship between heart rate and QT interval during atrial stimulation.* Pace, 1991. **14**: p. 783.

29.   Sagie, A., M. Larson, and R. Goldberg, *An improved method for adjusting the QT interval for heart rate (the Framingham Heart Study).* Am J Cardiol, 1992. **70**: p. 797.

30.   Rautaharju, P., S. Zhou, and S. Wong, *Functional characteristics of QT prediction formulas - the concepts of QTmax and QT rate sensitivity.* Comp Biomed Res, 1992. p. 548.

31.   Attwell, D., I. Cohen, and D. Eisner, *Activity dependent changes in mammalian ventricular muscle.* J Physiol, 1977. **271**: p. 17.

32.   Boyett, M. and B. Jewell, *A study of the factors responsible for rate-dependent shortening of the action potential in mammalian ventricular muscle.* J Physiol (London), 1978. **285**: p. 359.

33.   Rickards, A. and J. Norman, *Relation between QT interval and heart rate - new design of physiological adaptive cardiac pacemaker.* Br Heart J, 1981. **45**: p. 56.

34.   Milne, J., A. Camm, and D. Ward, *Effect of intravenous propranolol on QT interval. A new method of assessment.* Br Heart J, 1980. **43**: p. 1.

35.   Abildskov, J., *Neural mechanisms involved in the regulation oj ventricular repolarization.* Eur Heart J, 1985. **6 (Suppl)**: p. 31.

36. Boudoulas, H., P. Geleris, and R. Lewis, *Effect of increased adrenergic activity on the relationship between electrical systole and mechanical systole.* Circulation, 1981. **64**: p. 1.

37. Cappato, R., P. Alboni, and G. Gilli. *Sympathetic and vagal influence on rate dependent changes of Q-T.* in *Proceedings, 31st International symposium on vectorcardiography.* September, 1990. Florence, Italy.

38. Stern, S. and S. Eisenberg, *The effect of propranolol (Inderal) on the lectrocardiogram of normal subjects.* Am Heart J, 1969. **77**: p. 192.

39. Seides, S., M. Josephson, and W. Batesford, *The electrophysiology of propranolol in man.* Am Heart J, 1974. **88**: p. 733.

40. Birkhead, J., H. Vaughan Williams, and D. Gwilt, *Heart rate and QT interval in subjects adapted to beta-blockade: bradycardia and hypotension as uncorrected adaptions.* Cardiovasc Res, 1983. **17**: p. 649.

41. Surawicz, B. and S. Knoebel, *Long QT: Good, bad, or indifferent?* J Am Coll Cardiol, 1984. **4**: p. 398.

42. Lecocq, B., V. Lecocq, and P. Jaillon, *Physiologic relation between cardiac cycle and QT duration in healthy volunteers.* Am J Cardiol, 1989. **64**: p. 481.

43. Yanowitz, F., J. Preston, and J. Abildskov, *Functional distribution of right and left stellate innervation of the ventricles: Production of neurogenic electrocardiographic changes by unilateral alteration of sympathetic tone.* Circ Res, 1966. **18**: p. 416.

44. Kraluos, F., L. Martin, and M. Burgess, *Local ventricular repolarization changes due to sympathetic nerve branch stimulation.* Am J Physiol, 1975. **228**: p. 1621.

45.   Autenrieth, G., B. Surawicz, and C. Kuo, *Primary T-wave abnormalities caused by uniform and regional shortening of ventricular monophasic action potential in dog.* Circulation, 1975. **51**: p. 668.

46.   Till, J., E. Shinebourne, and J. Pepper, *Complete denervation of the heart in a child with congential long QT deafness.* Am J Cardiol, 1988. **62**: p. 1319.

47.   Finley, J. and J. Armour, *Cardiac denervation and long QT interval.* The Am Journal of Cardiol, 1989. **64**: p. 696.

48.   Savard, P., R. Cardinal, and R. Nadeau, *Epicardial distribution of ST segment and T wave changes produced by stimulation of intrathoractic ganglia of cardiopulmonary nerves in dogs.* Journal of Autonomic Nervous System, 1991. **34**: p. 47.

49.   Macfarlane, P. and T. Veitch Lawie, *The normal electrocardiogram and vectorcardiogram,* in *Comprehensive Electrocardiography - Theory and Practice,* P. Macfarlane and T. Veitch Lawrie, Editors. 1989, Pergamon Press: New York. p. 407-457.

50.   Ashman, R., *The normal duration of QT interval.* Am Heart J, 1942. **23**: p. 522.

51.   Kujath, G., *The electrocardiographic QT interval* . 1989, Dalhousie University, Halifax, Nova Scotia:

52.   Rautaharju, P., S. Zhou, and S. Wong, *Sex differences in the evolution of the elctrocardiographic QT interval with age.* Can J Cardiol, 1992. **8**: p. 690.

53.   Moss, A. and P. Schwartz, *Delayed repolarization (QT or QTU prolongation) and malignant ventricular arrhythmias.* Mod Concepts Cardiovasc Dis, 1982. **51**: p. 85.

54.   Levin, H., *Prolonged QT interval syndrome*. JAMA, 1986. **256**: p. 2985.

55.   Schwartz, P. and H. Stone, *Unilateral stellectomy and sudden death*, in *Neural Mechanisms in Cardiac Arrhythmias*, P. Schwartz and A. Zanchetti, Editors. 1978, Raven Press: New York. p. 107-122.

56.   Zehender, M., T. Meinertz, and S. Hohnloser, *Incidence and clinical relevance of QT prolongation caused by the new selective serotonin antagonist ketaserin*. AM J Cardiol, 1989. **25(Suppl)**: p. 826.

57.   Schwartz, P. and S. Wolf, *QT interval prolongation as predictor of sudden death in patients with myocardial infarction*. Circulation, 1978. **57**: p. 1074.

58.   Algra, A., J. Tijssen, and J. Roelandt, *QTc prolongation measured by standard 12 lead electrocardiogram is an independent risk factor for sudden death*. Circulation, 1991. **83**: p. 1888.

59.   Schouten, E., J. Dekker, and P. Meppelink, *QT-interval prolongation predicts cardiovascular mortality in an apparently healthy population*. Circulation, 1991. **84**: p. 1516.

60.   Schwartz, P., *Sympathetic imbalance and cardiac arrhythmias*. Nervous Control of Cardiovascular Function, ed. W. Randall. 1983, New York: Oxford University Press. 225 - 252.

61.   Vedin, A., L. Wilhelmsen, and H. Wedel, *Predictor of cardiovascular deaths and non-fatal reinfarctions after myocardial infarction*. Acta Med Scand, 1977. **201**: p. 309.

62.   Moller, M., *QT interval in relation to ventricular arrhythmias and sudden cardiac death in postmyocardial infarction patients*. Acta Med Scand, 1981. **210**: p. 73.

63.   Clerc, L., *Directional differences of impulse spread in trabecular muscle from mammalian heart*. J Physiol (London), 1976. **255**: p. 335.

64.   Corbin, L. and A. Scher, *The canine heart as an electrocardiographic generator: Dependence on cardiac cell orientation*. Circ Res, 1977. **41**: p. 58.

65.   Grant, R., *Architectures of the heart*. Am Heart J, 1953. **46**: p. 405.

66.   Hoffman, B. and E. Suckling, *Relationship between cardiac cellular potentials and the deflections of the electrogram*. Am J Physiol, 1952. **171**: p. 737.

67.   Rosenbaum, M., M. Elizari, and J. Lazzari, *The Hemiblocks*. 1970, Oldsmar, Florida: Tampa Tracings. p. 1-269.

68.   Tawara, S., *Das reitzleotungssytem des saugetierherzens*, in *Eine anatomisch-histologische studie uber das atrioventrikularbundel und die Purkinjeschen Faden*. 1906, Gustav Fischer Verlag: Jena.

69.   Demoulin, J. and H. Kulbertus, *Pathological findings in patients with left anterior hemiblock*, in *Vectorcardiography*, I. Hoffman and R. Hamby, Editors. 1976, North-Holland Publishing Company: Amsterdam. p. 123-127.

70.   Durrer, D., Van Dam, R. Th, and G. Freud, *Total excitation of the isolated human heart*. Circulation, 1970. **41**: p. 899.

71.   Weidmann, S., *Elektrophysiologie der Herzmuskelfaser*. 1956, Berne: Huber.

72.   Scher, A., *An excitation of the heart*, in *Handbook of Physiology*, W. Hamilton and P. Dow, Editors. 1962, Saunders: Philadelphia. p. 287-322.

73. Scher, A. and A. Young, *The pathway of ventricular depolarization in the dog*. Circ Res, 1956. **4**: p. 461.

74. Cassidy, D., J. Vassallo, and F. Marchlinski, *Endocardial mapping in human in sinus rhythm with normal left ventricles: Activation patterns and characteristics of electrograms*. Circluation, 1984. **70**: p. 37.

75. Van Dam, R.T., *Activation of the heart*, in *Comprehensive Electrocardiography - Theory and Practice*, P. Macfarlane and T. Veitch Lawrie, Editors. 1989, Pergamon Press: New York. p. 101 - 126.

76. Wyndham, R., M. Wyndham, and T. Smith, *Epicardial activation in patients with LBBB*. Circulation, 1980. **61**: p. 696.

77. Arisi, G., E. Macchi, and S. Baruffi, *Potential fields on the ventricular surface of the exposed dog heart during normal excitation*. Circ Res, 1983. **52**: p. 706.

78. Boineau, J. and M. Spach, *The relationship between the electrocardiogram and the electrical activity of the heart*. J Electrocardiol, 1968. **1**: p. 5.

79. Selvester, R., C. Collier, and E. Pearson, *Analog computer model of the vectorcardiogram*. Circulation, 1965. **31**: p. 45.

80. Grant, R., *Grant's Clinical Electrocardiography. Spatial vector approach*. 1972, New York: McGraw-Hill. p.126.

81. Rodriquez, M. and D. Sodi-Pallares, *Mechanism of complete and incomplete bundle branch block*. Am Heart J, 1952. **44**: p. 715.

82. Becker, R., A. Scher, and R. Erickson, *Ventricular excitation in experimental left bundle branch block*. Am Heart J, 1958. **55**: p. 547.

83. Sodi-Pallares, D., A. Bisteni, and M. Testelli, *Ventricular activation and the vectorcardiogram in bundle branch blocks: Clinical and experimental studies with a critical appraisal of the vectorcardiographic methods of Frank and Grishman*. Circ Res, 1961. **91**: p. 1098.

84. Wu, D., P. Denes, and K. Rosen, *Bundle branch block. Demonstration of the incomplete nature of some "complete" bundle branch and fascicular blocks by the extra-stimulus technique*. Am J Cardiol, 1974. **33**: p. 583.

85. Lev, M., P. Unger, and K. Rosen, *The anatomic substrate of complete left bundle branch block*. Circulation, 1974. **50**: p. 479.

86. Pruitt, R., H. Essex, and B. Burchell, *Studies on the spread of excitation through the ventricular myocardium*. Circulation, 1951. **3**: p. 418.

87. Vassallo, J., D. Cassidy, and F. Marchlinski, *Endocardial activation of left bundle branch block*. Circulation, 1984. **69**: p. 914.

88. de Padua, F., A. Pereirina, and M. Lopes, *Conduction defects*, in *Comprehensive Electrocardiography - Theory and Practice*, P. Macfarlane and T. Veitch Lawrie, Editors. 1989, Pergamon Press: New York. p. 459-509.

89. Sodi-Pallares, D., A. Estandia, and J. Sobrson, *Left intraventricular potential of the human heart. II Criteria for diagnosis of incomplete bundle branch block*. Am Heart J, 1950. **40**: p. 655.

90. Schamroth, L. and B. Bradlow, *Incomplete left bundle branch block*. Brit Heart J, 1964. **26**: p. 285.

91. Sodi-Pallares, D. and R. Galder, *New Bases of Electrocardiography*. 1956, St. Louis: C.V. Mosby Co. p. 289.

92. Moore, E., J. Boineau, and D. Patterson, *Incomplete right bundle branch block: an electrocardiographic enigma and possible misnomer*. Circluation, 1971. 4*, p. 678.

93. Chou, J., *Electrocardiography in Clinical Practice*. 1979, New York: Grune & Stratton. 93-145.

94. Lyons, C., *Site of functional right bundle branch block*. Am Heart J, 1980. **100**: p. 653.

95. Van Dam, R.T., *Ventricular activation in human and canine bundle branch block*, in *The Conduction System of the Heart*, H. Wellens, K. Lie, andM. Janse, Editors. 1976, Leiden: HE Stenfert Kroese: BV. p. 377-392.

96. Moore, E., H. BF, and D. Patterson, *Electrocardiographic changes due to delayed activation of the wall of the right ventricle*. Am Heart J, 1964. **68**: p. 347.

97. Dodge, H. and R. Grant, *Mechanism of QRS complex proplongation in man: Right ventricular conduction defects*. Am J Med, 1956. **21**: p. 534.

98. Surawicz, B., *T wave abnormalities*, in *Frontiers of Cardiac Electrophysiology*, M. Rosenbaum and M. Elizari, Editors. 1983, Martinus Nijhoff Publishers: Boston. p. 40.

99. Einthoven, W., G. Fahr, and A. De Waart, *Uber die richtung und die manifeste grosse der potential schwankungen im menschlichen herzen und fiber den einfluss der herziage auf die form des elektrokardiogramms*.

(Translation: Hoff, HE, Sekelf, P. On the direction and manifest size of the variations of potential in the human heart and on the influence of the position of the heart on the form of the electrocardiogram. Pfuegers Arch, 1903. **150**.

100. Burdon-Sanderson, J. and F. Page, *On the time relations of excitatory process in the ventricle of the heart of the frog.* J Physiol (London), 1880. **2**: p. 384.

101. Burdon-Sanderson, J. and F. Page, *On the electrical phenomena of the excitatory process in the heart of the frog and of the tortoise, as investigated photographically.* J Physiol (London), 1883. **4**: p. 327.

102. Waller, A., *A demonstration on man of electromotive changes accompanying the heart's beat.* J Physiol (London), 1887. **8**: p. 229.

103. Bayliss, W. and E. Starling, *On the electromotive phenomena of the mammalian heart.* Monthly International Journal of Anatomy and Physiology, 1892. **9**: p. 256.

104. Hoffman, A., *Zur deutung dec elektrokardiograms.* Pfliigers Archiv, 1901. **133**: p. 522.

105. Samojloff, A., *Weitere beitrage zur elektrophysiologic des herzens.* Pfiigers Archiv, 1910. **135**: p. 417.

106. Wilson, F., A. MacLeod, and P. Barker, *The demonstration and significance of areas of the ventricular deflections of the elctrocardiograms.* Am Heart J, 1931. **10**: p. 46.

107. Van Dam, R.T. and D. Durrer, *The T wave and ventricular repolarization.* Am J Cardiol, 1964. **14**: p. 294.

108. Burgess, J., L. Green, and K. Millar, *The sequence of normal ventricular recovery.* Am Heart J, 1972. **84**: p. 660.

109.   Abildskov, J., *The sequence of normal recovery of excitability in the dog heart.* Circulation, 1975. **52**: p. 442.

110.   Inoue, M. and M. Hori, *Theoretical analysis of T wave polarity based on a model of cardiac electrical activity.* J Electrocardiol, 1978. **11**: p. 171.

111.   Higuchi, T. and Y. Nakaya, *T wave polarity related to the repolarization process of epicardial and endocardial ventricular surfaces.* Am Heart J, 1984. **108**: p. 290.

112.   Franz, M., K. Bargheer, and W. Rafflenbeul, *Monophasic action potential mapping in human subjects with normal electrocardiograms: direct evidence for the genesis of the T wave.* Circulation, 1987. **75**: p. 379.

113.   Harumi, K., M. Burgess, and J. Abildskov, *A theoretic model of the T wave.* Circulation, 1966. **135**: p. 657.

114.   Burgess, M., B. Steinhaus, and K. Spitzer, *Effects of activation sequence on ventricular refractory periods of ischemic canine myocardium.* J Electrocardiol, 1985. **18**: p. 325.

115.   Spach, M., P. Dolber, and J. Heidlage, *Interaction of inhomogeneities of repolarization with anisotropic propagation in dog atria: a mechanism for both preventing and initiating reentry.* Circ Res, 1989. **65**: p. 1612.

116.   Noble, D. and I. Cohen, *The interpretation of the T wave of the ECG.* Cardiovasc Res, 1978. **12**: p. 13.

117.   Cohen, I., W. Giles, and D. Noble, *Cellular basis for the T wave of the electrocardiogram.* Nature, 1976. **262**: p. 657.

118. Toyoshima, H., R. Lux, and R. Wyatt, *Sequence of early and late phases of repolarization on dog ventricular epicardium.* J Electrocardiol, 1981. **14**: p. 143.

119. Rautaharju, P., M. Davignon, and F. Soumis, *Evolution of QRS-T realtionship from birth to adolesence in Frank-lead orthogonal electrocardiogram of 149 normal children.* Circulation, 1979. **60**: p. 196.

120. Autenrieth, G., B. Surawcz, and C. Kuo, *Sequence of repolarization in the ventricular surface in the dog.* Am Heart J, 1975. **89**: p. 463.

121. Solberg, L., D. Singer, and R. Ten Eick, *Glass microelectrode studies on intramural papillary muscle cells. Description of preparation and studies on normal dog papillary muscle.* Circ Res, 1974. **34**: p. 783.

122. Watanabe, T., L. Delbridge, and O. Bustamanate, *Heterogeneity of the action potential in isolated rat ventricular myocytes and tissue.* Circ Res, 1983. **52**: p. 280.

123. Geselowitz, D.B., *The ventricular gradient revisited: relation to the area under the action potential.* IEEE Transactions on Biomedical Engineering, 1983. **1-BME-230**: p. 76.

124. MacLeod, A., *The electrocardiogram of cardiac muscle, an analysis which explains the regression on T deflection.* Am Heart J, 1938. **15**: p. 165.

125. Toyoshima, H. and M. Burgess, *Electrotonic interaction during canine ventricular repolarization.* Circ Res, 1978. **43**: p. 348.

126. Kuo, C., J. Amlee, and K. Munakata, *Dispersion of monophasic action potential duration and activation time during atrial pacing, ventricular pacing and ventricular premature stimulation in canine ventricles.* Cardiovasc Res, 1983. **19**: p. 152.

127. Cowan, J., C. Hilton, and C. Griffiths, *Sequence of epicardial repolarization and configuration of the T wave*. Br Heart J, 1988. **60**: p. 424.

128. Hoffman, B., P. Cranefield, and P. Lepeschkin, *Comparison of cardiac monophasic action potential recorded by intracellular and suction electrodes*. Am J Physiol, 1959. **196**: p. 1297.

129. Franz, M., D. Burkhoff, and H. Spurgeon, *In vitro validation of a new cardiac catheter technique for recording monophasic action potentials*. Eur Heart J, 1986. **7**: p. 34.

130. Saraek, N., J. Roberts, and J. Leonard, *A new method to measure nonuniformity in the intact heart*. J Electrocardiol, 1972. **5**: p. 341.

131. Watanabe, T., P. Rautaharju, and T. McDonald, *Ventricular action potentials, ventricular extracellular potentials and the ECG of guinea-pig*. Circ Res, 1985. **57**: p. 362.

132. Mirvis, D., *Ventricular repolarization*, in *Body Surface Electrocardiographic Mapping*, D. Mirvis, Editor. 1988, Klumer Academic Publishers: Boston. p. 97-108.

133. Abildskov, J., *Effects of activation sequence on the local recovery of ventricular excitability in the dog*. Cir Res, 1976. **38**: p. 240.

134. Sridharan, M., N. Flowers, and J. Wilson, *Recurrent resemblance in potential topography at different instants during ventricular depolarization and repolarization*. J Electrocardiol, 1989. **72**: p. 211.

135. Simonson, E., *Differentiation between normal and abnormal QT interval in electrocardiography*. 1961, St. Louis: C.V. Mosby.

136. Schaefer, H. and H. Haas, *Electrocardiography*, in *Handbook of Physiology. Circulation*, W. Hamilton and P. Dow, Editors. 1962, Am Physiol Soc: Wasington DC. p. 323-415.

137. Daoud, F., B. Surawicz, and L. Gettes, *Effect of isoproterᵢₒₗ on the abnormal T wave*. Am J Cardiol, 1972. **30**: p. 810.

138. Reynolds, E. and C. Van der Ark, *An experimental study of the origin of T waves based on determination of effective refractory period from epicardial and endocardial aspects of the ventricle*. Circ Res, 1959. **8**: p. 943.

139. Plan And Operation Of The Second national Health And Nutrition Examination Survey 1976-1980, *Programs and Collection Procedures Series 1, No. 15. DHHS Publication No. (PHS) 81-1317*, 1981, US Department of Health and Human Services, Public Health Service, Office of Health Research, Statistics and Technology, National Center for Health Statistics, Hyattsville MD:

140. Plan And Operation Of The Hispanic National Health And Nutrition Examination Survey 1982-1984, *Programs and Collection Procedures Series 1, No. 19. DHHS Publication No. (PHS) 85-1321*, 1985, U.S. Department of Health Services, Public Health Services, Office oₗ Health Research, Statistics, and Technology. National center for Health Statistics, Hyattsvilla, MD:

141. Blackburn, H., A. Keys, and E. Simonson, *The electrocardiogram in population studies. A classification system*. Circulation, 1960. **21**: p. 1160.

142. Rautaharju, P., P. MacInnis, and J. Warren, *methodology oₗ ECG interpretation in the Dalhousie program: NOVACODE ECG classification procedures for clinical trials and population health surveys*. Meth Inform Med, 1990. **29**: p. 362.

143. Spodick, D., *Reduction of QT-interval imprecision and variance by measuring the JT interval*. J Electrocardiol, 1990. p.103.

144. Cowan, J., K. Yusoff, and M. Moore, *Importance of lead selection in QT interval measurement.* Am J Cardiol, 1988. **61**: p. 83.

145. Osaka, T., I. Kodama, and N. Tsuboi, *Effects of activation sequence and isotropy cellular geometry on the repolarization phase of action potential of dog ventricular muscles.* Circulation, 1987. **76**: p. 226.

146. Rosenbaum, M., H. Blanco, and M. Elizari, *Electrotonic modulation of the T wave and cardiac memory.* Am J Cardiol, 1982. **50**: p. 213.

147. Rautaharju, P., A. Nissimen, and J. Pekkanes, *QRS axis left shift with age in elderly men: dominating influence of the progression of left ventricular hypertrophy.* Unpublished manuscript, 1994.

148. Friedman, H., *Diagnostic Electrocardiography and Vectorcardiography.* 2nd ed. 1977, New York: McGraw-Hill. 80-85.

149. Browne, K., E. Prystowsky, and H. Heger, *Prolongation of the QT interval in man during sleep.* Am J Cardiol, 1983. **52**: p. 55.

150. Gerstenblith, G., J. Fredericksen, and F. Yin, *Echocardiographic assessment of a normal adult aging population.* Circulation, 1977. **56**: p. 273.

151. Zhou, S., S. Wong, and P. Rautaharju, *Should the JT rather than QT interval be used to detect prolongation of ventricular repolarization.* J Electrocardiol, 1992. **25** (**Suppl**): p. 131.

152. Broback, J., *Best & Tayler's Physiological Basis of Medical Practice.* 1979, Baltimore: The Williams & Eilkins Company. 52-53.

153. Armour, J. and W. Randall, *Structural basis for cardiac functions*. Am J Physiol, 1970. **218**: p. 1517.

154. Streeter, D.J., H. Spotnitz, and D. Patel, *Fiber orientation in the canine left heart during diastole and systole*. Circ Res, 1969. **24**: p. 339.

155. Spach, M., S. Huang, and C. Ayers, *Electrical and anatomic study of the Purkinje system of the canine heart*. Am Heart J, 1962. **65**: p. 664.

156. Fox, C. and G. Hut~i~ns, *The architecture of the human ventricular myocardium*. John Hopkins Med J, 1972. **130**: p. 289.

157. Taccardi, B., R. Lux, and E. PR. *Seventeenth International Congress of Electrocardiology*. in *The Seventeenth International Congress of Electrocardiology*. September, 1990. Florence, Italy.

158. Antzelevitch, C. and S. Sicouri, *Clinical relevance of cardiac arrhythmias generated by after depolarization*. Am Coll Cardiol, 1994. **23**: p. 259.

159. Lab, M.J., *Transient depolarization and action potential alterations following mechanical changes in isolated myocardium*. Cardiovascular research, 1980. **14**: p. 624.

160. Huang, M.H., Wolf, S.G. Armour, J.A., *Sympathetically induced shortening of the QT interval of the EKG is associated primarily with changes in ventricular contractility rather than heart rate*. (in press).

161. Rautaharju, P., T. Manolio, and B. Psaty, *Correlates of QT prolongation in older adults (the Cardiovascular Health Study)*. Am J Cardiol, 1994. **73**: p. 999.